Dissertation

Mitochondrial Ca^{2+} homeostasis and its contribution to metabolism-secretion coupling in pancreatic β-cells

submitted by

Muhammad Rizwan ALAM

MSc, MPhil

for the Academic Degree of

Doctor of Philosophy

(PhD)

at the

Medical University of Graz

Institute of Molecular Biology and Biochemistry

under the supervision of

Univ.-Prof. Dr. Wolfgang F. GRAIER

2013

DECLARATION

I hereby declare that this dissertation is my original work and that I have fully acknowledged by name all those individuals and organizations that have contributed to the research for this dissertation. Due acknowledgement has been made in the text to all other materials used. Throughout this dissertation and in all related publications I followed the guidelines of “Good Scientific Practice”.

Graz ---------- ----------

DEDICATED TO

MY LATE BROTHER-IN-LAW

MUHAMMAD SALEEM BUTT

ACKNOWLEDGEMENTS

In the name of Allah the most beneficent and the most merciful who has provided me plentiful courage and motivation to accomplish this work. He is the one who has created this universe and has blessed the human being with knowledge, wisdom and power to explore the exquisite beauties of life.

With all my sincerity, I express my deepest gratitude to Prof. Dr. Wolfgang Graier who provided me an enormous opportunity to join his lab and successfully complete my PhD. Dr. Graier is a great scientist who was a source of continuous inspiration and enthusiasm for me. I am duly obliged for his persistent support, guidance and encouragement in different aspects of my work which played a major role in my professional development. I appreciate his efforts in arranging and providing all possible resources required to accomplish this task.

I am also very thankful to my co-supervisor, Dr. Roland Malli, whose exceptional guidance greatly helped me in the accomplishment of this thesis. His intelligent and skillful opinions always contributed strongly throughout the course my studies. Special thanks also goes to Prof. Dr. Berthold Huppertz and Prof. Dr. Dirk Strunk who as a part of my thesis committee provided many valuable suggestions during our annual meetings.

I consider it worthwhile to acknowledge my adorable colleagues, Lukas Groschner, Muhammad Jadoon Khan, Markus Waldeck-Weiermair, Claire Jan-Quartier, Neelanjan Vishnu, Rene Rost, Alexander Bondarenko, Sonja Barth, Sandra Blass, Andras Deak, Felix Karsten, Warisara Parichatikanond, Corina Madreiter, Therese Macher, Christiane Klec, Florian Enzinger and Anna Schreilechner, for their company and assistance during my stay in the lab. It was also a great pleasure to work with Elisabeth Seles, Stefan Dobersberger, Alexandra Barbulescu, Ismene Fertschai and Shamim Naghdi. I duly acknowledge the contribution and support of Lukas, Warisara and Liang Kuo for performing some experiments and for helping me to publish this work successfully. I am also obliged to all the colleagues and friends who have directly or indirectly provided their assistance during my stay and PhD research at the institute of molecular biology and biochemistry.

I am indebted and grateful to my Pakistani folks in Graz for their great support and company. My special thanks go to Jadoon, Khurram, Mudassar and Tanveer Bhai for their

cooperation and unforgettable company through thick and thin. Taking this opportunity I also thank my friends and well-wisher back in Pakistan.

Finally, I convey my greatest gratitude to my loving parents, sisters, brother, my wife, nephews and niece who provided me an unconditional support and encouragement throughout my stay in Austria. All of them prayed persistently and patiently for the successful completion of my PhD. They are the greatest asset of my life and I am short of words to express my love for all of them. May Allah (SWT) bless them with a successful and beautiful life both in this world and the next – Aameen.

Muhammad Rizwan Alam

Graz, Austria

TABLE OF CONTENTS

ABBREVIATIONS

ADP/ATP	Adenosine di/triphosphate
AMPK	AMP-activated protein kinase
Bcl-2	B-cell lymphoma 2 proteins
BLAST	Basic local alignment search tool
bp	Base pair
BSA	Bovine serum albumin
$[Ca^{2+}]_{cyto}$	Cytosolic free calcium concentration
$[Ca^{2+}]_{mito}$	Mitochondrial free calcium concentration
CaM	Calmodulin
CCDC190A	Coiled-coil domain containing 109A proteins (also known as MCU)
Cch	Carbachol
cDNA	Complementary DNA
CFP/GFP/YFP	Cyan/Green/Yellow fluorescent protein
dNTPs	Deoxyribonucleoside triphosphates
DroCRC	*Drosophila melanogaster* Ca^{2+} release channel
EB	Experimental buffer
EGTA	Ethylene glycol tetraacetic acid
ER	Endoplasmic reticulum
FAD/ $FADH_2$	Flavin adenine dinucleotide: oxidized/reduced
FASTA	Fast accurate search tool alignment
FRET	Förster (fluorescent) resonance energy transfer
Fura-2 AM	Fura-2 acetoxymethyl ester
GAPDH	Glycerol-3-phosphate dehydrogenases
GDP/GTP	Guanosine di/triphosphate
GLP-1	Glucagon-like peptide-1
GLUT1/2	Glucose transporter ½
GPCR	G-protein coupled receptor
GSIS	Glucose-stimulated insulin secretion
HBSS	Hank's balanced salt solution
HCE	Proton calcium exchanger
hMCU	Human mitochondrial Ca^{2+} uniporter

hMICU1	Human mitochondrial Ca^{2+} uptake-1
IMM	Inner mitochondrial membrane
INS-1	Insulinoma-1 cell line
IP_3	Inositol triphosphate
IP_3R	Inositol trisphosphate receptor
K_{ATP}	ATP-sensitive potassium channel
KHE	Potassium proton exchanger
LB	Laura Bertani
LETM1	Leucine zipper-EF-hand containing transmembrane protein 1
M13	Myosin light chain kinase peptide
MCUR1	Mitochondrial Ca^{2+} uniporter regulator-1
MCU	Mitochondrial Ca^{2+} uniporter
MDa	Mega Dalton
MFN2	Mitofusin-2
MICU1	Mitochondrial Ca^{2+} uptake-1
mPTP	Mitochondrial permeability transition pore
mtDsRed	Mitochondrial *Discosoma* sp. red fluorescent protein
NAD/ NADH	Nicotinamide adenine dinucleotide: oxidized/reduced
NCBI	National center for biotechnology information
NCLX	Sodium calcium lithium exchanger
NCX	Sodium calcium exchanger
OMM	Outer mitochondrial membrane
PCR	Polymerase chain reaction
Pi	Inorganic phosphate
PLC-β	Phospholipase C-beta
PM	Plasma membrane
PMCA	Plasma membrane Ca^{2+} ATPase
RaM	Rapid uptake mode
RIPA	Radioimmuno precipitation assay buffer
ROCC	Receptor-operated Ca^{2+} channel
ROS	Reactive oxygen species
RRP	Readily releasable pool

RyR	Ryanodine receptor
S100A1	S100 calcium-binding protein A1
SERCA	Sarco/endoplasmic reticulum Ca^{2+} ATPase
siRNA	Small interfering RNA
SLC25A25	SLC25A25 solute carrier family member A25
SOC	Store-operated Ca^{2+} channel
SOCE	Store-operated Ca^{2+}-entry
T2D	Type 2 diabetes mellitus
TM	Transfection mixture
TRP	Transient receptor potential channels
UCP2/3	Uncoupling proteins 2/3
VDAC	Voltage-dependent anion channel
VGCC /VDCC	Voltage-gated/dependent Ca^{2+} channel

ABSTRACT

Mitochondria Ca^{2+} uptake is an important physiological process which contributes in many cellular functions. In addition to its involvement in the modulation of mitochondrial metabolism and cytosolic Ca^{2+} homeostasis, it has also emerged as a central hub in many cell survival/death pathways such as apoptosis, necrosis and autophagy. In pancreatic β-cells, mitochondrial Ca^{2+} uptake promotes metabolism – secretion coupling by activation of some rate limiting enzymes in the matrix. This accelerates the process of oxidative phosphorylation which generates ATP and other coupling factors necessary for glucose – stimulated insulin secretion (GSIS). Thus transfer of Ca^{2+} signals from the cytosol to mitochondria plays a crucial role in boosting the oxidative metabolism and any interference with mitochondrial Ca^{2+} transport may disrupt the metabolism-secretion coupling and compromise GSIS. This study was designed to identify the contribution of recently identified MICU1 and, MCU, along with other putative candidates LETM1 and UCP2 in mitochondrial Ca^{2+} homeostasis, ATP production and GSIS in clonal pancreatic β-cells. Using a combination of siRNA – mediated silencing and Ca^{2+} measurement with FRET – based genetic sensor, we found that MICU1 and MCU are involved in mitochondrial Ca^{2+} sequestration upon Ca^{2+} mobilization with both IP_3 – generating agonists and plasma membrane depolarization. In contrast, knockdown of UCP2 and LETM1 solely diminished mitochondrial Ca^{2+} uptake in response to either intracellular Ca^{2+} release or Ca^{2+} entry from extracellular side, respectively. Moreover, a simultaneous knockdown of both MICU1 and MCU did not yield any additional effect on mitochondrial Ca^{2+} response which ruled out the association of these proteins with other pathways of Ca^{2+} transport. Based on the involvement of MICU1 and MCU in both pathways of Ca^{2+} uptake, we further explored their role in mitochondrial metabolism and GSIS. Glucose, the major trigger for insulin secretion, induced cytosolic Ca^{2+} oscillations which were also transferred to mitochondria. However, the silencing of MICU1 and MCU hampered the relay of these Ca^{2+} transients into the mitochondria. Conversely this was not accompanied by an inhibition or increase of global cytosolic Ca^{2+} signals. Furthermore glucose – triggered elevation of cytosolic ATP and insulin secretion was also diminished upon suppression of MICU1 and MCU. In summary this data provides convincing evidence about the role of MICU1 and MCU in the physiology of pancreatic β-cells and makes them a compelling target for therapy to improve the GSIS by modulation of mitochondrial Ca^{2+} in patients with type 2 diabetes mellitus.

ZUSAMMENFASSUNG

Die Aufnahme von Ca^{2+} durch die Mitochondrien stellt einen physiologischen Prozess von enormer Wichtigkeit dar, der unzählige zelluläre Funktionen maßgeblich beeinflusst. Abgesehen von Stoffwechsel und zytosolischem Ca^{2+}-Haushalt, gibt es eine Vielzahl weiterer zellulärer Signalwege, wie etwa Apoptose, Nekrose oder Autophagie, die in unmittelbarem Zusammenhang mit der mitochondrialen Ca^{2+}-Aufnahme stehen. In den β-Zellen des Pankreas verstärkt mitochondriales Ca^{2+} die Kopplung zwischen Stoffwechsel und Sekretion indem es geschwindigkeitsbestimmende Stoffwechselenzyme aktiviert. Dies wiederum beschleunigt die oxidative Phosphorylierung und damit die Synthese von ATP and anderen Faktoren, die eine Glucose-stimulierte Insulinsekretion (GSIS) ermöglichen. Die Fortleitung von Ca^{2+}-Signalen aus dem zytosolischen in das mitochondrielle Kompartiment ist daher von essentieller Bedeutung für den oxidativen Metabolismus. Eine Störung des mitochondrialen Ca^{2+}-Transports könnte demnach die Stoffwechsel-Sekretionskopplung und damit auch die GSIS negativ beeinflussen. Die vorliegende Studie hat zum Ziel, die Rolle der beiden unlängst identifizierten Proteine MICU1 und MCU, sowie die von LETM1 und UCP2, in der mitochondrialen Ca^{2+}-Homöostase einer klonalen β-Zelllinie der Ratte zu untersuchen. Weiters soll der Beitrag dieser Proteine zur Stoffwechsel-Sekretionskopplung in pankreatischen β-Zellen erforscht werden.

Mit Hilfe von siRNA-vermitteltem Gen-silencing konnte die Expression der jeweiligen Proteine selektiv vermindert werden. Fluoreszenzmikroskopische Messungen unter Anwendung eines genetisch kodierten, auf FRET basierenden Ca^{2+}-Sensors ermöglichten in Folge die Aufzeichnung mitochondrialer Ca^{2+}-Signale und zeigten, dass MICU1 und MCU an der mitochondrialen Ca^{2+}-Aufnahme in β-Zellen beteiligt sind. Gen-Kockdown von MICU1 wie auch von MCU verminderte die mitochondriale Ca^{2+}-Aufnahme, sowohl auf IP_3-vermittelte Ca^{2+}-Freisetzung, als auch auf Depolarisation der Zelle hin. Knockdown von UCP2 oder LETM1 hingegen zeigte einen selektiven Effekt, entweder in Reaktion auf intrazelluläre Ca^{2+}-Mobilisierung oder auf Ca^{2+}-Einstrom über die Plasmamembran. Der simultane Knockdown von MICU1 und MCU hatte keinen zusätzlichen Effekt, was darauf schließen lässt, dass diese beiden Proteine, unabhängig von der Ca^{2+}-Quelle, am selben Ca^{2+}-Transportweg teilhaben. Aufbauend auf der zentralen Rolle von MICU1 und MCU, wurde in Folge deren Beitrag zur Stoffwechsel-Sekretionskopplung untersucht. Glucose, der wichtigste Auslöser der Insulinsekretion, rief Ca^{2+}-Oszillationen in der mitochondrialen Matrix hervor, welche durch Gen-silencing von MICU1 und MCU unterdrückt wurden,

während die zytosolische Ca^{2+}-Aktivität unverändert blieb. Auch der Glucose-induzierte Anstieg der zytosolischen ATP-Konzentration sowie die GSIS konnten durch Knockdown von MICU1 und MCU signifikant vermindert werden. Diese Arbeit liefert die erste Evidenz für eine integrale Rolle von MICU1 und MCU in der Physiologie der pankreatischen β-Zelle und macht sie somit zu einem neuen vielversprechenden Ziel für die Therapie des Typ 2 Diabetes mellitus.

1. INTRODUCTION

Mitochondria are essential cellular organelles required to maintain a bioenergetic balance along with their contribution to Ca^{2+} homeostasis, stress responses, cell death and various intracellular signaling pathways (1,2). Historically mitochondria are believed to be endosymbionts which work as cell's powerhouse and contribute to energy production by oxidation of nutrient metabolites. However, over the past few decades their role as a central hub in regulating a number of biological activities ranging from metabolism to cell death has been firmly established (1). Their direct and indirect involvement in the etiopathogenesis of a number of human diseases has made this organelle a compelling target for the scientist both in translational medicine and basic research (3,4).

1.1 Historical Perspective

First recognized in the middle of 19th century, these organelles were lately named as bioblasts and were considered as "elementary organisms" living within a cell. Later the endosymbiotic theory also narrated a similar concept due to resemblance of these so-called intracellular organisms with bacteria (5). Carl Benda was the first to introduce these organelles as "mitochondria" and this word was derived from the Greek "mitos" (thread) and "chondros" (granules) which described their appearance during spermatogenesis. The 20th century brought a lot of major discoveries in this field, some of which include isolation of structurally and functionally preserved mitochondria from tissue, high resolution electron micrographs revealing their structure, Peter Mitchell's chemiosmotic theory, Ca^{2+} uptake by energized mitochondria, discovery of the respiratory chain, isolation and sequencing of mitochondrial genome, identification of fusion and fission processes and many more (6,7,5,3). Accumulation of this data has provided us a deep insight of the structure and function of this indispensable organelle and its crucial contribution to cell physiology and pathology (3). Over the last 30 years most of the information about mitochondria has been obtained from the patients suffering from diseases with defects in mitochondrial respiratory chain proteins. A number of mutations in the mitochondrial genome have been linked to many diverse human disorders but we still do not have a deep understanding of the molecular mechanisms underlying such defects (4). The participation of mitochondria in cellular Ca^{2+} homeostasis has emerged as a biological phenomenon of prime importance in the last two decades and it is of absolute physiological and pathological relevance (8,9,10).

1.2 Mitochondria and cellular Ca^{2+} homeostasis

The characterization of Ca^{2+} as a major and ubiquitous signaling molecule with its involvement in a variety of cellular functions has provided us a deep understanding of its importance in animal physiology. This divalent cation transforms the input of many extracellular stimuli and regulates the cellular functions both in health and disease conditions (11,12). The energy – associated accumulation of Ca^{2+} in the mitochondria was first described in 1960s and this ushered in a new era in the field of cellular Ca^{2+} homeostasis (13,14). Figure 1.1 narrates a story of the development of conceptual basis of mitochondrial Ca^{2+} uptake since its first demonstration in early 1960s. The phenomenon of mitochondrial Ca^{2+} sequestration is of fundamental importance and it has been convincingly demonstrated to play a pivotal role in many cellular functions such as ATP production (15), cytosolic Ca^{2+} buffering (16,17,18) and hormone secretion (19). Moreover disruption of pathways involved in relaying of cytosolic Ca^{2+} signals into mitochondria may trigger disease – associated mitochondria – dependent processes such as apoptosis and necrosis which may culminate in cell death (20,21,22,1).

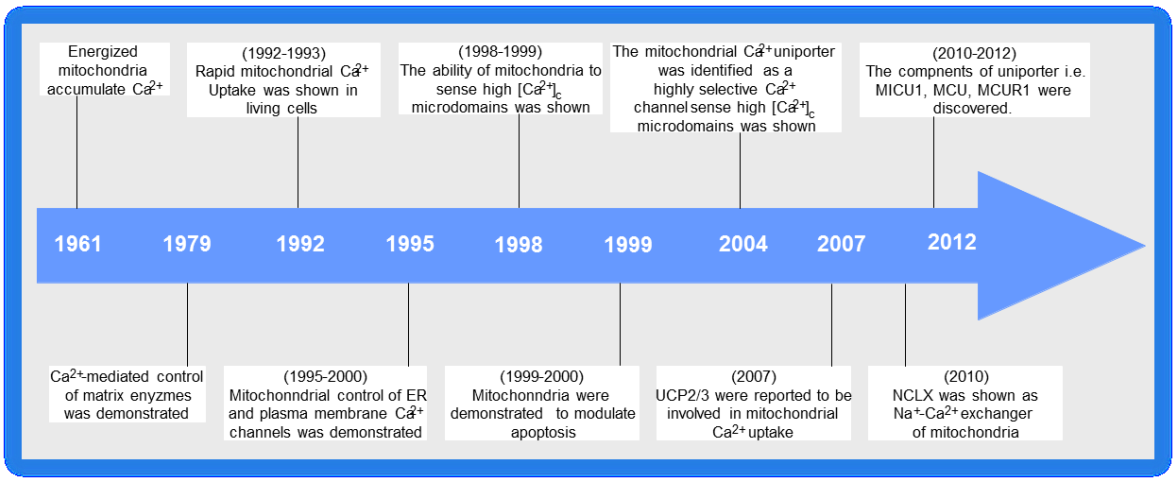

***Figure 1.1**: The history of mitochondrial* Ca^{2+}*- A Timeline (modified and adopted from Rizzuto et al. 2012)* (1)

Mitochondria play a crucial role in modulation of cellular Ca^{2+} homeostasis. Their ability to accumulate large amounts of Ca^{2+} (1-10 µM) depends upon an electrochemical gradient across the inner mitochondrial membrane (IMM) (20). This gradient is generated by the transport of protons across IMM into intermembrane space by electron transport chain. Pumping of protons out of the mitochondrial matrix produces a negative membrane potential of ~ -180 mV which is the major driving force for transport of Ca^{2+} ions into

mitochondria (20,23,24). The balance of matrix Ca^{2+} is very critical for maintenance of a physiological state and is controlled by combination of many influx and efflux pathways along with Ca^{2+} - buffering processes. Various mechanisms increase the intracellular Ca^{2+} leading to a subsequent mitochondrial Ca^{2+} uptake. Elevation of cytosolic Ca^{2+} occurs mainly by mobilization from intracellular stores and by Ca^{2+} influx from the extracellular milieu by opening of numerous ion channels in the plasma membrane. Mitochondria shape these cytosolic transients by uptake/release of Ca^{2+} and regulate a number of important cellular functions (23,24,1,25).

1.3 Ca^{2+} mobilization from endoplasmic reticulum

Endoplasmic reticulum (ER) is the largest intracellular Ca^{2+} store (~500 μM) which contributes to a number of cellular functions. It harbors many proteins in its membrane which contribute to Ca^{2+} release/refilling, translocation of nascent polypeptides and establishment of contacts sites with other organelles like mitochondria, golgi bodies and nucleus (25,24). This dynamic store can be stimulated to release its Ca^{2+} via different channels and serves as a mandatory component which provides Ca^{2+} for many intracellular signal transduction pathways (24,26).

Inositol 1, 4, 5-trisphosphate receptor (IP_3R*)* is the main player in the release of Ca^{2+} from ER and it is activated by soluble IP_3 molecules which are generated by G-protein-coupled receptor (GPCR) – mediated phospholipase C-β (PLC-β) pathways. IP_3, a lipid secondary messenger, binds and causes the opening of IP_3R which results in a fast release of sequestered ER Ca^{2+} (27,24). The functional regulation of IP_3R requires its interaction with many other proteins within ER lumen and on the cytosolic domain as well (28). There are three different isoforms of human IP_3R and each of which is composed of 4 subunits. IP_3R has a long cytosolic N – terminus which contains a binding site for IP_3 along with many phosphorylation sites serving as targets for post-translational modifications by various enzymes which play an important role in its regulation (29,30). Ryanodine receptors (RyR) are another group of ER membrane proteins which are involved in Ca^{2+} release and are primarily activated by a rise in intracellular Ca^{2+}. They have three isoforms (RyR 1-3) which are found in a wide variety of cell types. They are the biggest ion channels reported so-far with a molecular weight of approximately 2.2 MDa and are generally believed to be involved in Ca^{2+}- induced Ca^{2+} release and act as a facilitator in the amplification of the cytosolic Ca^{2+} signals. They are mostly famous for their vital contribution to excitation –

contraction coupling in muscle cells (31,32). Sarco/endoplasmic reticulum ATPase (SERCA) is a protein which resides in ER membrane and plays a very important role in pumping Ca^{2+} back into the lumen of ER against a steep gradient at the cost of ATP. It has three isoforms which are adapted to specific functions in different tissues. They play a crucial role in maintenance of ER Ca^{2+} homeostasis on one hand and regulate the cytosolic Ca^{2+} concentration on the other hand (33). ER Ca^{2+} leak is a phenomenon of passive Ca^{2+} leak from the ER that contributes in many aspects of cellular Ca^{2+} homeostasis. In addition to IP_3R and RyRs which can cause Ca^{2+} leakage in some pathological conditions, the existing data suggest the existence of many candidate proteins which contribute to the Ca^{2+} leak from ER both in normal and disease conditions (34). Some of the reported candidates which contribute to ER Ca^{2+} leak include translocon (35), polycystins (36), presenilins (37) and Bcl-2 protein family (38).

1.4 Ca^{2+} influx from extracellular milieu

Ca^{2+} transport across the plasma membrane is mediated by a variety of channels and carriers with cell type specificities (8). These include voltage-gated Ca^{2+} channels (VGCCs) and receptor-operated Ca^{2+} channels (ROCCs) which are mainly active in electrically excitable cells while store-operated Ca^{2+} channels (SOCs) are believed to be the major players in non-excitable cells (39,12,40). Transient receptor potential (TRP) channels are another large group of ion channels which are involved in Ca^{2+} transport across the plasma membrane. However they are relatively non-selective and allow the permeation of other cations as well (41,42).

To maintain a robust intracellular Ca^{2+} homeostasis plasma membrane is also equipped with pumps and exchangers which contribute to the extrusion of Ca^{2+} from the cells such as plasma membrane Ca^{2+} ATPases (PMCAs) and Na^{+}-Ca^{2+} exchangers (NCXs). Both of these protein families have many isoforms and work at different Ca^{2+} affinities. For instance PMCA which has a high affinity for Ca^{2+} maintains low level of cytosolic Ca^{2+} while NCX having a low affinity for Ca^{2+} is better suited for removing larger amounts of Ca^{2+} from the cytosol in exchange with extracellular sodium (43,33,44). Due to a huge Ca^{2+} gradient between ER/extracellular space and cytosol cells maintain a tight control over Ca^{2+} release/influx and efflux pathways. This is regulated by a plethora of proteins in the plasma membrane and ER. In addition mitochondria and other organelles like lysosomes

also play a significant role in shaping the spatial and temporal patterns of cellular Ca^{2+} signals (45,9,46,47)

1.5 Mitochondrial Ca^{2+} transport

The outer mitochondrial membrane (OMM) is relatively permeable to ions and small molecules. Voltage-dependent anion channel (VDAC) is a group of non-selective pores which allow the diffusion of small molecules including Ca^{2+} ions across the OMM (48). The IMM however is impermeable to most of the ions and small molecules and they are transported via tightly regulated channels and carrier proteins. Mitochondria start accumulating Ca^{2+} in response to cytosolic Ca^{2+} elevation by agonist – induced Ca^{2+} release from ER or Ca^{2+} influx from extracellular space. Mitochondrial Ca^{2+} balance is maintained by specific influx and efflux pathways which have a role in many cellular functions ranging from metabolism to cell death (1,8,49) (Figure 1.2).

1.5.1 Mitochondrial Ca^{2+} uptake

Although the role of mitochondria in Ca^{2+} uptake has been established for many decades, the molecular players involved in Ca^{2+} influx and efflux pathways have been only recently discovered (50,51,52,53). The major route of mitochondrial Ca^{2+} uptake comprises a mitochondrial Ca^{2+} uniporter (MCU) whose physical characteristics were first recognized in 2004 by patch clamping of mitoplasts. MCU is proposed to be a highly selective ion channel which transports Ca^{2+} down the electrochemical gradient and this pathway of mitochondrial Ca^{2+} uptake is ruthenium red sensitive (54). However the molecular identity of MCU remained obscured for many years. RyR type 1 was the first candidate protein to be reported in mitochondrial Ca^{2+} uptake but its role seems specific only to cardiac muscle cells (55,56,1). The discovery of uncoupling proteins 2/3 (UCP2/3), which, in addition to their role in H+ transport, were reported to be involved in mitochondrial Ca^{2+} uptake in some specific cell types, raised a lot of interest in this field (57). Initially reported to be fundamental for mitochondrial Ca^{2+} uniport, UCP2/3 were later shown to be involved in mitochondrial uptake of Ca^{2+} released from ER and not in store – operated Ca^{2+} entry. In subsequent studies they were proposed to be the modulators of MCU rather than MCU themselves (58,59). The participation of these proteins in mitochondrial Ca^{2+} uptake is debated (20,24,1) and further studies are required to rule out the possibilities of changes in cellular metabolism (60) or any indirect modulation of MCU-mediated Ca^{2+} uptake (8). Leucine zipper EF hand-containing transmembrane proteins 1 (LETM1), which was

originally believed to be involved in mitochondrial K^+/ H^+ exchange (KHE) (61) has also been demonstrated to play a role in the modulation of mitochondrial structure, its biogenesis, metabolism and in the pathogenesis of Wolf-Hirschhorn syndrome (62,63,64). More recently KHE function of LETM1 has been shown to be important in ER Ca^{2+} uptake in combination with small conductance Ca^{2+} - activated potassium channels. Its contribution to sequestration of matrix Ca^{2+} in exchange with H^+ implies its role in mitochondrial Ca^{2+} uptake (53,65). However this function of LETM1 is largely debated and demands further investigation (66). Some studies have also discovered other routes of mitochondrial Ca^{2+} uptake which include rapid mode of Ca^{2+} uptake (RaM) (67), involvement of Coenzymes Q 10 (68), mCa1/2 (69) and DroCRC (70) and these are summarized in Figure 2. A recent study by our group utilizing the patch clamp technique has highlighted the existence of three and two Ca^{2+} currents in mitoplasts isolated from HeLa and endothelial cells respectively (46).

1.5.2 Discovery of Mitochondrial Ca^{2+} uptake 1 (MICU1) - A breakthrough

Using a combination of comparative physiology, evolutionary genomics and organelle proteomics, Mootha group was the first to discover Mitochondrial Ca^{2+} uptake 1 (MICU1) an EF hand-containing protein playing a major role in MCU – mediated mitochondrial Ca^{2+} sequestration. On the basis of its expression in most mammalian tissues, localization in inner mitochondrial membrane, absence in yeast, diminished mitochondrial Ca^{2+} uptake in MICU1 silenced cells and presence of one transmembrane domain made it the most plausible candidate to act as a regulator of MCU – mediated Ca^{2+} uptake (50). However its role in mitochondrial Ca^{2+} uptake was challenged by Madesh and co-workers who called this protein as a gatekeeper and demonstrated in different cell models that it plays a role in the regulation of basal mitochondrial Ca^{2+} by inhibition of MCU – mediated Ca^{2+} uptake under unstimulated conditions (71). However, while some unpublished findings from our lab indicate a more dynamic role of MICU1 in different cell types depending upon its expression and interaction with MCU, we need further studies to elucidate the enigmatic contribution of MICU1 to mitochondrial Ca^{2+} transport in various cell models.

1.5.3 Mitochondrial Ca^{2+} Uniporter

The remarkable discovery of MICU1 in 2010 led researchers to resolve the long – standing mystery of MCU a year later. Two groups in parallel identified CCDC190A, now known as Mitochondrial Ca^{2+} Uniporter (MCU), as an essential component of MCU – mediated Ca^{2+}

uptake pathway (52,51). This protein has all the major characteristics of long – known MCU which is a highly selective ion channel. MCU physically interacts with MICU1 and exists as an oligomer in a large protein complex. siRNA – mediated silencing of MCU resulted in a strong inhibition of mitochondrial Ca^{2+} uptake in both intact and permeabilized cells while its overexpression significantly increased the mitochondrial Ca^{2+} sequestration. Reconstitution of recombinant MCU in lipid bilayers showed an electrophysiological activity while mutation of the pore forming amino acids blunted the Ca^{2+} currents. It has two predicted transmembrane domains while both of its C – and N – terminal ends, which have sites for post-translational modifications, are located in the mitochondrial matrix (72,51,73). There is a large tissue variation in MCU – mediated mitochondrial Ca^{2+} current which might have a role in regulating the mitochondrial Ca^{2+} overload in cells containing large numbers of mitochondria or cells with frequent cytosolic Ca^{2+} activity (74). However this concept needs further clarification in its relevance to physiology and disease. A very recent study also reported the identification of a new protein which physically interacts with MCU and has been named as MCU regulator 1 (MCUR1). This protein has been proposed as a crucial component of MCU complex and its silencing has been shown to impair MCU – mediated Ca^{2+} uptake and mitochondrial metabolism without affecting the localization of MCU. Intriguingly, knockdown of MCUR1 led to an increased expression of MCU (75). The discovery of MCU and its regulatory partners MICU1 and MCUR1 has opened a new molecular era in the field of mitochondrial Ca^{2+} transport. In addition to raising new questions these discoveries have unlocked new directions to explore the contribution of these proteins in cell physiology and diseases along with finding new targets for therapy.

1.5.4 Mitochondrial Ca^{2+} extrusion

During Ca^{2+} signaling events, mitochondria located at some crucial strategic positions such as those close to ER and mouth of channels in the plasma membrane may accumulate a huge amount of Ca^{2+}. Some part of this Ca^{2+} is buffered by the formation of calcium phosphate precipitates which have pathophysiological relevance (76). To restore normal concentrations of matrix Ca^{2+}, the IMM is also equipped with certain proteins carriers which contribute to the extrusion of excess Ca^{2+}. The kinetics of mitochondrial Ca^{2+} efflux varies between excitable and non-excitable cells and different proteins are believed to participate in this phenomenon. Na^{+}/Ca^{2+} exchanger (NCX) which transports Ca^{2+} out of the matrix in exchange with Na^{+} while H^{+}/Ca^{2+} exchanger (HCE) are considered to be

responsible for outward transport of mitochondrial Ca^{2+} with exchange of H^{+} (20). Although the phenomenon of Na^{+}- mediated Ca^{2+} efflux in mitochondria was first reported many decades ago (77), a serendipitous finding of Sekler's group about a mitochondrial isoform (78) of NCX led them to finally characterize the molecular identity of this transporter in 2010. This protein is now known as NCLX (Na^{+}- Ca^{2+}- Li^{+} exchanger) and is believed to be responsible for mitochondrial Ca^{2+} release which is dependent on the presence of Na^{+} but can also be substituted with Li^{+}. The discovery of NCLX has now enabled researchers to find its contribution in different cellular functions (79,80,78,77). The molecular identity of HCE is not known so far (20). Another pathway which has been proposed to participate in mitochondrial Ca^{2+} efflux involves the so – called mitochondrial permeability transition pore (mPTP) (81). Although this pore has been proposed to function under physiological conditions (81,82), it can also trigger cell death signaling under conditions of matrix Ca^{2+} overload (83).

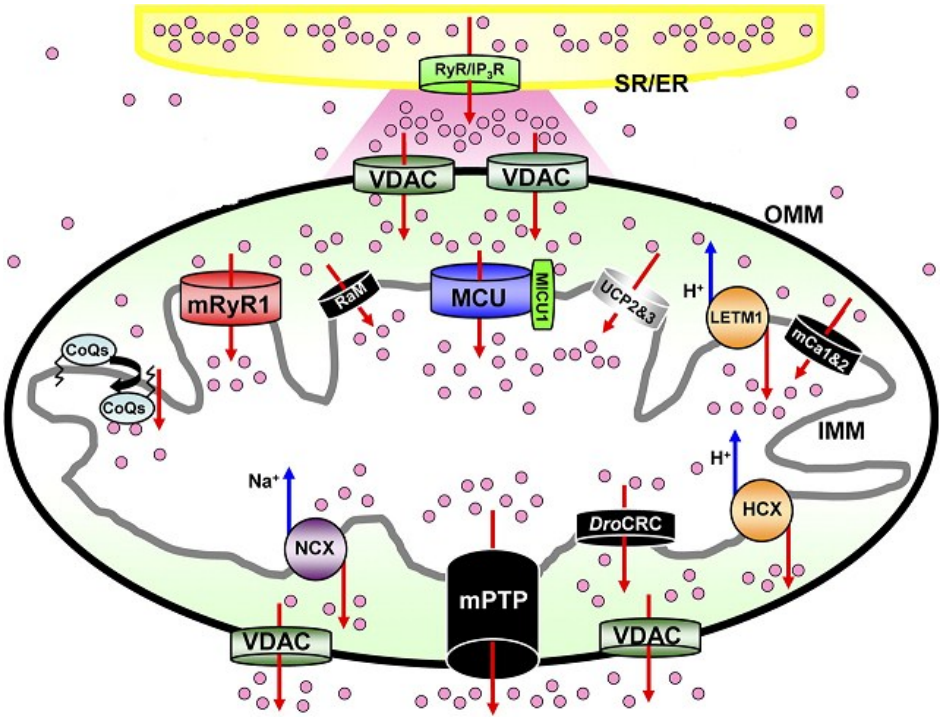

***Figure 1.2**: Mitochondrial Ca^{2+} transport mechanisms (modified and adopted from O-Uchi et al. 2012)* (10).

1.6 Ca^{2+} as an activator of mitochondrial metabolism

Matrix Ca^{2+} modulates the activity of many mitochondrial proteins which in turn accelerate oxidative metabolism and ATP production. Chelation of extracellular Ca^{2+} can significantly reduce their function resulting in a compromised respiration and oxidative phosphorylation. There are many mitochondrial proteins (mostly enzymes) which are modulated by free Ca^{2+} and are briefly described in the following sections (84)

i) Pyruvate dehydrogenase phosphatase

Pyruvate dehydrogenase is a part of pyruvate dehydrogenase complex required for the conversion of pyruvate to acetyl-CoA which then can enter either citric acid cycle or fatty acid biosynthesis pathways. This is a rate limiting enzyme which is regulated by phosphorylation or dephosphorylation of specific amino acid by either pyruvate kinase or pyruvate phosphatase respectively. Acetyl-CoA which is a product of the reaction catalyzed by pyruvate dehydrogenase complex itself modulates the activity of this enzyme. Ca^{2+} binding increases the activity of pyruvate phosphatase which in turn dephosphorylates and enhances the activity of pyruvate dehydrogenase complex. This increases the rate of citric acid cycle and ATP production by enhancing oxidative phosphorylation (85,86,84,87).

ii) α – Ketoglutarate dehydrogenase

Also known as oxoglutarate dehydrogenase, it is a complex of three enzymes (E1. E2 and E3). This multisubunit enzyme catalyzes the rate – limiting step of citric acid cycle i.e. conversion of α – Ketoglutarate to succinyl-CoA. It is activated by direct binding of free Ca^{2+} to E1 subunit (85,84,88,89).

ii) Isocitrate dehydrogenase

Isocitrate dehydrogenases has a low sensitivity to Ca^{2+} which increases the concentration range in which matrix Ca^{2+} can modulate its activity. It catalyzes the decarboxylation of isocitrate to α – ketoglutarate in the third step of citric acid cycle (84,90).

iv) ATP synthase

The ATP synthase, also known as F_1, F_0 ATPase is the biggest protein complex in the IMM. It catalyzes the formation of ATP by transportation of H+ across the IMM using a proton motive force. F_0 subunit is a proton carrier while F_1 works like a hub protruding towards the matrix side of the mitochondria. The head of F_1 subunit is formed of

alternating α- and β-subunits with β-subunits having catalytic activity (91,92). Matrix free Ca^{2+} is proposed to regulate the activity of ATP synthase by modulation of its post – translational modification (phosphorylation) and by Ca^{2+} - dependent binding of S100A1 protein to its F_1 subunit which also enhances the ATP production (93,94,95,84).

Other mitochondrial proteins which are potential targets of Ca^{2+} include FAD -glycerol 3-phosphate dehydrogenase (96), cytochrome oxidase (97), citrin, aralar 1, malate-aspartate shuttle (98), ATP-Mg^{2+}/Pi transporter (SLC25A25) (96) and β-hydroxybutyrate dehydrogenase. Ca^{2+} modulates the activity of these proteins within mitochondria or on the cytosolic side either indirectly by their post – translational modification or by direct interaction with specific Ca^{2+} - binding domains (84,90).

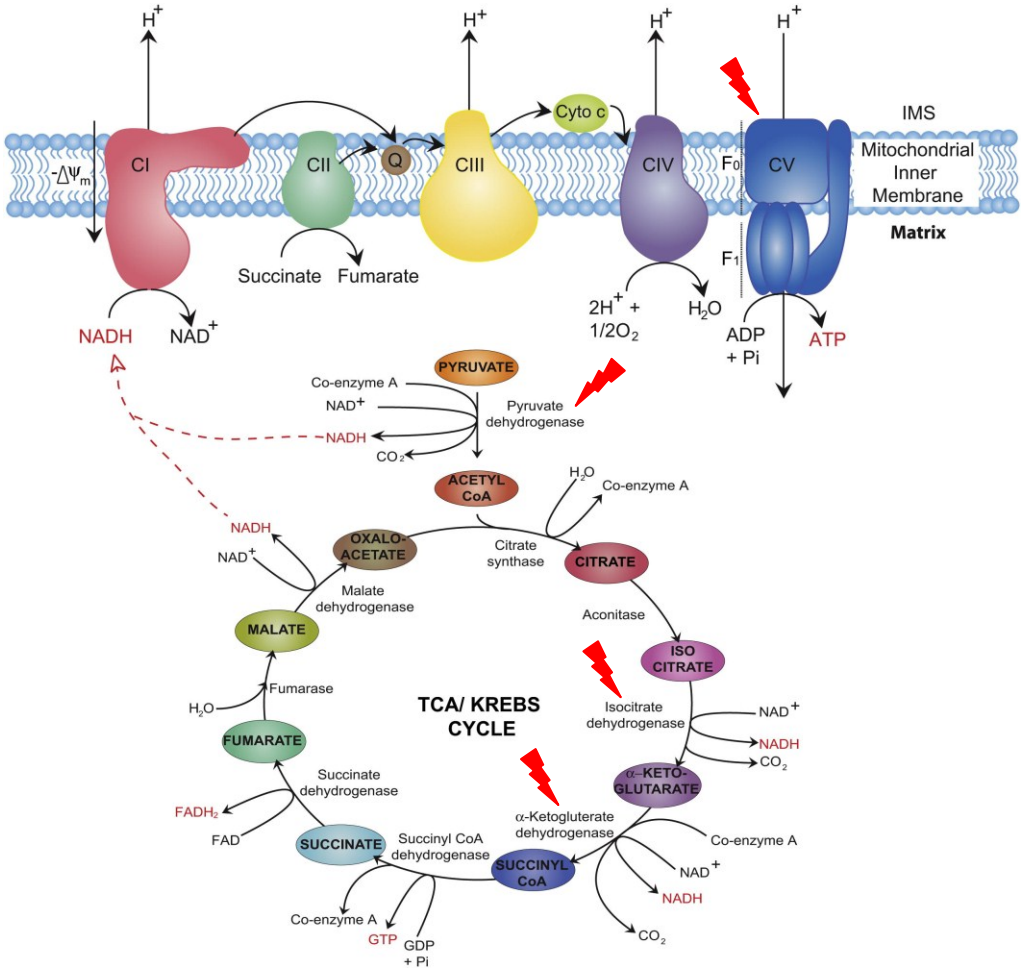

Figure 1.3: *A schematic model of Krebs cycle and electron transport chain. Major proteins which are modulated by* Ca^{2+} *are pointed with red flash symbols. (Modified ad adopted from Osellame LD et al. 2012)* (99)

1.7 Role of mitochondria in cytosolic Ca^{2+} buffering

In addition to many Ca^{2+} - binding proteins, mitochondria also buffer cytosolic Ca^{2+} by rapidly accumulating Ca^{2+} released from the ER or Ca^{2+} entering the cell from extracellular space. However, in contrast to Ca^{2+} - binding proteins, mitochondria can sequester huge amounts of Ca^{2+} and they can act as dynamic reservoirs at many Ca^{2+} microdomains in the cell. Their capacity to take up Ca^{2+} depends on their energy status and this influences cellular Ca^{2+} signals by different manners depending upon the cell type (1). For instance mitochondrial Ca^{2+} uptake from some subplasmalemmal domains reduces the inactivation of SOCE channels (100,101) and in neurons mitochondria Ca^{2+} accumulation at the synapses modulates the local Ca^{2+} dynamics which affect the release of neurotransmitters (102). In addition mitochondrial Ca^{2+} sequestration from sub-cellular domains modulates the function of other channels such as IP_3R, RyR in the ER and L-type channel residing in the plasma membrane (7,103). Moreover mitochondria also participate in controlling the spatiotemporal patterns of Ca^{2+} signals at specific microdomains and their strategic positioning restricts the diffusion of Ca^{2+} out of these critical regions like in pancreatic acinar cells (104). Thus location and movement of mitochondria in defined regions of the cells are very crucial and defects in this positioning have been reported to contribute to the pathogenesis of many diseases (105,1).

1.8 Mitochondrial Ca^{2+} controls cell survival

Mitochondrial Ca^{2+} uptake also has implications in different cell death pathways. Matrix Ca^{2+} overload due to excessive or consistent cytosolic Ca^{2+} release e.g. due to hyperstimulation of cells in excitotoxicity, have been reported to disrupt the bioenergetics balance resulting in increased reactive oxygen species (ROS) production and collapse of the membrane potential. These changes may lead to opening of the mPTP, causing swelling of the mitochondria and loss of ATP culminating in cell death via necrosis. Ca^{2+}-triggered opening of mPTP also plays a role in the initiation of intrinsic mechanisms of apoptotic cell death. This occurs in combination with other apoptotic stimuli such as oxidative stress and generation of some ceramide derivatives. The release of apoptosome components from mitochondria leads to the activation of executioner caspases which contribute to apoptotic damage. Many pro – and anti – apoptotic proteins of the Bcl-2 family also regulate this mode of cell death by modulating the Ca^{2+} levels of ER and mitochondria. Dysfunction of mitochondrial Ca^{2+} homeostasis and matrix Ca^{2+} overload leading to cell death has been observed in many diseases (106,1,2).

Mitochondrial Ca^{2+} has also been demonstrated to be involved in autophagy which is an adaptive response of cells to nutrient deprivation. Inhibition of IP_3 – mediated Ca^{2+} transfer to mitochondria compromises the bioenergetic status of the cell causing an activation of AMPK (AMP kinase) and initiation of the pro – survival process of autophagy. A constitutive transfer of Ca^{2+} from ER to mitochondria via IP_3R is essential for normal cellular respiration and suppression of autophagy (107,108).

1.9 Mitochondrial function in pancreatic β-cells

The pancreatic β-cells are neuroendocrine cells which secrete insulin to maintain D-glucose (glucose) homeostasis. The release of insulin is increased in response to circulating nutrients, gastrointestinal hormones and neurotransmitters secreted by the autonomic nervous system. Glucose is the major nutrient secretagogue which is sensed by β-cells causing a release of insulin into the bloodstream. In addition, long chain amino acid e.g. leucine and fatty acids also promote insulin secretion by metabolism or by acting on cell surface receptors. Release of acetylcholine and glucagon like peptide 1 (GLP-1) further potentiate insulin exocytosis by initiating a signaling cascade after binding the respective receptor on plasma membrane (109).

Nutrients and their metabolites trigger insulin granule exocytosis by stimulating mitochondrial metabolism and oxidative phosphorylation causing an enhanced ATP production (84,109). The transport of ATP into cytosol increases ATP/ADP ratio which inhibits the ATP – sensitive K^+ channels (K_{ATP} channel) causing plasma membrane depolarization. As a result VGCCs, which are sensitive to changes in plasma membrane electrical potential, are opened causing an influx of Ca^{2+} into the cytosol. The entering Ca^{2+} activates the exocytosis of readily releasable pool (RRP) of insulin granules. This is referred to as the triggering phase of insulin secretion which is followed by a long lasting amplifying phase (109). Part of the Ca^{2+} entering the cytosol is also taken up by mitochondria which further boosts respiration and ATP production along with the generation of other coupling factors such as GTP, glutamate, glutamine, α-ketoglutarate and superoxides (110,111,19,109). These processes are proposed to be responsible for a more sustained insulin secretion. Figure 1.4 summarizes a consensus model of glucose-stimulated insulin secretion (GSIS) in which mitochondria play a fundamental role in coupling of oxidative metabolism of glucose (and other nutrient secretagogue) to insulin secretion.

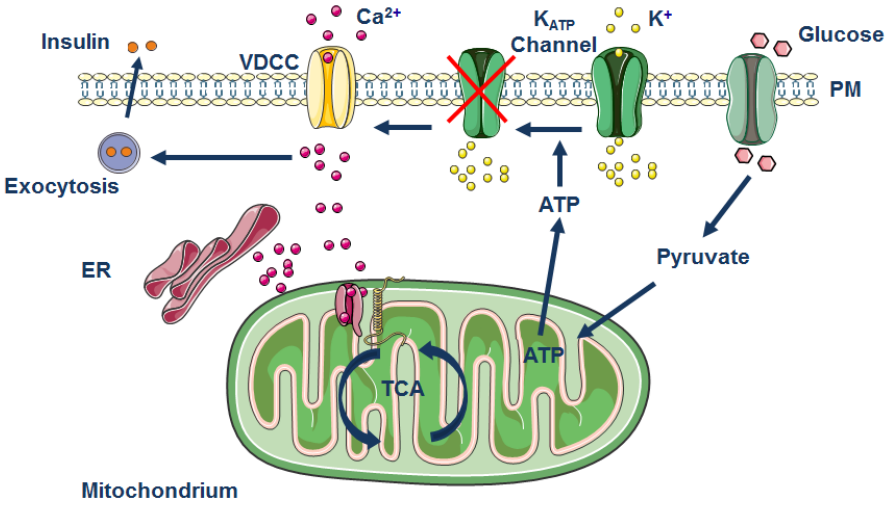

***Figure 1.4**: A model of glucose-stimulated insulin secretion.*

Most of the information about this consensus model of GSIS has been derived from experiments in rodents. However recent studies have shown considerable differences among human and mouse beta cells some of which are briefly summarized in the table below (112).

***Table 1.1:** Differences between human and rodent pancreatic β-cells.*

β-cell function/phenotype	Human	Rodents
Innervation (112)	Sparse	Extensive
Main glucose transporters (with Km for glucose) (112)	GLUT1 (6 mM)	Glut2 (1 mM)
Non – fasting plasma glucose (112)	~ 5 mM	7-10 mM
Pyruvate carboxylase activity level and activity (113)	Low	High
ATP citrate lyase level and activity (113)	Low	High
Succinyl-CoA:3-ketoacid-CoA transferase Acetoacetyl-CoA synthetase (113)	High	Low
Glucose threshold for half maximal insulin secretion (112)	~ 6 mM	~ 11 mM in mice
Resting membrane conductance (112)	60 pS/pF	0.7 nS/pF in mice

Threshold potential (112)	-60 mV	-50 mV ?? mice
Proportions of β-cells in islets (114)	55 %	77 %
Association of β-cells with other endocrine cells within an islet (114)	29 %	71 %
Distribution of β-cells in islets (114)	Throughout the islets	Mostly in the center forming a core
Extra – islet β-cells (115)	~15 %	Rare
Proliferation capability	Low (< 0.1 %) (116,117)	High (> 20 %) (118)
Oscillatory activity throughout the cells (114)	Not coordinated	Coordinated

1.10 Influence of mitochondrial Ca^{2+} on insulin secretion

Mitochondria play an essential role in the physiology of β-cells and their dysfunction has been associated with type 2 diabetes mellitus (T2D) (119). Nutrient stimulation causes cytosolic Ca^{2+} rises in β-cells which are then transferred to mitochondria via MCU (120,121). Matrix Ca^{2+} elevation accelerate oxidative phosphorylation by activation of various matrix dehydrogenases and other proteins as described previously. Therefore any interference with the relay of cytosolic Ca^{2+} signals into mitochondria may contribute to impairment of mitochondrial metabolism resulting in compromised insulin secretion which is a major factor contributing to the pathogenesis of T2D. An excessive matrix Ca^{2+} may also trigger the opening of mPTP directly or due to enhanced ROS production initiating a signaling cascade culminating in cell death. This phenotype of β-cells is observed in gluco – or lipotoxic conditions which are often associated with obesity and T2D which are a hallmark of metabolic syndrome (119).

Despite a crucial contribution of mitochondrial Ca^{2+} uptake in the physiology of pancreatic β-cells the actual identity of proteins involved in mitochondrial Ca^{2+} sequestration was unknown when this work was started. Therefore this study was designed to elucidate the function of recently discovered MCU and MICU1 as components of mitochondrial Ca^{2+} uniporter in addition to finding a possible contribution of UCP2 and LETM1 in mitochondrial Ca^{2+} uptake in pancreatic β-cells.

Aims of this dissertation

Based on the existing knowledge about the importance of mitochondrial Ca^{2+} sequestration, candidate transport proteins and crucial contribution of mitochondrial Ca^{2+} in pancreatic β-cells, this study was designed to achieve following goals.

i) To characterize mitochondrial Ca^{2+} signals and spatiotemporal patterns of Ca^{2+} transfer from cytosol to mitochondria in INS-1 cells

ii) To identify the role of MICU1, MCU, LETM1 and UCP2 in mitochondrial Ca^{2+} uptake under different stimulatory conditions.

iii) To elucidate the function of these proteins in mitochondrial metabolism and GSIS.

2. MATERIALS AND METHODS

2.1 Cell Culture

All experiments were carried out in a rat insulinoma cell line INS-1 832/13 except the expression of MICU1 and MCU which was also tested in freshly isolated mouse pancreatic β-cells. INS-1 832/13 (INS-1) cell line has been derived from a previously available clonal INS-1 cells and has a stably transfected human proinsulin cDNA (122). These cells have a potent response to glucose with half-maximal insulin secretion at 6 mM D-glucose. INS-1 cells were kindly provided by Dr. C. B Newgard (Duke University, School of medicine, Durham, NC, USA) and were cultured in RPMI-1640 (RMPI) medium containing 10 mM glucose supplemented with 10 % fetal calf serum, 10 mM HEPES, 50 µg of penicillin, 100 µg of streptomycin, 1 mM sodium pyruvate, 50 µM β-mercaptoethanol and were grown at 37 ˚C in 5 % CO2 in a humidified environment. Most of the experiments were done between 47-70 population doublings.

2.2 Mouse islet isolation

Pancreatic islets were isolated from 9-12 weeks old C57/BL6 mice by collagenase digestion as described elsewhere (123). The euthanized mice were opened and pancreas was perfused with ~3 ml of collagenase solution containing 1,000 U/L collagenase XI. Distended pancreas was carefully removed and incubated at 37 ˚C in 2 ml of fresh collagenase solution. Digestion was terminated at by putting the tubes on ice and digested pancreatic tissue was washed 2-3 times with Hank's balanced salt solution (HBSS) and resuspended pellet was put into a 70 µM strainer. Strainer containing the digested tissue was washed again with HBSS. It was turned upside down over a cell culture dish and islets were collected with 15 ml of RPMI medium. Islets were handpicked under an inverted microscope and maintained in RPMI medium until further processing.

2.3 Transfection of cells

The best way to elucidate the function of a protein is by obtaining a gain or loss of its function within the cell. Small interfering RNAs (siRNAs) are commonly used to transiently silence the gene expression while cDNAs cloned in an expression vector are used for overexpression. We used both siRNA-mediated knock-down and overexpression approaches to identify the function of target proteins.

2.3.1 Transfection of siRNAs with/without plasmid DNA

INS-1 cells were grown in 6 well plates with or without glasses to 60-70% density and were transfected with specific siRNA or scrambled control siRNA with or without a plasmid DNA depending on the requirement of the experiment. The transfection mixture (TM) was prepared in DMEM medium (without serum and antibiotics/antifungals) using Promega TransFastTM transfection medium as given below.

Components	Volume/well*
DMEM medium	0.5 ml
siRNA	100-200 pmoles
Plasmid DNA	1-1.5 µg
TransFastTM reagent	4 µl/well

**Volume for 1 well of a 6-well plate*

The TM was mixed well and incubated at room temperature for 10-15 minutes to allow the formation of liposomes. This mixture was layered onto the cells after removal of the medium and incubated at 37 ˚C for 1 hour. Another 0.5 ml of the DMEM medium was added to each well upon completion of 1 hour incubation period and kept in the incubator for overnight. After an overnight (16-20 hours) incubation period the transfection mixture was replaced with complete RMPI-1640 medium and experiments were performed after 48 or 72 hours of transfection. The sequences of siRNA used in this study are listed in Table 1.

2.3.2 Transfection of plasmid DNA

The cells were transfected with plasmid DNA using a slightly different protocol. The recipe for the preparation of the TM is given as below.

Component	Volume/well*
DMEM medium	1.0 ml
Plasmid DNA	1.5 – 2 µg
TransFastTM reagent	4 µl/well

**Volume for 1 well of a 6-well plate*

The rest of the protocol for incubation was the same as described in 2.3.1 with a little variation. 1 ml of TM was layered onto the cells for 4-5 hours and then it was replaced

with complete RMPI medium and experiments were carried out 48 or 72 hours after incubation.

2.4 Ca^{2+} measurements

Over the past two decades there has been immense progress in the approaches to measure free intracellular Ca^{2+}. The development of Ca^{2+} sensors, ranging from synthetic dyes to genetically – encoded proteins based indicators, have greatly helped to demystify various aspects of cellular signaling pathways in physiology and disease processes.

The present work has mostly employed the FRET based genetically – encoded Ca^{2+} sensors which include 4mtD3cpv (mito-cameleon) and D3cpv (cyto-cameleon) both of which can nicely be used for ratiometric imaging of free Ca^{2+} in the mitochondrial matrix and cytosol respectively. The fundamental design of these sensors consists of a Ca^{2+} sensitive peptide from calmodulin (CaM) and a CaM binding region of myosin light-chain kinase (M13) flanked by two GFP-derived fluorophores on N – and C – termini. Upon Ca^{2+} binding a conformational change brings the two fluorophores in close vicinity increasing the FRET signal. The design of two sensors is similar (Fig. 2.1) with the exception of 4mtD3cpv which has an additional mitochondrial targeting sequence at the N – terminus.

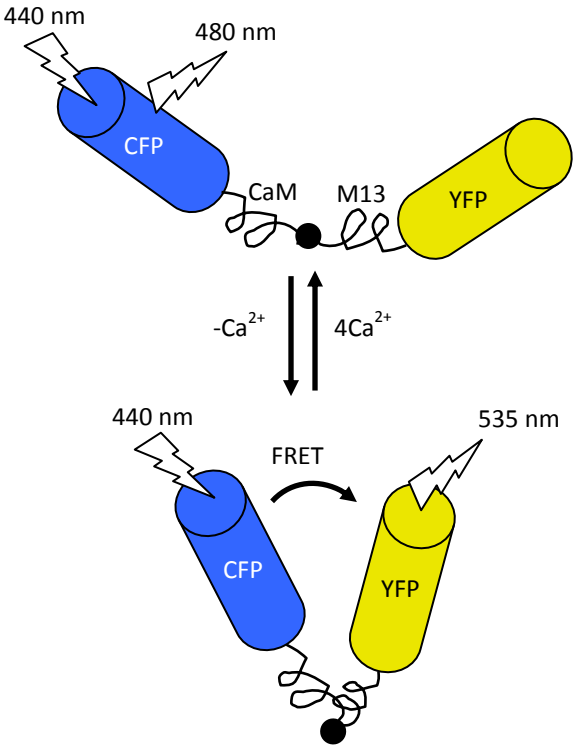

Figure 2.1: *Basic design of a CFP/YFP based genetically – encoded* Ca^{2+} *sensor. Flash symbols indicate the excitation and emission wavelengths.*

In addition to cameleon sensors a membrane permeable chemical indicator Fura-2 AM (Fura-2) which is an EGTA – derived synthetic dye was also used for cytosolic Ca^{2+} measurements. Fura-2 allows ratiometric imaging of intracellular Ca^{2+} with a minimum problem of photobleaching and uneven loading. The peak excitation of Fura-2 shifts from 340 nm to 380 nm in Ca^{2+} bound and Ca^{2+} free states respectively and its peak fluorescence intensity is observed at 500 nm. Therefore when measuring cytosolic Ca^{2+} with Fura-2 an elevated Ca^{2+} concentration leads to an amplification of signal at 340 nm while fluorescence decreases when the dye is excited at 380 nm (Fig. 2.2).

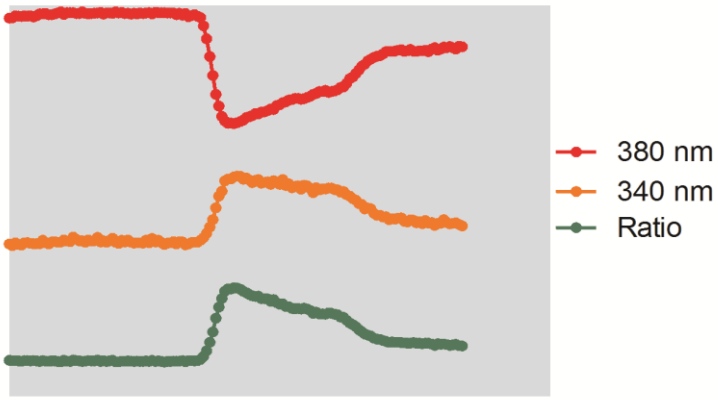

Figure 2.2: *Fura-2 excitation in* Ca^{2+} *free (380 nm) and* Ca^{2+} *bound (340 nm) states.*

2.4.1 Mitochondrial Ca^{2+} measurement

INS-1 cells were cultured on glasses in 6-wells dishes and mitochondrial Ca^{2+} uptake was measured 48-72 hours after transfection with mito-cameleon and respective siRNA/plasmid DNA. INS-1 cells can be stimulated by different means to mobilize Ca^{2+} from intracellular stores or to cause Ca^{2+} influx from the extracellular medium, both leading to a rise in intracellular Ca^{2+} which is then transferred to mitochondria via channels in the inner and outer mitochondrial membranes.

Following protocols were used to measure mitochondrial Ca^{2+} uptake in these cells:

i) Ca^{2+} *mobilization from intracellular stores*

Cells were washed and maintained at room temperature in HEPES-buffered solution (EH-loading buffer) containing in (in mM): 138 NaCl, 5 KCl, 2 $CaCl_2$, 1 $MgCl_2$, 1 HEPES, 2.6 $NaHCO_3$, 0.44 KH_2PO_4, 0.34 Na_2HPO_4, 10 D-glucose, 0.1% vitamins, 0.2% essential amino acids, and 1% penicillin/streptomycin, pH adjusted to 7.4. During imaging cells

were perfused for 1 minute with an experimental buffer (EB) containing (in mM): 138 NaCl, 5 KCl, 2 $CaCl_2$, 1 $MgCl_2$, 10 D-glucose, and 10 HEPES, pH adjusted to 7.4. This was followed by 2 – 3 minutes of perfusion with a Ca^{2+}-free EB and then stimulated with a combination of IP_3 – generating agonists i.e. carbachol (Cch: 100 µM) and ATP (200: µM). This leads to Ca^{2+} release mainly from endoplasmic reticulum which is then rapidly taken up mitochondria.

ii) Influx of extracellular Ca^{2+}

INS-1 cells are electrically excitable and they can take up large amounts of Ca^{2+} via L-type voltage – gated Ca^{2+} channels (VGCCs). VGCCs are activated by depolarization of plasma membrane which can be achieved by manipulating ATP-sensitive K^+ (KATP channel) either by elevated intracellular ATP:ADP ratio or by an increased extracellular potassium concentration. A global rise in cytosolic Ca^{2+} causes mitochondria to sequester this Ca^{2+}. In this study INS-1 cells cultured on glasses were perfused during imaging with EB for 1 – 2 minutes followed by a short pulse of 30 mM KCl – containing EB (isotonic conditions was maintained by substituting 25 mM NaCl with KCl). This leads to depolarization of plasma membrane allowing a rapid Ca^{2+} influx and an uptake by mitochondria.

Glucose is a physiological stimulator of VGCC – mediated Ca^{2+} influx and acts via its metabolism in mitochondria by accelerating the production of ATP. To monitor glucose-stimulated mitochondrial Ca^{2+} uptake cells were pre-incubated in HBSS containing (in mM) 114 NaCl, 4.7 KCl, 2.5 $CaCl_2$, 1.2 $MgSO_4$, 2 HEPES, 1.2 KH_2PO_4, 25 $NaHCO_3$, 0.2% bovine serum albumin (BSA), and 3 glucose. This was followed by a wash with glucose – free EB and a further incubation in the same buffer for 10 – 15 minutes. This additional treatment was done to minimize the cytosolic Ca^{2+} oscillations on the one hand and to achieve a maximum Ca^{2+} signal upon exposure to high glucose on the other hand. During Ca^{2+} imaging cells were treated with 16 mM glucose – containing EB following a 3 minutes perfusion with glucose – free EB.

2.4.2 Cytosolic Ca^{2+} measurement

Global cytosolic Ca^{2+} was measured with either cyto-cameleon or Fura-2 using the protocols described in 2.4.1. Fura-2 loading was done by incubation of the cells in EH – loading solution containing 2 µM Fura-2 at room temperature for 30 – 45 minutes. Cells were washed for two times with EB to remove extracellular Fura-2 and were maintained in EB for the whole period of experiment.

2.4.3 Single cell imaging and data acquisition

Single cell Ca^{2+} imaging was performed on two different inverted microscopy systems. The technical specifications of both systems are as follows: Zeiss Axiovert inverted microscope (Zeiss, Vienna, Austria) provided with a polychromator illumination system (VisiChrome High Speed, Xenon lamp, Visitron Systems, Puchheim, Germany) and a thermo-electric-cooled CCD camera (Photometrics Coolsnap HQ, Visitron Systems), Nikon Eclipse TE300 inverted microscope (Japan) equipped with a polychromator lamp (Opti Quip 770, USA) and a liquid-cooled charged coupled device (CCD) camera (Photometrics Quantix KAF, Roper Scientific, Tucson, AZ, USA). Cells were imaged with a 40 x oil immersion objective (Zeiss, Vienna, Austria or Plan Fluor 40 x oil objective, Nikon) with continuous perfusion in EB with or without stimulants. Excitation of the cameleon sensors was accomplished at 440 ± 10 nm (440AF21, Omega Optical, Brattleboro, USA), and emission was recorded at 480 nm and 535 nm using a beam splitter (Optical Insights, Visitron Systems). Excitation filters were adjusted through a filter-wheel (MAC 6000/5000, Ludl Electronic Products, Hawthorne, NY, USA). Fura-2 was measured at 340 and 380 nm excitation (340HT15, 380HT15, Omega Optical, Brattleborough, VT, USA) and 510 nm emission filters (510WB40, Omega Optical). MetaFluor 4.6r3 or VisiView 2.0.3 (Universal Imaging, Visitron Systems) were used for controlling both systems and for the acquisition of data. GraphPad Prism version 5.00 for Windows (GraphPad Software, San Diego, CA, USA) was used to analyze the acquired data.

2.4.4 Simultaneous measurement of cytosolic and mitochondrial Ca^{2+}

Our lab has recently developed a red – shifted mitochondrial cameleon sensor (4mtD1GO-Cam) for simultaneous measurement of free Ca^{2+} in the cytosol and mitochondrial in combination with Fura-2. For this purpose INS-1cells were transfected with 2 µg of 4mtD1GO-Cam (see section 2.3.2 for description transfection protocol) and used for the experiment after 48 hours. Cells were loaded with Fura-2 (see section 2.4.2 for Fura-2 loading protocol) for 30 minutes and proceeded for co-imaging of Ca^{2+} in both the cellular compartments. Till iMIC (Till Photonics Graefelfing, Germany), a digital wide field imaging system, was deployed to image the cells using a 40X objective (alpha Plan Fluar 406, Zeiss, Gottingen, Germany). Polychrome V (Till Photonics) which is an ultra fast switching monochromator was used for illumination of Fura-2 and the 4mtD1GO-Cam. Fura-2 was excited alternatively at 340 nm and 380 nm and the 4mtD1GO-Cam was excited at 477 nm. To avoid contamination of the emission channels with excitation light

the system was equipped with an excitation filter (E500spuv, Chroma Technology Corp, Rockingham Vermont, USA) including a dichroic filter (495dcxru). Emission light was simultaneously captured at 510 nm (fura-2 and GFP of GOCam) and at 560 nm (FRET-channel of GO-Cam) using a single beam splitter (Dichrotome, Till Photonics) that was provided with a dual band emission filter (59004m ET Fitc/Tritc Dual Emitter, Chroma Technology Corp) and a second dichroic filter (560dcxr, Chroma Technology Corp). The light path and spectra for the filters used for the co-imaging experiments are illustrated in Figure 2.3. CCD camera (AVT Stringray F145B, Allied Vision Technologies, Stadtroda, Germany) was used for capturing the images. For data acquisition and the control of the digital fluorescence microscope, live acquisition software version 2.0.0.12 (Till Photonics) was used.

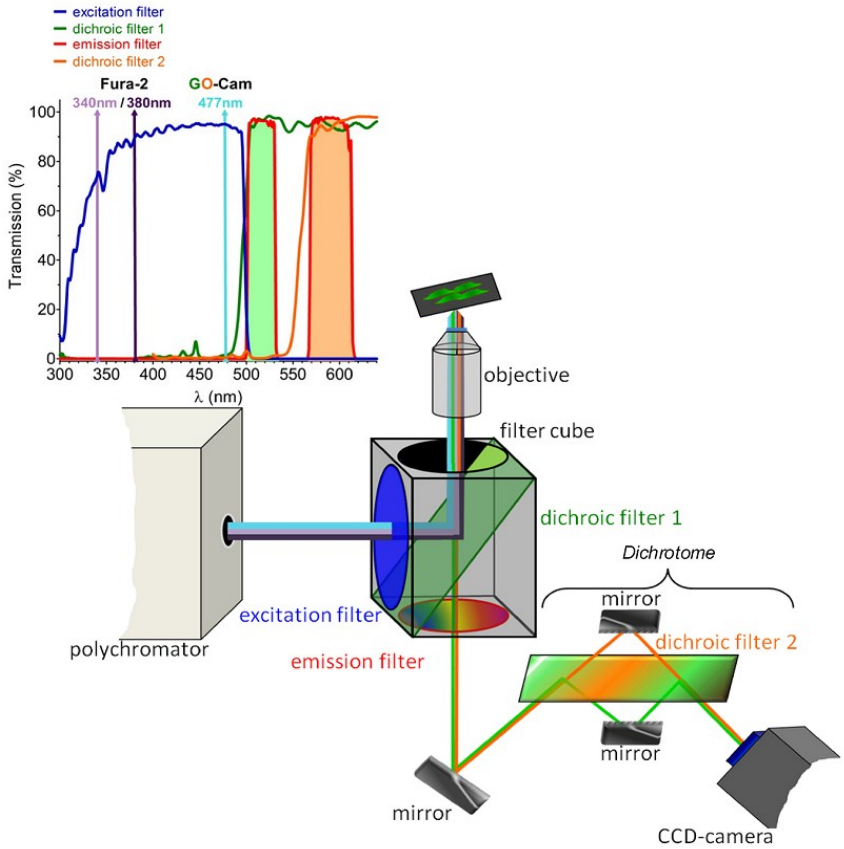

Figure 2.3: *Schematic representation of the Till iMIC imaging system showing the light paths of the excitation (violet = 340 nm, dark blue = 380 nm, and light blue 477 nm) and emission (green = 510 nM and orange = 560 nM). Optical filters used to simultaneously image fura-2 and the novel red-shifted cameleons are also illustrated (Adopted and modified from Waldeck-Weiermair et al. 2012)* (47).

2.5 Analysis of mitochondrial morphology

Mitochondrial structure was analyzed in hMICU1 – citrine or mtDsRed overexpressing INS-1 cells 48 hours after transfection. High resolution images of cells were taken with array confocal laser scanning microscope (Axio Observer.Z1 from Zeiss, Gottingen, Germany) equipped with 100X objective (Plan-Fluor x100/1.45 Oil, Zeiss), a motorized filter wheel (CSUX1FW, Yokogawa Electric Corporation, Tokyo, Japan) on the emission side, AOTF – based laser merge module for laser line 405, 445, 473, 488, 551, and 561 nm (Visitron Systems) and a Nipkow – based confocal scanning unit (CSU-X1, Yokogawa Electric corporation). hMICU1 - citrine and mtDsRed were excited with 488 and 551 laser lines respectively and emission was acquired with a charged CCD camera (CoolSNAP-HQ, Photometrics, Tucson, AZ, USA). The system was controlled with VisiView acquisition software (Visitron systems).

2.6 ATP measurement

Cytosolic ATP was measured using luciferase assay as using a cytosolic version of luciferase construct as described previously (15). INS-1 cells were seeded on white – walled 96-well microplates (PerkinElmer Inc., USA) and cotransfected with plasmid DNA encoding cytosolic Luciferase and respective siRNA. 48 hours after transfection the cells were pre-incubated in HBSS containing 0.2 % BSA and 3 mM glucose for 1 hour. The buffer was then replaced with HBSS containing 3 mM glucose and 1 mM beetle luciferin (Promega) and luminescence was measured on a VICTOR Mulitlabel Reader (PerkinElmer Inc., USA) at 37°C. Cells were stimulated with 16 mM glucose during the measurement.

2.7 Insulin measurement

INS1- cells were cultured in 6-well plates and transfected with respective siRNA at 70-80 % density using a protocol mentioned in 2.3.1. After 48 hours of transfection cells were washed with warm PBS and pre-incubated for 1 hour in HBSS – containing 0.2% BSA and 3 mM glucose at 37 °C gassed with 5 % CO2. Buffer was replenished with HBBS – containing 3mM glucose after another washing step and incubated for another 1 hour. An aliquot of supernatant was collected after 1 hour of incubation for basal insulin secretion. The buffer was then replaced with HBSS – containing 16 mM glucose and another sample was collected after 1 hour. These samples were centrifuged to remove any cells or debris and subjected to further analysis. For estimation of total insulin content cell lysis was performed with RIPA buffer – containing protease inhibitor cocktail and total protein was

quantified with Pierce BCA proteins assay kit (Thermo Fisher Scientific Inc. USA) for normalization of the results. Insulin content in the supernatant samples and cell lysate was determined by a sandwich enzyme linked immunosorbant assay kit (Mercodia, Sweden).

2.8 Molecular Biology Methods

2.8.1 Isolation of total cellular RNA

Total cellular RNA was isolated with a spin column – based RNA isolation kit (PEQLAB Biotechnologie GmbH, Erlangen, Germany) using a protocol provided by the manufacturer. Cells grown in 6-well plates were washed twice with PBS followed by a treatment with 300 µl of cell lysis buffer. The lysate was transferred to a DNA removing column and centrifuged at 12,000 g for 1 minute. The DNA binding column was discarded and the flow through was mixed with an equal volume of cold 70% ethanol. The solution was mixed well and transferred to a RNA binding column followed by a centrifugation step at 10,000 g for 1 minute. The flow through was discarded and the column was reinserted into a fresh collection tube. Two washing steps were performed with 500 µl and 600 µl of wash buffer 1 and wash buffer 2 respectively at a centrifugation speed of 10,000 g for 1 minute. After the second washing the empty column was centrifuge at 10,000 g for another 2 minutes to remove the traces of ethanol – containing wash buffer 2. RNA was eluted in 20 µl eppendorf tubes with 20 µl of nuclease – free water by centrifuging at 8000 g for 1 minute and stored at -70 ˚C until further processing.

2.8.2 cDNA synthesis

The concentration of RNA was estimated on a spectrophotometer (UviLine 9400, SCHOTT Instruments, Mainz, Germany) and 2 µg of RNA was reversed transcribed with a High Capacity cDNA Reverse Transcription Kit (Applied Biosystems) using a thermal cycler (PEQLAB Biotechnologie GmbH). The reverse transcription master mix recipe and thermal protocol are given in the box below. RNasin® Plus RNase inhibitor (Promega) was used to minimize any chances of RNA degradation.

Reverse Transcription Master Mix	
Components	**Volume/20 µl reaction**
2X RT buffer	2.0 µl
2X Random Primers	2.0 µl

100 mM dNTPs mix	0.8 µl
Reverse Transcriptase	1.0 µl
RNase inhibitor	1.0 µl
Nuclease-free H2O	3.2 µl
Thermal Protocol	
Step (Temperature)	**Time**
Step 1 (25 ˚C)	10 minutes
Step 2 (37 ˚C)	120 minutes
Step 3 (85 ˚C)	5 minutes
Step 4 (4 ˚C)	∞

2.8.3 Polymerase chain reaction

The polymerase chain reaction (PCR) was carried out from cDNA synthesized to detect the expression of target genes using a GoTaq® Green Master Mix. The recipe for PCR master is given in the box below. The same sets of primers were used to execute both conventional and real time PCR and their sequences are listed in the Table 1. A three step PCR cycling protocol was as follows: Initial denaturation at 95 ˚C for 5 minutes (1 cycle), cycling (40 times for 1 min each) at 95 ˚C, 60 ˚C and 72 ˚C and a final extension at 72 ˚C for 10 minutes (1cycle).

PCR Master Mix	
Components	**Volume/20 µl reaction**
2X GoTaq Master Mix	10.0 µl
Forward Primer (10 µM)	1.0 µl
Forward Primer (10 µM)	1.0 µl
Nuclease-free H2O	7.0 µl
cDNA	1 µl

2.8.4 Real Time PCR

Real time PCR is a very sophisticated and sensitive technique which is based on the use of fluorescent DNA-binding dyes and a thermal cycler equipped with a detection system usually a CCD camera or a photomultiplier tube. This allows the detection of the PCR

product during the run; hence the name real time PCR. This procedure is widely used for both relative and absolute quantification of mRNA in various types of samples. In this study the relative quantification of mRNA was performed with real rime PCR on a Light Cycler 480 (Roche Diagnostics, Vienna, Austria) using QuantiFast® SYBR Green PCR kit (Qiagen, Hilden, Germany). The reactions were performed in white 96 well plates which were sealed with transparent stickers to prevent any evaporation during the run. Rat GAPDH was used as a housekeeping gene to normalize well to well variation occurred during pipetting. The sequences of primers used for real time PCR are given in Table 1 and their efficiencies were assessed by running them with three different dilutions of a pooled cDNA sample. The recipe used to prepare real time master mix along with the cycling protocol is given in the box below. The threshold cycle values obtained from the real time data were analyzed to estimate the changes in the expression of target genes using Relative Expression Software Tool (Qiagen, Germany).

Real Time Master Mix	
Component	**Volume/10 µl reaction**
5X Master Mix	2.0 µl
Forward Primer (10 µM)	1.0 µl
Forward Primer (10 µM)	1.0 µl
Nuclease-free H2O	Variable
cDNA (10 – 50 x dilution)	1-3 µl
Thermal cycling protocol	
Step (Temperature)	**Time**
Heat activation at 95 ˚C	5 minutes
Two step cycling (40 cycles)	
Denaturation at 95 ˚C	10 seconds
Annealing and extension at 60 ˚C	30 seconds

2.8.5 Cloning of MICU1 and MCU

Human MICU1 and MCU were used for overexpression of these proteins in INS-1 cells due to their strong homology (>90%) with the rat counterparts. MICU1 and MCU were amplified using a human cDNA obtained from human umbilical vein endothelial derived cell line EA.hy926 cells using gene specific primers containing restriction sites as 5’

overhangs (see Table 1 for primers sequences and cutting sites). The amplified product was resolved on 1 % agarose gel and DNA was purified with a spin – column based gel extraction kit according to manufacturer's protocol. (Promega, Germany). The purified products were digested with appropriate restriction enzymes for 3 – 4 hours at 37 ˚C with a compatible buffer. The digested product was purified by agarose gel electrophoresis and a gel extraction kit and inserted into multiple cloning site of pcDNA 3.1 mammalian expression vector (Invitrogen, Austria). The purified product was ligated with the digested vector in a 3:1 ratio using a T4 DNA ligase (Promega, Germany or Fermenats, Germany (now Thermo Scientific, USA)). The ligation mixture was prepared according to the recipe in the box below and incubated in a thermal cycler at 22 ˚C overnight.

Ligation mixture	
Components	**Volume/20 µl reaction**
10X T4 DNA ligase buffer	2 µl
T4 DNA ligase	1-5 U
Vector DNA	100-200 ng
Insert DNA	Variable
Nuclease-free H2O	Make up to 20 µl

The ligated product was transformed into TOP10 chemically competent E. coli strain according to manufacturer's protocol (Invitrogen, Austria). Positive clones were selected by overnight culturing on Lauria Bertaini (LB) agar (Tryptophan: 10g + NaCl: 10g + yeast extract: 5g in 1 L. pH: 7-7.5) plates containing 100 µg/ml ampicillin. The colonies were handpicked and cultured in 2 ml of LB broth containing 100 µg/ml of ampicillin and placed in a shaking incubator at 37 ˚C overnight. Bacteria were harvested in the next morning and plasmid DNA was extracted with a spin column – based miniprep kit according to a protocol described by the manufacturer (Promega, Germany). To confirm the ligation and correct orientation of the insert plasmid DNA was digested with appropriate restriction enzymes and the product was separated on 1% agarose gel for detection of the positive clones. The bacterial culture from positive colonies were mixed with 20 % glycerol and stored at -70 ˚C for future use. For isolation of larger amounts of plasmid DNA bacteria were cultured in 200 ml of ampicillin – containing LB broth at 37 ˚C in a shaking incubator overnight. Plasmid DNA was isolated from 200 ml of culture

using PureYieldTM Plasmid Maxiprep System (Promega, Germany) as instructed in the product manual. The isolated plasmid DNA was quantified and stored at 4 ˚C for further use.

Table 2.1: *Sequences of primers*

Primers for Real Time PCR			
Name	Sequence (5'-3')	Tm (˚C)	Product (bp)
rat	AGATGGTGTTCGAGTTGCTG	60	138
rat	AGGGTCTCTGCGTTTTCATG	60	
mouse	TCGACCTAGAGAAATACAATCAGC	60	137
mouse	CACGGTCATCTCGGATCATTC	60	
rat	ACTAAGCGGAGACTGATGTTG	60	149
rat	GTCCTTGCTCTTCCCCTTATC	60	
mouse	TTGACTTGAATGGAGACGGAG	60	138
mouse	AACATAAGCCAGACTTGAGGG	60	
rat	TCCGCATTGGCCTCTACGACTCT	60	175
rat	TCGACAGTGCTCTGGTATCTCCGA	60	
rat	TCTTCCGTCTAGTACCCTTCC	60	142
rat	CTCCTTCTTCAGCCTTTCCTC	60	
rat	CTGGTGCTGAGTATGTCGTGGA	60	197
rat	AGTTGGTGGTGCAGGATGCATT	60	
Primers for cloning			
MCU_HindIII-F	GGAAGCTTAGTTGAGAGATGGCGGCCGCC		
MCU_EcoRI-R	GGGAATTCTCAATCTTTTTCACCAATTTGTCGGAG		
MICU1_BamHI-F	ACGGATCCACCATGTTTCGTCTGAACTCAC		
MICU1_EcoRI-R	ACGAATTCCTGTTTGGGTAAAGCGAAGTCC		

Table 2.2: *List of siRNAs.*

Name	**Sequence (5'-3')**	**Reference**
rat MICU1 Si-1	GUAAUGGAGUAUGAGAAUA	Self designed
rat MICU1 Si-2	CGAACCUGGUGAAACUGAA	Self designed

rat MCU Si-1	GCCAGAGACAGACAAUACU	Stefani D et al, 2011
rat MCU Si-2	AAAGTCTCGTTTCGACCTA	Self Designed
rat UCP2 Si	CGUAGUAAUGUUUGUCACC	Affourtit C et al, 2008
rat LETM1 Si	UCCACAUUUGAGACCCAGU	Self Designed
rat Control Si	AGGTAGTGTAATCGCCTTG	Self Designed

2.9 Bioinformatics Tools

Many online and computer based tools were used for different application during this study.

2.9.1 Primer designing

Primes were used in cloning and for performing conventional and real time PCR. For designing the primers for cloning purposes MS Dos – based software Primers Designer version 2.0 (Scientific and Educational Softwares) was used. This tool requires the loading of cDNA sequence in FASTA format included in a *.txt file and allows the insertion of overhangs at the 5' ends of the primers. This program also provides the opportunity to customize the default primer parameters for selecting the best possible primers pair.

For performing real time PCR, primers were designed with an online tool provided under the Scitools option on the website of Integrated DNA technologies and can be accessed by using following link (http://eu.idtdna.com/scitools/Applications/RealTimePCR/). In order to design the primers this program requires either the Genbank ID of the target gene or a full length sequence in FASTA format with information of intronic and exonic regions. It offers to customize all the primer parameters and designs the primers at exon – intron junctions.

2.9.2 siRNA designing

siRNAs can be efficiently used to transiently knockdown the genes of interest and it allows the measurement of knockdown effect at functional level within 48-96 hours. The structure and physical properties of a siRNA has to be good for efficient working in a mammalian system. The siRNA can either be obtained from already published studies or they can be designed by many online tools which offer free services for designing. For this study siRNAs were designed by a web – based tool provided on the website of Microsynth AG,

Switzerland and can be accessed with following link (http://www.microsynth.ch/de/10116/siRNA-%E2%80%94-Overview.html).

2.9.3 Genbank Database

The mRNA sequences for designing the primers and siRNA were obtained from the Genbank database of National Centre for Biotechnology Information (NCBI) and it was accessed by the web address www.ncbi.nlm.nih.gov.

2.9.4 Sequence alignment

Homologies between different genes were investigated using an online tool ClustalW2 using the option of pairwise sequence alignment. This web – based alignment tool is available at the following link.

http://www.ebi.ac.uk/Tools/psa/emboss_needle/nucleotide.html

2.9.5 Basic Local Alignment Search Tool (BLAST)

In order to compare the short and long sequences with the genes and proteins databases of different organisms, nucleotide and protein BLAST were used. It can be accessed from the NCBI websites using the following link.

http://blast.ncbi.nlm.nih.gov/

3. RESULTS

3.1 Characterization of Ca^{2+} signals in INS-1 cells

INS-1 832/13 (INS-1) cells are of neuroendocrine origin which allows Ca^{2+} mobilization by two pathways in these cells, i) IP_3 – mediated Ca^{2+} release from ER and/or ii) depolarization – induced Ca^{2+} influx from extracellular medium. The consequential cytosolic Ca^{2+} transients are rapidly relayed to mitochondria. In this work a FRET – based genetic sensor (4mtD3cpv) has been employed for Ca^{2+} measurements in INS-1 cells. Although this is a quite bulky sensor yet it demonstrated a very good transfection rate (~60 %) with only a small proportion of cells showing mistargeting after 48 hours of transfection. Figure 3.1 illustrates three INS-1 cells with correct targeting of 4mtD3cpv to mitochondria.

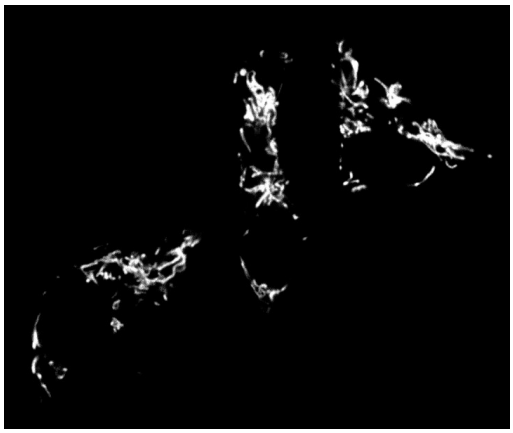

Figure 3.1: *A grayscale high resolution image of INS-1 cells transiently transfected with a plasmid DNA encoding 4mtD3cpv. 48 hours after transfection cells were imaged with an array confocal laser scanning microscope using a 100X objective.*

3.1.1 IP_3 – generating agonists and depolarization evoked rapid mitochondrial Ca^{2+} transients

The stimulation of INS-1 cells with a mixture IP_3 – generating agonist i.e. carbachol (100 μM) and ATP (200 μM) (Cch+ATP) resulted in a fast rise in mitochondrial Ca^{2+} ($[Ca^{2+}]_{mito}$). (Figure 3.2a). A short pulse of 30 mM KCl also evoked a similar response in the mitochondria which confirmed the presence of L-type VGCC channels in these cells (Figure 3.2c). In order to confirm the accurate targeting of 4mtD3cpv mitochondrial Ca^{2+}

was measured in the presence of a mixture of oligomycin (2 µM) and antimycin (10 µM), which inhibit the ATP synthase and complex III respectively. These drugs depolarize the mitochondria and block the energy – dependent Ca^{2+} uptake (124). A reduction of more than 80% was observed in mitochondrial Ca^{2+} uptake in the presence of oligomycin and antimycin (O+A). The matrix Ca^{2+} sequestration was abolished both upon stimulation of cells with Cch+ATP (Figure 3.2 a & b) and 30 mM KCl (Figure 3.2 c & d). This data verifies the use of 4mtD3cpv for estimation of mitochondrial Ca^{2+} in INS-1 cells.

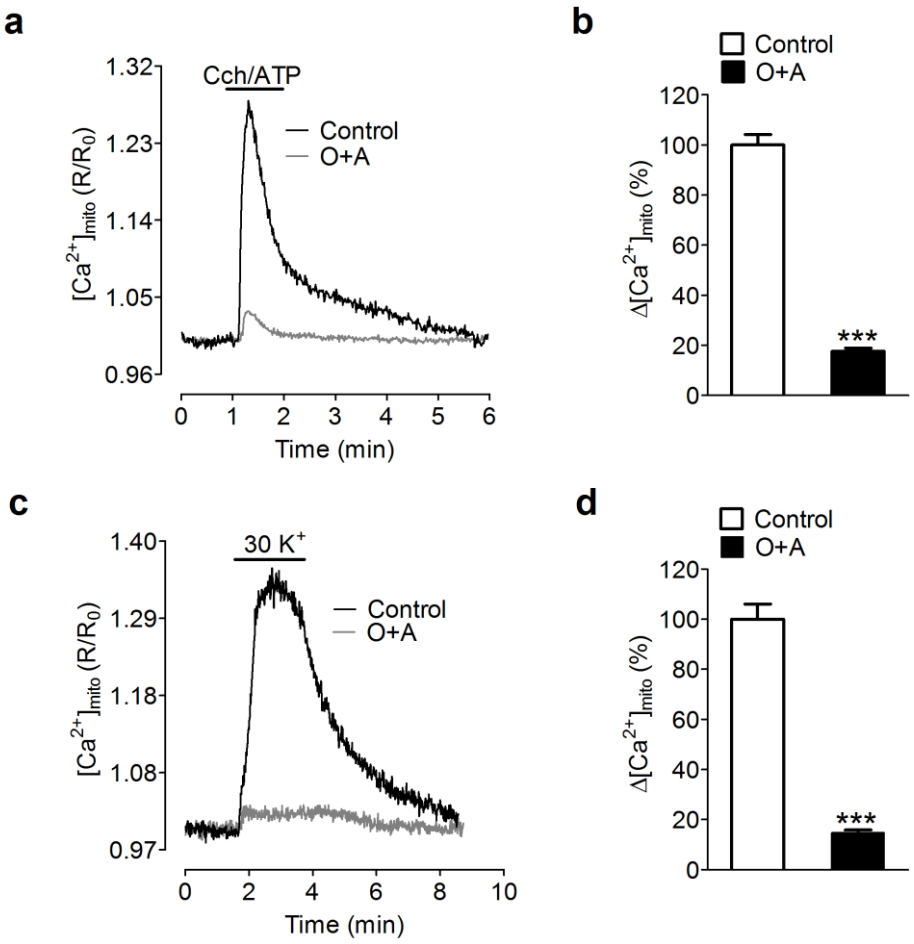

Figure 3.2: *Mitochondrial* Ca^{2+} *was measured in INS-1 cells 48 hours after transfection with 4mtD3cpv. a & c) Average curves representing* $[Ca^{2+}]_{mito}$ *(corrected ratios) upon stimulation with* Cch+*ATP and 30 mM KCl (*$30K^{+}$*) respectively. Black and gray curves represent cells treated with and without a mixture of oligomycin (2 µM) and antimycin (10 µM) (O+A) respectively. b & d)* $[Ca^{2+}]_{mito}$ *amplitude in control and O+A treated cells upon stimulation with* Cch+*ATP (n=3) and* $30K^{+}$ *(n=3). Columns indicate* $\Delta[Ca^{2+}]_{mito}$ *as a percentage of control and is represented as mean ± sem. (***P<0.0001)*

3.1.2 Simultaneous measurement of mitochondrial and cytosolic Ca^{2+} reveals important clues about the kinetics of Ca^{2+} transport in INS-1 cells

The recent development of a red – shifted mitochondrial Ca^{2+} sensor (4mtD1GO-Cam) provided us an opportunity to explore the kinetics of Ca^{2+} transients in cytosol and mitochondria of individual INS-1 cells. This was achieved by simultaneous measurement of $[Ca^{2+}]_{mito}$ and cytosolic Ca^{2+} ($[Ca^{2+}]_{cyto}$) within individual cells using a combination of 4mtD1GO-Cam (Figure 3.3) and Fura-2 probes.

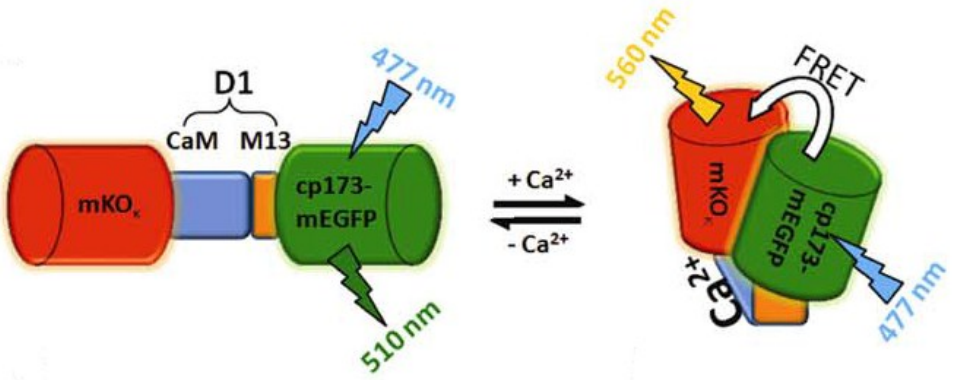

Figure 3.3: *A schematic model of 4mtD1GO-Cam without 4mt signal sequence. This is composed of a* Ca^{2+} *- binding peptide from calmodulin (CaM) and myosin light chain kinase (M13) At the flanks it contains an orange fluorescent protein (mKOK) and a circularly permutated green fluorescent protein (cp173-mEGFP) at the N- and C- termini respectively. The binding of* Ca^{2+} *brings the two fluorophores in close vicinity increasing the FRET signal. The excitation and emission wavelengths are shown as flash symbols. (Adopted and modified from Waldeck-Weiermair et al. 2012)*

3.1.3 Spatiotemporal correlation of $[Ca^{2+}]_{mito}$ and $[Ca^{2+}]_{cyto}$ in INS-1 cells upon activation of VGCCs

The simultaneous measurement of Ca^{2+} was performed after Fura-2 loading 4mtD1GO-Cam expressing cells. The stimulation of cells with 130 mM KCl – containing buffer ($130K^{+}$) evoked a fast cytosolic Ca^{2+} transient in the cytosol which was relayed to mitochondria with a slight delay in the uptake (Figure 3.4a). Although the slope of Ca^{2+} elevation both in cytosol and mitochondria were approximately similar (Figure 3.4b) the rate of Ca^{2+} extrusion was much faster in the cytosol (Figure 3.4a). Moreover the onset of

mitochondrial Ca^{2+} uptake was significantly slower in cells stimulated with $30K^+$ (5.17 ± 0.47) as compared to $130K^+$ (1.45 ± 0.22) (Figure 3.4c).

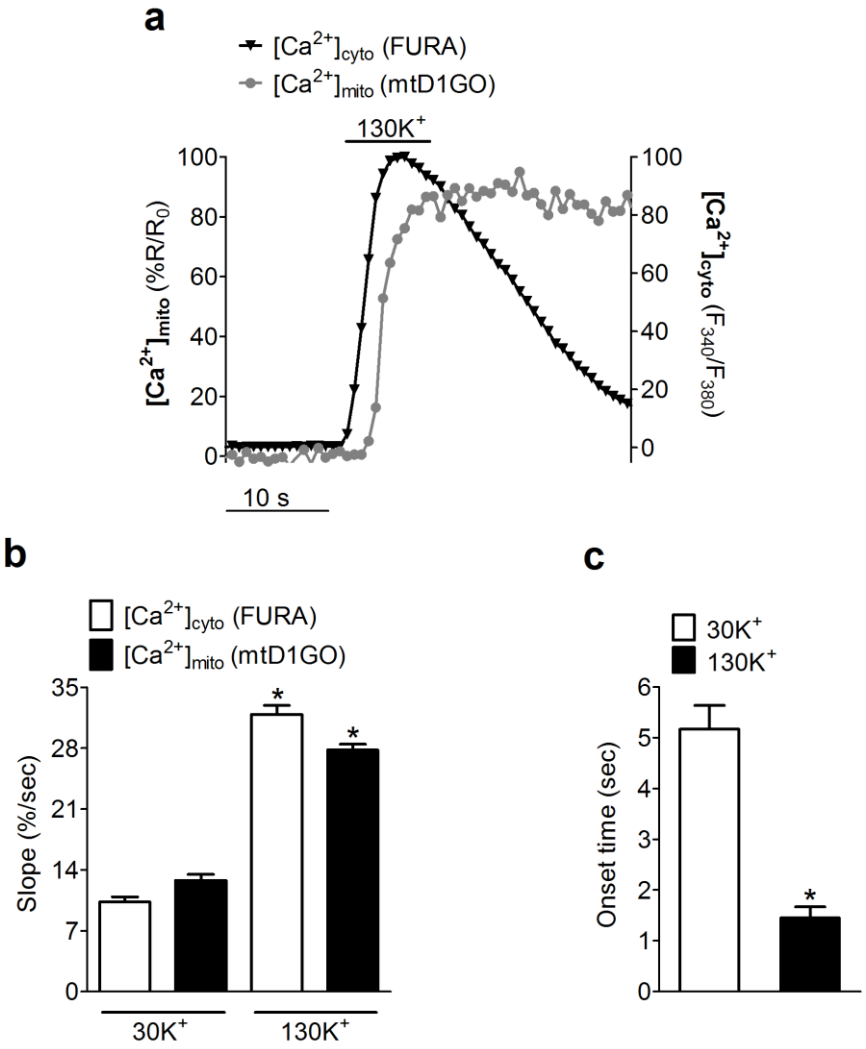

Figure 3.4: *The simultaneous measurement* $[Ca^{2+}]_{mito}$ *and* $[Ca^{2+}]_{cyto}$ *in fura-2 loaded 4mtD1GO-Cam expressing cells INS-1 cell. a) Cells were stimulated with 130 mM KC (*$130K^+$*) (or 30 mM KCl in Figure 3.4b & c) in the presence of extracellular* Ca^{2+}*. Curves represent traces of one cell and are expressed as percentage of maximum* Ca^{2+} *response. b) Slope of mitochondrial and cytosolic* Ca^{2+} *calculated from the percentage curves and expressed as %/second upon stimulation with* $130K^+$ *(n=21 cells) and* $30K^+$ *(n=32 cells). c) Analysis of time delay between mitochondrial and cytosolic* Ca^{2+} *response onset. (*$P<0.05$ *vs* $30K^+$*).*

3.1.4 Repetitive stimulation of VGCCs displays a Ca^{2+} - dependent desensitization of mitochondrial Ca^{2+} uptake

The repetitive stimulation of cells with 130 mM KCl resulted in cytosolic Ca^{2+} transients with every consecutive peak smaller than the previous one. The basal Ca^{2+} in the cytosol also remained high after first stimulation. However all the cytosolic Ca^{2+} transients did not evoked a corresponding mitochondrial Ca^{2+} response showing an inactivation of the mitochondrial uptake mechanism (Figure 3.5a). Moreover, the mitochondria were only able to start sequestrating Ca^{2+} again when they were allowed to recover from the first Ca^{2+} impulse (Figure 3.5b).

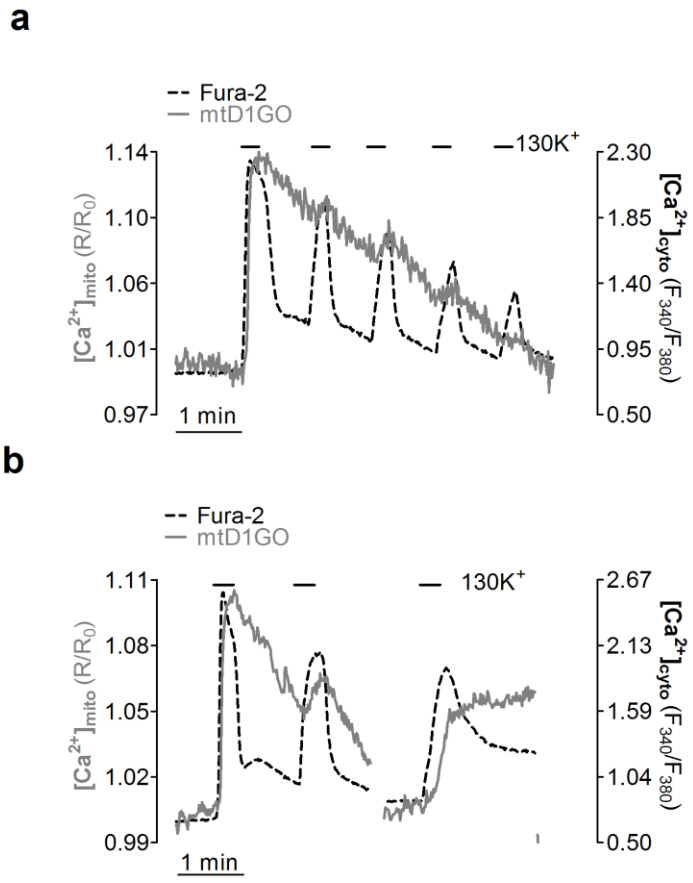

Figure 3.5: *Measurement of* $[Ca^{2+}]_{mito}$ *and* $[Ca^{2+}]_{cyto}$ *in Fura-2 loaded 4mtD1GO-cam expressing cells. The cells were repetitively stimulated with 130 mM KCl (*$130K^{+}$*) in the presence of extracellular* Ca^{2+}*. a) Representative curves from a cells showing mitochondrial (gray solid line) and cytosolic (black dotted line)* Ca^{2+} *transients. a) Traces of cells treated with two pulses of* $130K^{+}$ *followed by a third stimulation after the recovery time.*

3.2 Expression of MICU1, MCU, LETM1 and UCP2 in INS-1 cells

Before continuing with the functional experiments we investigated the expression of MICU1, MCU, LETM1 and UCP2 in INS-1 cells using a gene specific reverse transcriptase PCR. The expression of UCP2 has already been demonstrated in this cell line but there is not data about the other three candidate gene. Figure 3.6a represents an inverted agarose gel image showing the expression of these genes at mRNA level in INS-1 cells. In addition to INS-1 cells MICU1 and MCU mRNA were also detected in freshly isolated mice pancreatic islets using a similar protocol for cDNA synthesis and PCR (Figure 3.6b).

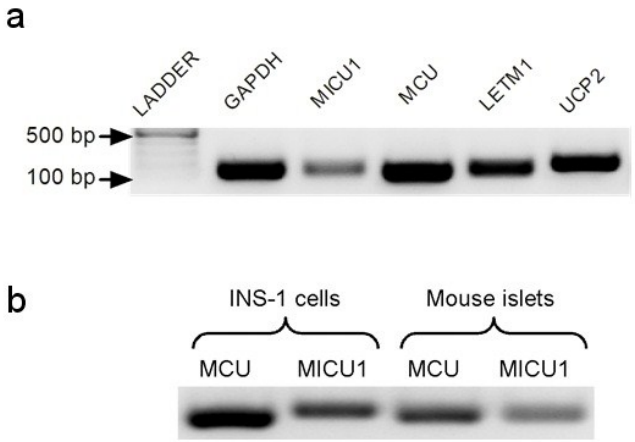

Figure 3.6: *Gene specific reverse transcriptase PCR was performed by using a cDNA synthesis kit followed by an amplification of the target cDNAs with a pair of gene-specific primers (see material and methods for primer sequences). GAPDH was amplified to control the quality of whole procedure and was used as a housekeeping gene. Amplified PCR products were electrophoretically detected on 1 % agarose gel using a 100 bp DNA ladder. b) Similar protocol was followed to detect the expression of MCU and MICU1 in freshly isolated mouse pancreatic islets (see materials and methods for mouse pancreatic islet isolation).*

3.3 Silencing of target genes and validation of siRNA efficiency

Gain or loss of the function of a gene is an excellent approach which can be employed to identify the role of unknown proteins. In this study a siRNA – mediated strategy was used to knockdown the mRNA level of candidate genes. The efficiency of each siRNA was validated by evaluating the expression levels of MICU1, MCU, LETM1 and UCP2 in cells

treated with mRNA - specific siRNA and control scrambled siRNA. Each siRNA (MCU, UCP2 and LETM1) or a combination of two siRNAs (MICU1) could significantly reduce the mRNA levels (Figure 3.7).

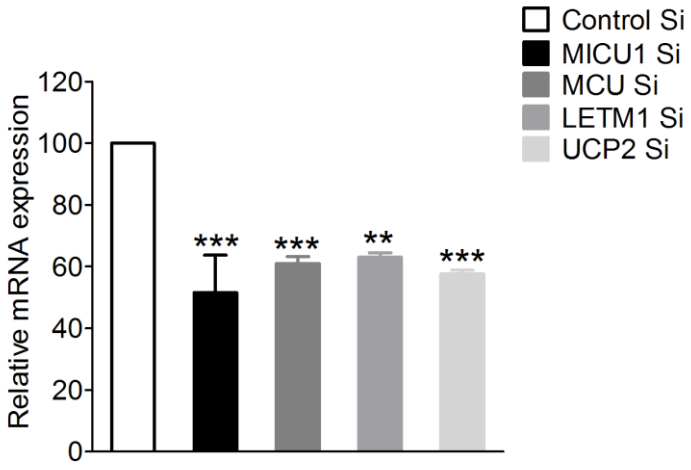

Figure 3.7: *The efficiency of siRNA-induced knockdown was investigated by quantitative real time PCR. Total RNA was isolated 48-72 hours after transfection of cells with siRNA against MICU1 (n=3), MCU (n=4), LETM1 (n=4) and UCP2 (n=4). Ct values obtained from real time data were converted into fold expression change and represented as percentage of respective controls. GAPDH was used as a housekeeping gene. The columns represent mean ± sem. (***P<0.001, **P<0.01 versus respective controls).*

3.4 Contribution of MICU1 and MCU to mitochondrial Ca^{2+} uptake in INS-1 cells

In order to investigate a possible role of MICU1 and MCU in mitochondrial Ca^{2+} uptake, cells transiently transfected with respective siRNAs and 4mtD3cpv were treated with the different Ca^{2+} mobilizing agents to elevate the cytosolic Ca^{2+} which led to a subsequent entry into mitochondria.

3.4.1 Silencing of MICU1 and MCU diminished IP_3 – induced mitochondrial Ca^{2+} uptake

The mobilization of Ca^{2+} stores by IP_3 – generating agonists (Cch+ATP) resulted in a fast increase in $[Ca^{2+}]_{mito}$ and this response was significantly diminished in cells with transient knockdown of MICU1 and MCU (Figure 3.8a & b). Peak $[Ca^{2+}]_{mito}$ amplitude was reduced to 58.5 ± 6.94 % and 67.8 ± 6.5 % in cells transfected with MICU1 and MCU siRNA respectively (Figure 3.8c & d). However there was a slight variation in reduction of

mitochondrial Ca^{2+} peak response among experiments due to slight day to day variation in silencing effect of MICU1 and MCU siRNAs (see section 3.4.4). This data confirm the involvement of both of these proteins in $[Ca^{2+}]_{mito}$ handling upon IP_3 – induced stimulation of INS-1 cells.

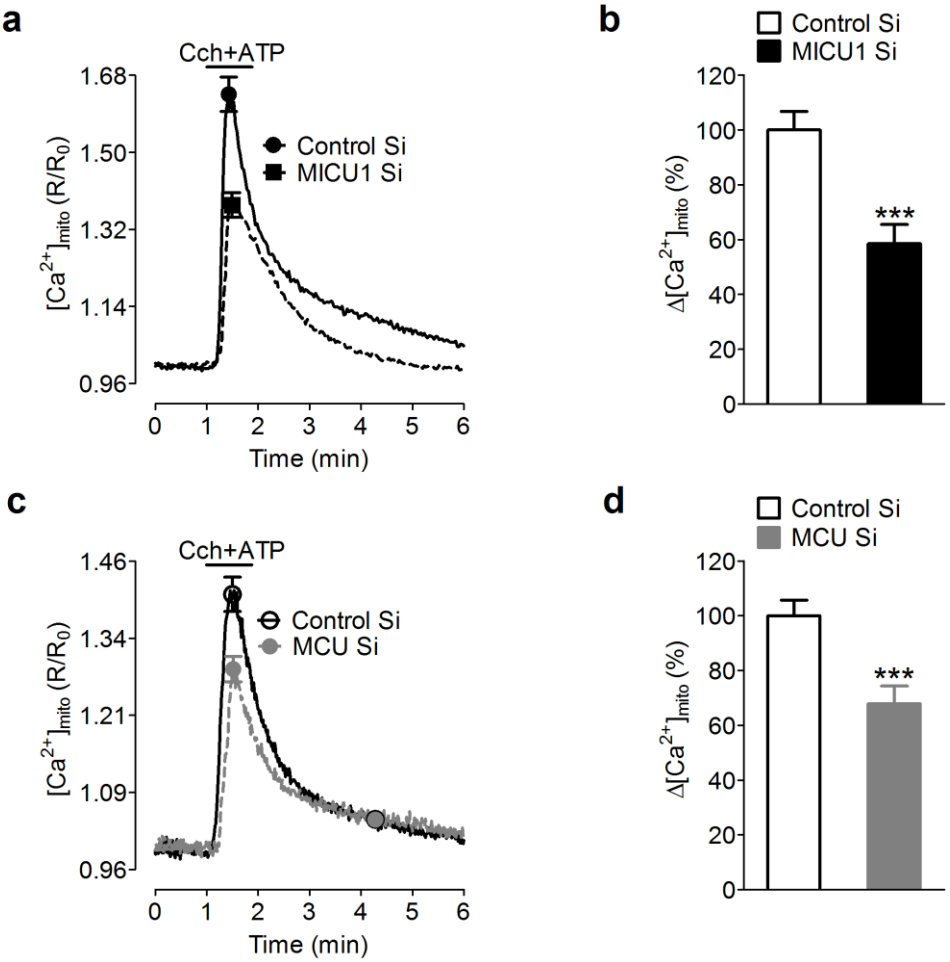

Figure 3.8: *$[Ca^{2+}]_{mito}$ measurement in MICU1 and MCU silenced cells. a & c) Average curves representing mitochondrial Ca^{2+} response (corrected ratios) upon stimulation with Cch+ATP (100+200 µM) in a Ca^{2+} - free experimental buffer. Black solid lines indicate cells treated with control siRNA while black and gray dotted lines represent cells transfected with MICU1 and MCU siRNA respectively. b & d) Peak $[Ca^{2+}]_{mito}$ amplitude in MICU1 (black column; n=9) and MCU (gray column; n=9) silenced cells represented as percentage of respective controls (white columns, n=9 for a & b). Data is shown as mean ± sem. (***P<0.0001 vs respective control)*

3.4.2 Direct depolarization - induced $[Ca^{2+}]_{mito}$ elevation was impaired upon silencing of MICU1 and MCU

In the next step connection of MICU1 and MCU with depolarization – induced mitochondrial Ca^{2+} sequestration was investigated. Direct depolarization of INS-1 cells with 30 mM KCl triggered a rapid influx of Ca^{2+} from the extracellular space with ensuing mitochondrial Ca^{2+} uptake (Figure 3.9 a & b) (also see data from simultaneous Ca^{2+} measurements) This protocol allows to measure the sequestration of Ca^{2+} by mitochondria upon its entry from outside the cell via VGCCs. A transient knockdown of MICU1 and MCU significantly reduced the import of Ca^{2+} into mitochondrial matrix providing a convincing evidence for the participation of these proteins in mitochondrial Ca^{2+} uptake upon a VGCC – mediated Ca^{2+} influx as a result of direct plasma membrane depolarization with KCl. In comparison to respective control cells the peak $[Ca^{2+}]_{mito}$ amplitude went down to 59.2 ± 4.2 % and 69.5 ± 4.57 % in cells with a suppression of MICU1 and MCU mRNA respectively (Figure 3.9c & d).

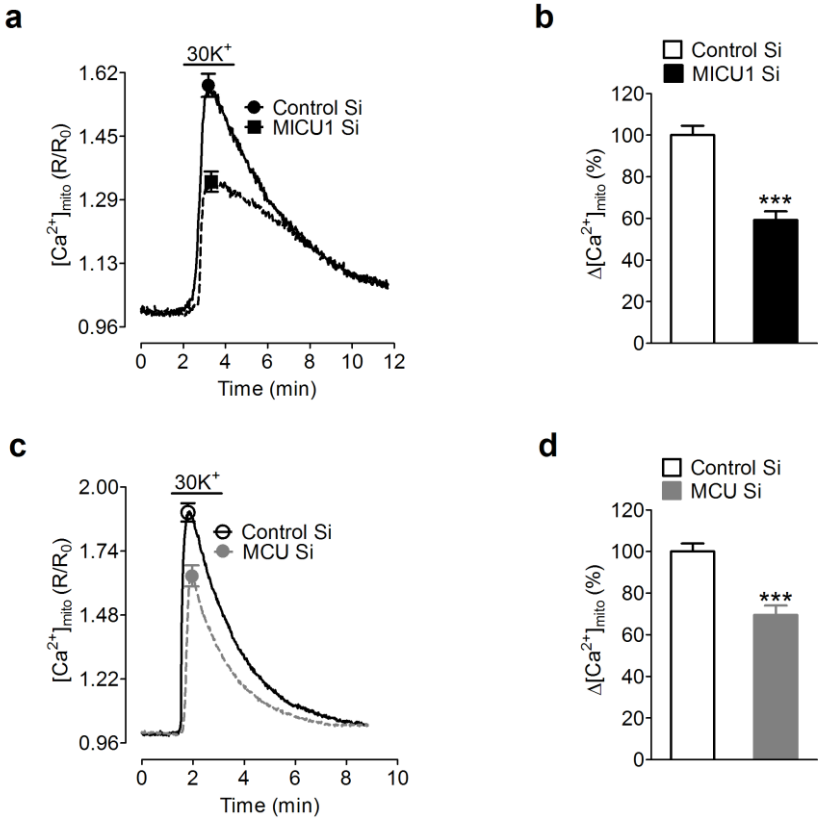

Figure 3.9: *$[Ca^{2+}]_{mito}$ estimation in MICU1 and MCU silenced cells upon plasma membrane depolarization with 30 mM KCl ($30K^+$) a & c) Average curves representing*

*$[Ca^{2+}]_{mito}$ response (corrected ratio) upon stimulation with $30K^{+}$ in the presence of extracellular Ca^{2+}. Black solid lines indicate cell treated with control siRNA while black and gray dotted lines represent cells transfected with MICU1 and MCU siRNA respectively. b & d) Peak $[Ca^{2+}]_{mito}$ amplitude in MICU1 (black column; n=9) and MCU (gray column; n=9) silenced cells represented as percentage of respective controls (white columns, n=9 for b & d). Data is shown as mean ± sem. (***P<0.0001 vs respective control)*

3.4.3 Influence of MICU1 and MCU knockdown on cytosolic Ca^{2+} signals

The reduction of mitochondrial Ca^{2+} uptake upon Ca^{2+} release from ER or Ca^{2+} influx via VGCCs can also be a consequence of reduced $[Ca^{2+}]_{cyto}$. In order to rule out this possibility a further set of experiments were carried out to measure $[Ca^{2+}]_{cyto}$ using a cytosolic Ca^{2+} i.e. D3cpv in MICU1 and MCU silenced cells. We merged two methods of Ca^{2+} mobilization into one protocol. Both plasma 30 0M KCl – mediated membrane depolarization and stimulation with Cch+ATP triggered fast cytosolic Ca^{2+} transients (Figure 3.10a & b) which were not affected by suppression of MICU1 and MCU mRNA levels.

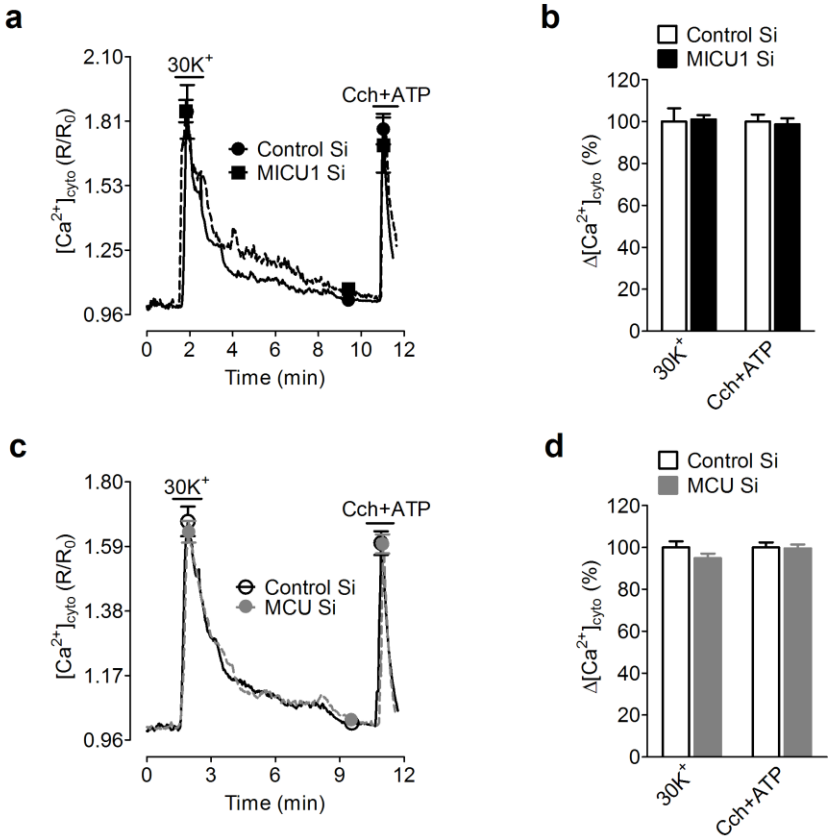

Figure 3.10: *Measurement of IP_3 - or depolarization – induced $[Ca^{2+}]_{cyto}$ rises in MICU1 and MCU silenced cells. $[Ca^{2+}]_{cyto}$ was measured in cells transiently transfected with D3cpv and respective siRNAs 48 or 72 hours after transfection. Cells were first treated with 30 mM KCl ($30K^+$) during perfusion (in the presence of extracellular Ca^{2+}) to activate VGCC – mediated Ca^{2+} influx which was followed by a wash-out and a subsequent stimulation with Cch+ATP (100+200 µm) in a Ca^{2+} - free buffer. a & c) Average curves representing $[Ca^{2+}]_{cyto}$ responses (corrected ratios) upon depolarization of cells with $30K^+$ or upon stimulation with Cch+ATP. b & d) Peak $[Ca^{2+}]_{cyto}$ amplitudes shown as percentage of control cells (white columns; n=3 (b), n=9 (d)) with knockdown of MICU1 (black columns; n=3), MCU (gray columns; n=9). Data is represented as mean ± sem.*

3.4.4 Simultaneous knockdown of MICU1 and MCU did not have any additional effect on $[Ca^{2+}]_{mito}$

MICU1 and MCU can be components of two independent mitochondrial Ca^{2+} uptake pathways and in such a scenario simultaneous knockdown of both MICU1 and MCU should be able to create an additional impeding effect on $[Ca^{2+}]_{mito}$. To explore this possibility $[Ca^{2+}]_{mito}$ was measured in INS-1 cells transiently transfected either with MICU1 and MCU siRNAs alone or with a combination of both. (Figure 3.11). Although silencing of MICU1 and MCU alone was able to diminish $[Ca^{2+}]_{mito}$ upon Ca^{2+} mobilization both with Cch+ATP (Figure 3.11a & b) and direct depolarization (Figure 3.11c & d), a combination of both siRNAs did not produce a significant additional inhibitory effect on mitochondrial Ca^{2+} sequestration (Figure 3.11c & d dotted columns).

Figure 3.11: *Measurement of IP_3 – or direct depolarization – induced $[Ca^{2+}]_{mito}$ in INS-1 cells with a combined knockdown of MICU1 and MCU. a & c) Average curves showing an increase in $[Ca^{2+}]_{mito}$ (correct ratios) upon stimulation of cells with Cch+ATP or 30 mM KCl ($30K^+$) respectively. b & d) Peak $[Ca^{2+}]_{mito}$ amplitude of each group represented as percentage of control. Silencing of MICU1 (black columns) and MCU (gray columns) diminished $[Ca^{2+}]_{mito}$ without having a considerable additional effect upon simultaneous knock-down of both proteins (dotted columns) in cells stimulated with Cch+ATP (n=6, ***P<0.001) or $30K^+$ (n=9, ***P<0.001) respectively. Data is represented as mean ± sem.*

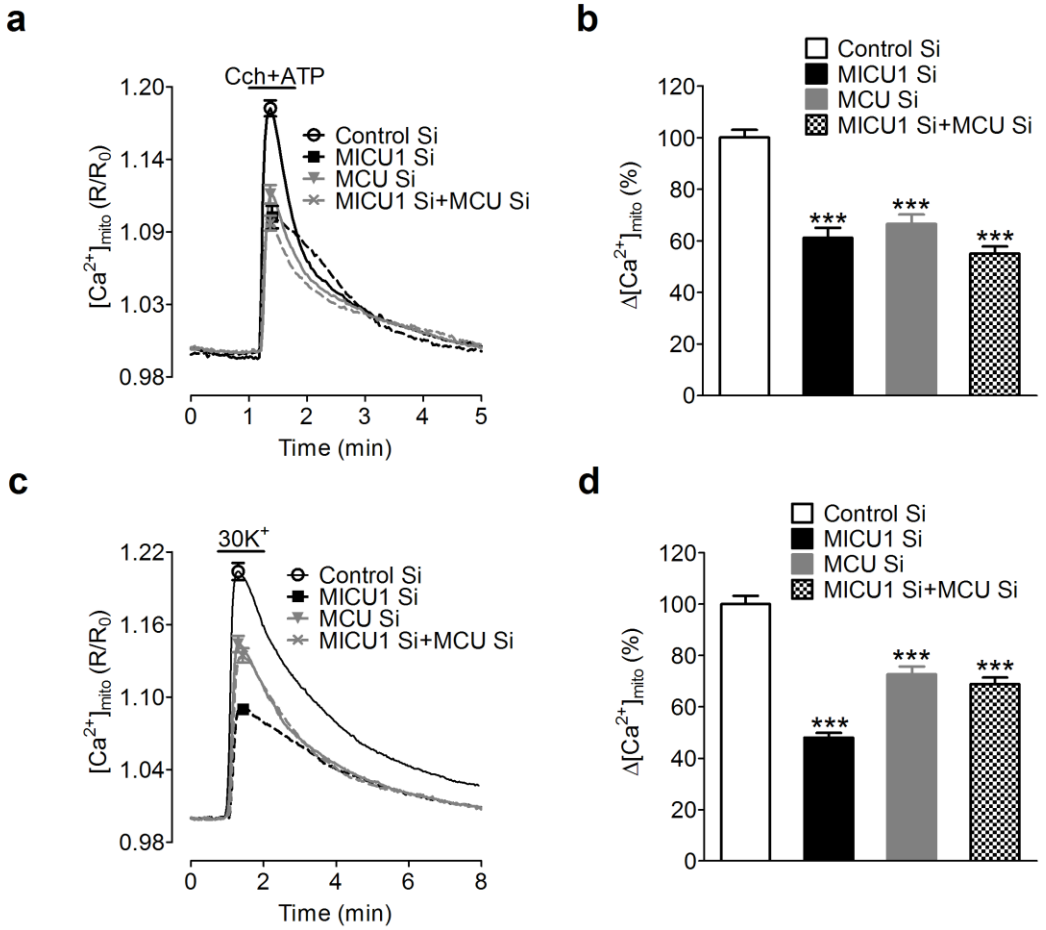

3.4.5 Inhibitory effect of MCU silencing on $[Ca^{2+}]_{mito}$ could be rescued by expression of human MCU

To further confirm the involvement of MCU in mitochondrial Ca^{2+} uptake we demonstrated a rescue of the inhibitory phonotype of MCU silencing. For this purpose human MCU, which is > 95 % homologous to rat MCU at proteins level (Figure 3.12a), was cloned and co-expressed with MCU siRNAs – 2. Rat MCU siRNA used in the previous experiments was not used here due to its homology with human MCU cDNA. Upon stimulation of cells with IP_3 – generating agonists there was fast uptake of Ca^{2+} by control cells and this response was diminished in cells transfected with MCU siRNA-2 which showed a small but significant effect on $[Ca^{2+}]_{mito}$. The inhibitory effect of mitochondrial Ca^{2+} sequestration was rescued (14.5 % increase) in cells overexpressing MCU siRNA-2 and human MCU cDNA (Figure 3.12b & c).

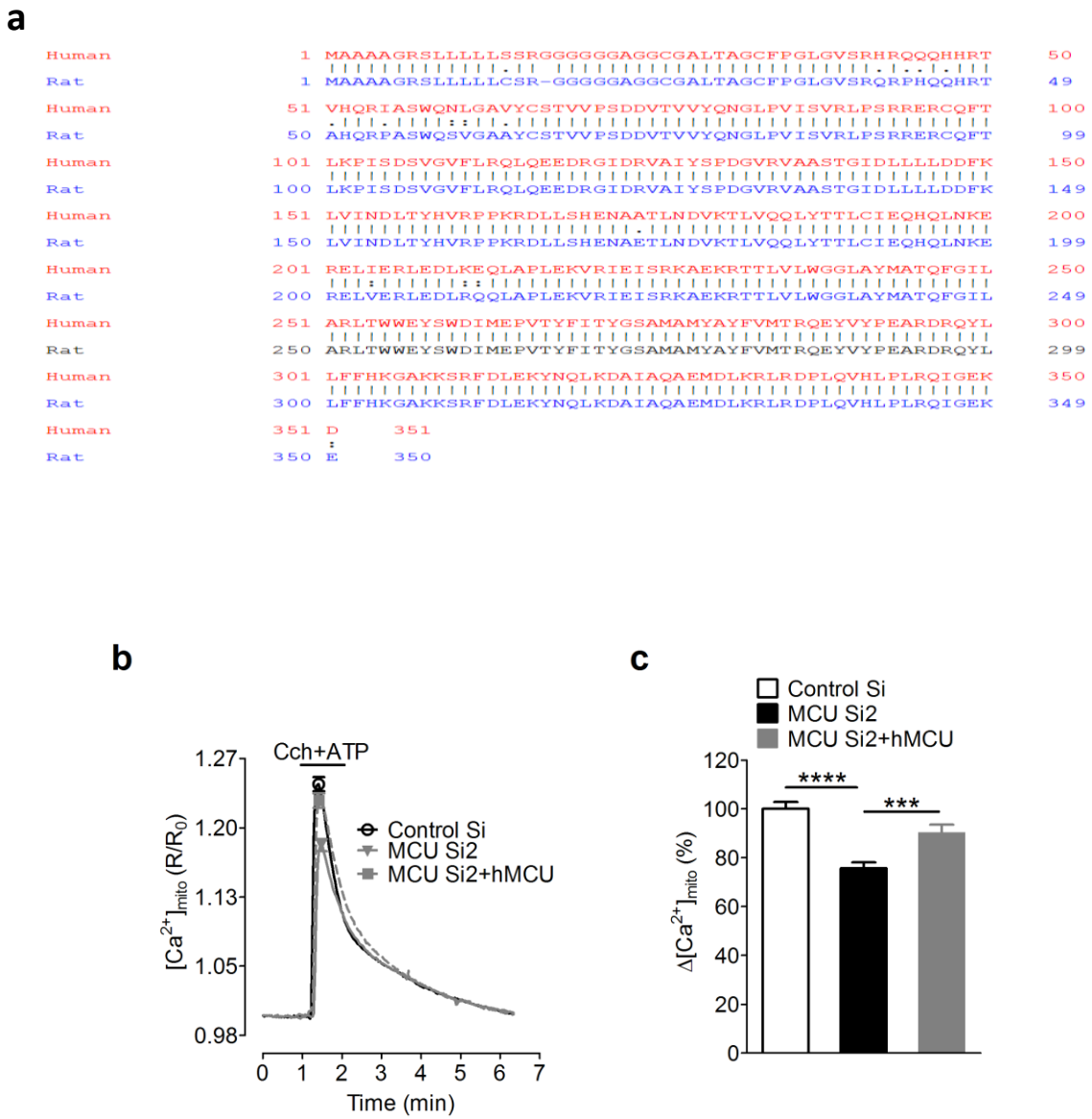

Figure 3.12: *Rescue of mitochondrial* Ca^{2+} *uptake in MCU silenced INS-1 cells with expression of human MCU. a) A pariwise amino acid alignment of human and rat MCU proteins. b) Average curves showing an increase in* $[Ca^{2+}]_{mito}$ *(corrected ratios) upon stimulation of cells with Cch+ATP. c) Peak* $[Ca^{2+}]_{mito}$ *amplitude of each group represented as percentage of control. Silencing of MCU (black column; n=6) reduced* $[Ca^{2+}]_{mito}$ *while expression of hMCU in MCU – silenced cells (gray column; n=6) could rescue this effect. Data is shown as mean ± sem. (****P<0.0001 vs control, ***P<0.001 vs MCU Si2).*

3.4.6 Human MICU1 expression in MICU1 – silenced INS-1 cells produced no considerable rescuing effect on $[Ca^{2+}]_{mito}$.

Similar to mitochondrial Ca^{2+} rescue effect of human MCU expression (>90 % homologous with rat MCU) further experiments were performed to investigate whether human MICU1 (hMICU1) expression in MICU1 silenced cells can yield the same results. Contrary to our expectations, while knockdown of rat MICU1 resulted in strong reduction in $[Ca^{2+}]_{mito}$ upon stimulation of cells with IP_3 – generating agonists, hMICU1 could not rescue $[Ca^{2+}]_{mito}$ when co-expressed with MICU1 siRNA (Figure 3.13a & b). Instead hMICU1 expression resulted in a further diminution of $[Ca^{2+}]_{mito}$ upon stimulation with Cch+ATP (Figure 3.13b gray column).

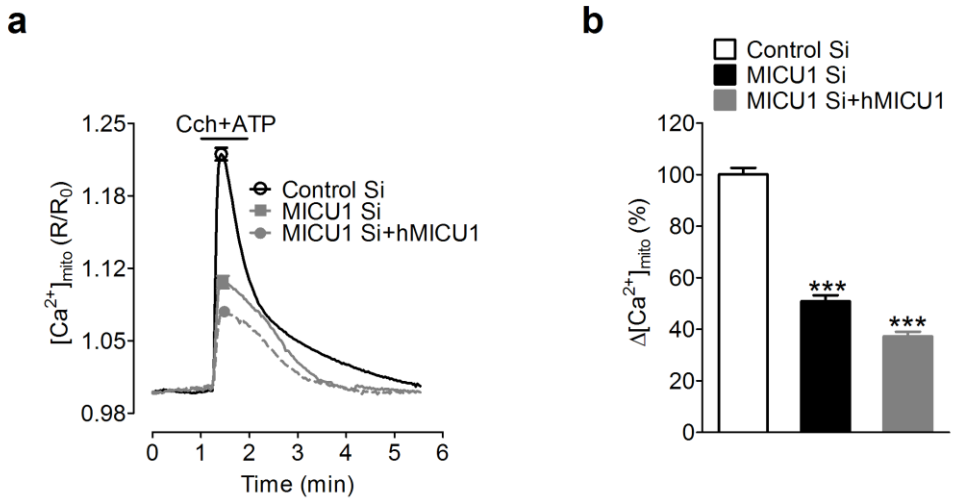

Figure 3.13: hMICU1 co-expression with MICU1 siRNA did not improve mitochondrial Ca^{2+} uptake. a) Average curves showing an increase in $[Ca^{2+}]_{mito}$ (corrected ratios) upon stimulation of cells with Cch+ATP. b) Peak $[Ca^{2+}]_{mito}$ amplitude of each group represented as percentage of control. Silencing of MICU1 (black column; n=9) significantly reduced $[Ca^{2+}]_{mito}$ while expression of hMICU1 in MICU1 - silenced cells (gray column; n=9) could not increase the inhibitory effect of siRNA. Data is shown as mean ± sem. (***P<0.001 vs control).

3.4.7 Human MICU1 expression yielded mitochondrial structural changes

As hMICU1 expression in MICU1 knockdown INS-1 cells could not rescue $[Ca^{2+}]_{mito}$, therefore the influence hMICU1 expression alone was further explored on the structure of mitochondria. In order to perform these experiments hMICU1 was cloned in pcDNA3.1

vector with citrin fluorescent protein at its 3' end. hMICU1 – citrine construct was expressed in INS-1 cells and mitochondrial morphology was analyzed from the confocal high resolution images. The cells were counted and divided into four different groups based on the morphology of mitochondria (Figure 3.14a). In comparison to mtDsRed – expressing control group, the percentage of cells containing mitochondrial in the form of short network and fragmented dots was significantly increased with a considerable reduction in cells having nicely distributed network in hMICU1-citrine group (Figure 3.14b).

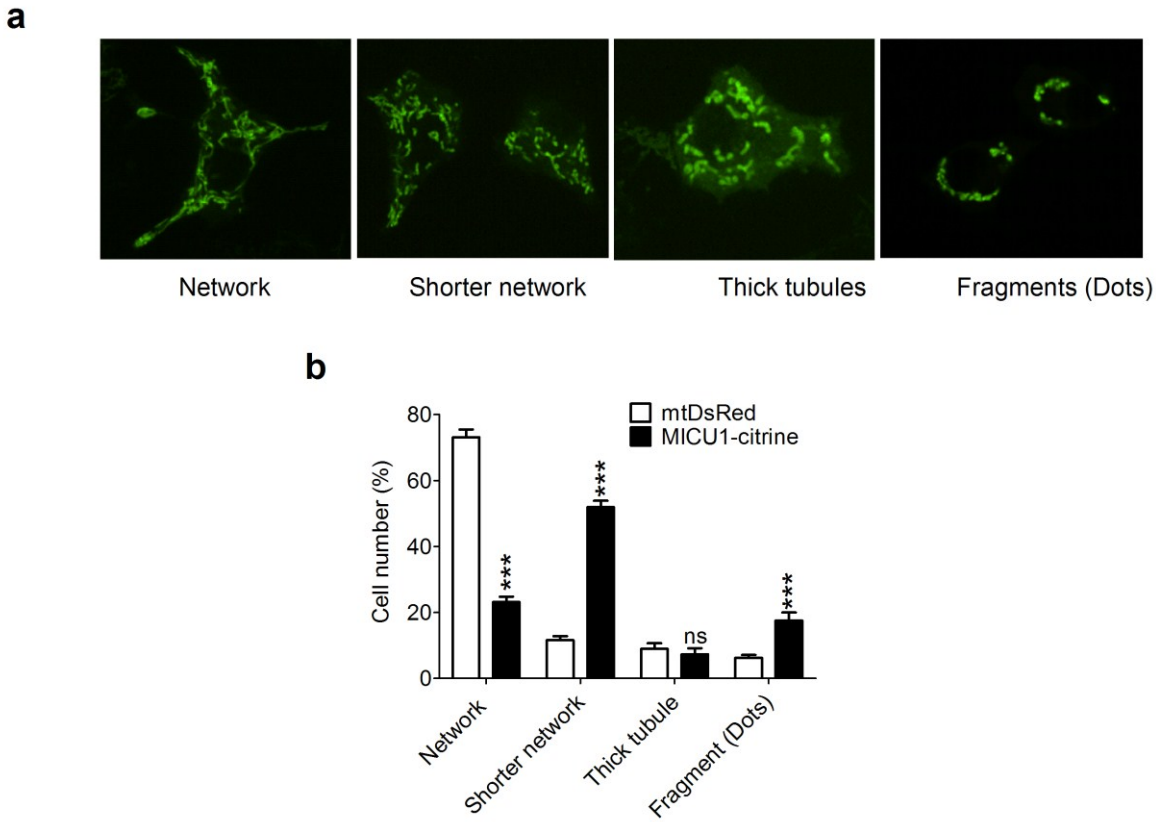

Figure 3.14: *Analysis of mitochondrial morphology in hMICU1 – citrine expressing cells. Mitochondrial morphology was analyzed 48 hours after transfection of cells with either MICU1-citrine or mtDsRed. Live images were taken with a confocal microscope using a 100X objective. A total of 570 and 860 cells were analyzed for mtDsRed and MICU1-citrine respectively. Cells were divided into four groups and percentage data were presented as mean ± sem. MICU1 – citrine expressing cells showed an alteration in the morphology of mitochondria as shown by the presence of reduced network structure and existence of shorter networks and fragments (dots). (***P<0.001 vs mtDsRed).*

3.5 Knockdown of LETM1 reduced depolarization – induced but not IP_3 - triggered mitochondrial Ca^{2+} uptake

In addition to role of LETM1 in mitochondrial integrity and metabolism it has been described to play a role in mitochondrial Ca^{2+} uptake in exchange with protons. Therefore further experiments were performed to investigate the involvement of LETM1 in mitochondrial Ca^{2+} transport. Transient knockdown of LETM1 significantly reduced $[Ca^{2+}]_{mito}$ upon stimulation of cells with direct depolarization with 30mM KCl (Figure 3.15c & d). However IP_3 – induced mitochondrial Ca^{2+} entry was not influenced by silencing of LETM1 (Figure 3.15a & b).

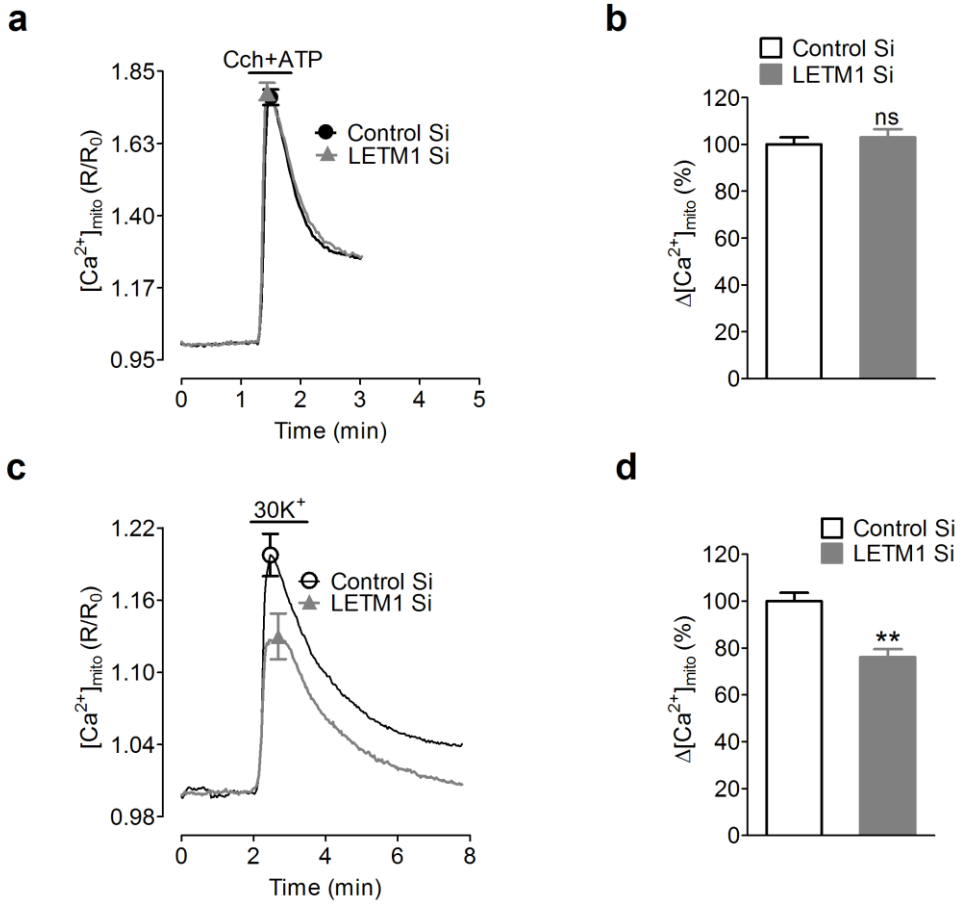

Figure 3.15: *Measurement of IP_3 – or direct depolarization – induced $[Ca^{2+}]_{mito}$ in INS-1 cells with a knockdown of LETM1. a & c) Average curves showing an increase in $[Ca^{2+}]_{mito}$ (correct ratios) upon stimulation of cells with Cch+ATP or 30 mM KCl ($30K^+$) respectively. b & d) Peak $[Ca^{2+}]_{mito}$ amplitude of each group represented as percentage of control (white columns). Silencing of LETM1 diminished $[Ca^{2+}]_{mito}$ upon stimulation with*

30 mM KCl (n=12, d) without any influence on Cch+ATP – induced $[Ca^{2+}]_{mito}$ *(n=5, b) respectively. Data is represented as mean ± sem. (**P=0.001, ns=not significant)*

3.6 UCP2 silencing altered mitochondrial Ca^{2+} transfer in a source dependent manner

UCP2 has been reported to participate in mitochondrial Ca^{2+} sequestration in some specific cells types in a mode – dependent fashion. Therefore this role of UCP2 was tested by transient knockdown of UCP2 in INS-1 cells. Figure 3.16a & b demonstrate a significant decline in mitochondrial Ca^{2+} uptake upon stimulation of cells with IP_3 – generating agonists in UCP2 knockdown cells while depolarization induced $[Ca^{2+}]_{mito}$ was not affected by suppression of UCP2 mRNA levels.

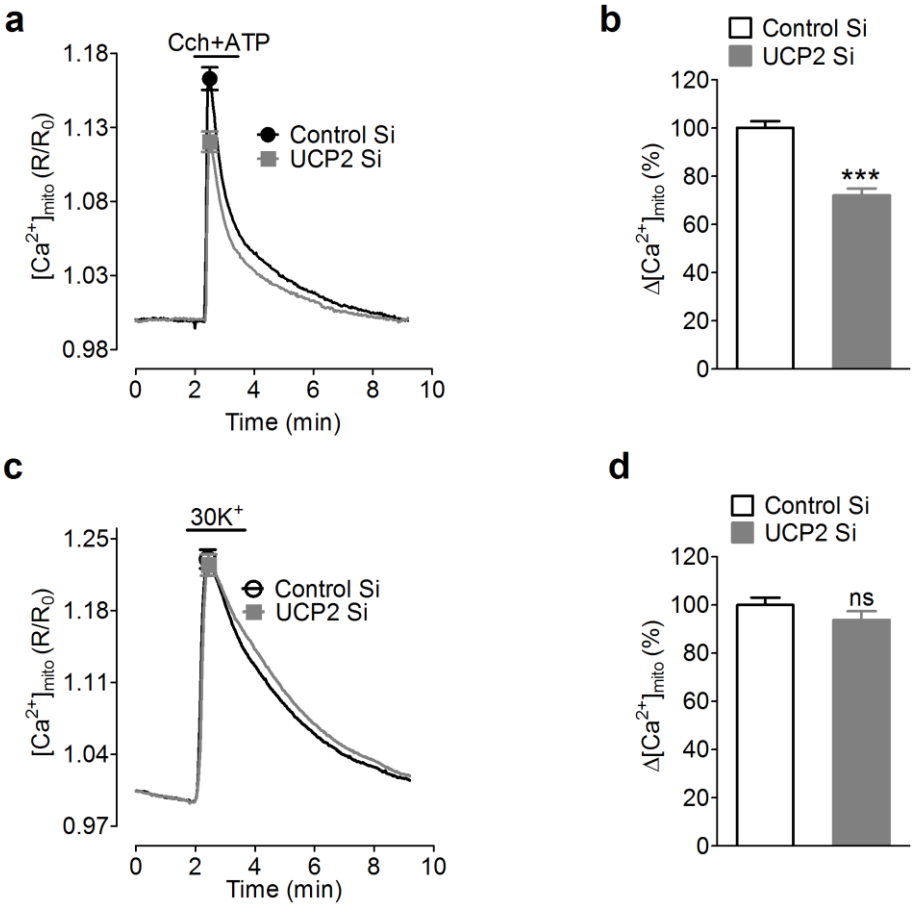

Figure 3.16: *Measurement of* IP_3 *– or direct depolarization – induced* $[Ca^{2+}]_{mito}$ *in INS-1 cells with a knockdown of UCP2. a & c) Average curves showing an increase in* $[Ca^{2+}]_{mito}$ *(correct ratios) upon stimulation of cells with Cch+ATP or 30 mM KCl (*$30K^{+}$*) respectively. b & d) Peak* $[Ca^{2+}]_{mito}$ *amplitude of each group represented as percentage of control (white columns). Silencing of UCP2 diminished* $[Ca^{2+}]_{mito}$ *upon stimulation with*

Cch+ATP (n=13) without any influence on depolarization – induced $[Ca^{2+}]_{mito}$ *(n=11) respectively. Data is represented as mean ± sem. (***P<0.0001, ns=not significant).*

3.7 UCP2 and LETM1 silencing did not influence IP_3 – and depolarization induced cytosolic Ca^{2+} transients

The diminishing effect of LETM1 and UCP2 knockdown on mitochondrial Ca^{2+} transport can also be attributed to alteration of cytosolic Ca^{2+} signals. However the data obtained from cytosolic Ca^{2+} measurements upon stimulation with Cch+ATP or KCl revealed a fast increase in Ca^{2+} transients in control cells without a considerable impairment of the signal in both LETM1 and UCP2 silenced cells (Figure 3.17). Similar to the results given in section 4.5.3 both methods of Ca^{2+} mobilization were combined into one protocol in this experiment which provided an opportunity to stimulate the cells with Cch+ATP following a first trigger with 30 mM KCl (Figure 3.17a & c).

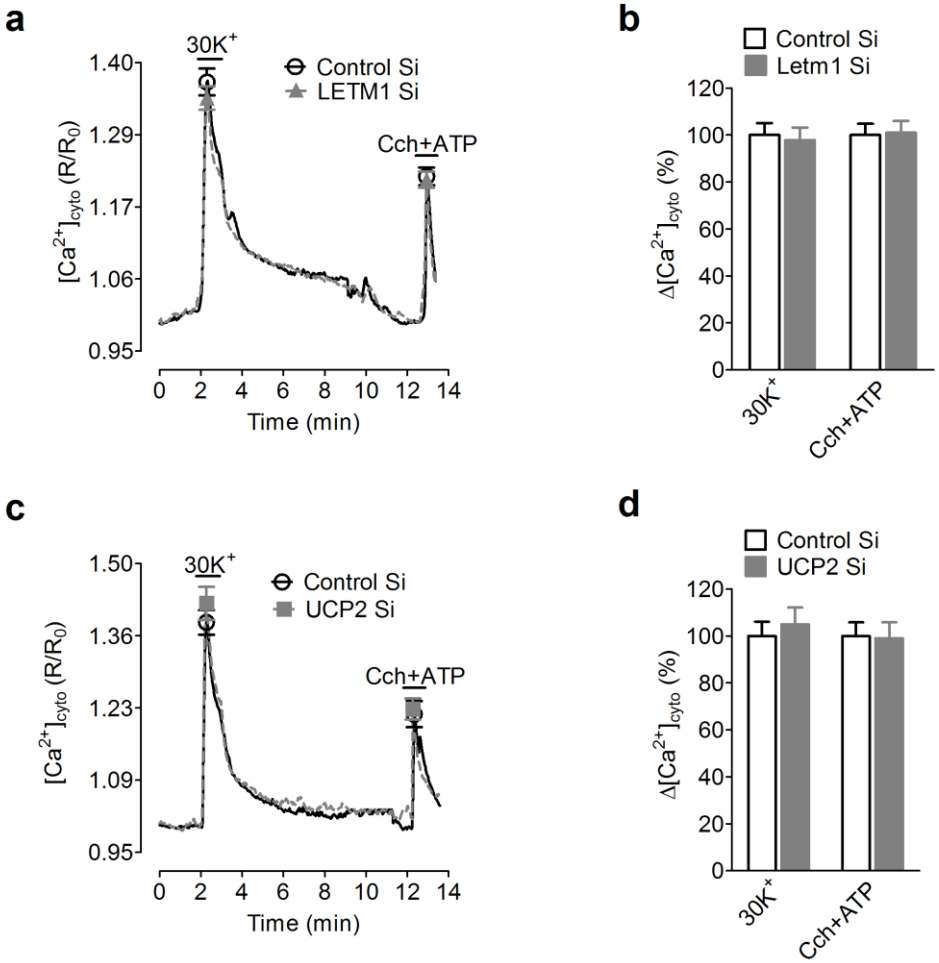

Figure 3.17: *Measurement of depolarization or IP_3 – induced $[Ca^{2+}]_{cyto}$ rises in LETM1 and UCP2 silenced cells. $[Ca^{2+}]_{cyto}$ was measured in cells transiently transfected with D3cpv and respective siRNAs 48 or 72 hours after transfection. Cells were first treated with 30 mM KCl ($30K^+$) during perfusion (in the presence of extracellular Ca^{2+}) to activate VGCC – mediated Ca^{2+} entry which was followed by a wash-out and a subsequent stimulation with Cch+ATP in a Ca^{2+} - free buffer. a & c) Average curves representing $[Ca^{2+}]_{cyto}$ responses (corrected ratios) upon depolarization of cells with $30K^+$ or upon stimulation with Cch+ATP. b & d) Peak $[Ca^{2+}]_{cyto}$ amplitudes shown as percentage of control cells (white columns, n=4) with knockdown of LETM1 (gray columns; n=4) and UCP2 (gray columns; n=4). Data is represented as mean ± sem.*

3.8 Glucose – induced mitochondrial Ca^{2+} uptake was diminished upon knockdown of MICU1 and MCU

Glucose induces Ca^{2+} oscillations in pancreatic β-cells by accelerating ATP production with a concomitant plasma membrane depolarization and a subsequent activation of VGCCs. These Ca^{2+} signals are also relayed into mitochondria where they further boost the oxidative phosphorylation and production of ATP. Thus glucose is a nutrient and physiological secretagogue which induces depolarization – induced mitochondrial Ca^{2+} uptake. Therefore it was empirical to investigate the contribution of MICU1 and MCU in glucose – stimulated mitochondrial Ca^{2+} uptake as they were the only proteins out of four candidates to be involved in mitochondrial Ca^{2+} sequestration upon stimulation of cells with both IP_3 – generating agonist and direct depolarization. For this purpose transfected INS-1 cells were incubated in low glucose followed by a short incubation in an experimental buffer without glucose (0G) to minimize the Ca^{2+} signals on one hand and to increase the response to high glucose on the other hand (see methods for detailed description). Upon stimulation of cells with 16 mM glucose (16G) the cells started responding heterogeneously both in control and MICU1/MCU – silenced cells (Figure 3.18). However, the statistical analysis showed a significant reduction in mitochondrial Ca^{2+} uptake in MICU1 (Figure 3.18c) and MCU (Figure 3.18f) knockdown cells as determined by total peak area of responding cells. Due to a large heterogeneity in mitochondrial Ca^{2+} signals among individual β-cells, data are shown as traces of three cells from each group with respective controls.

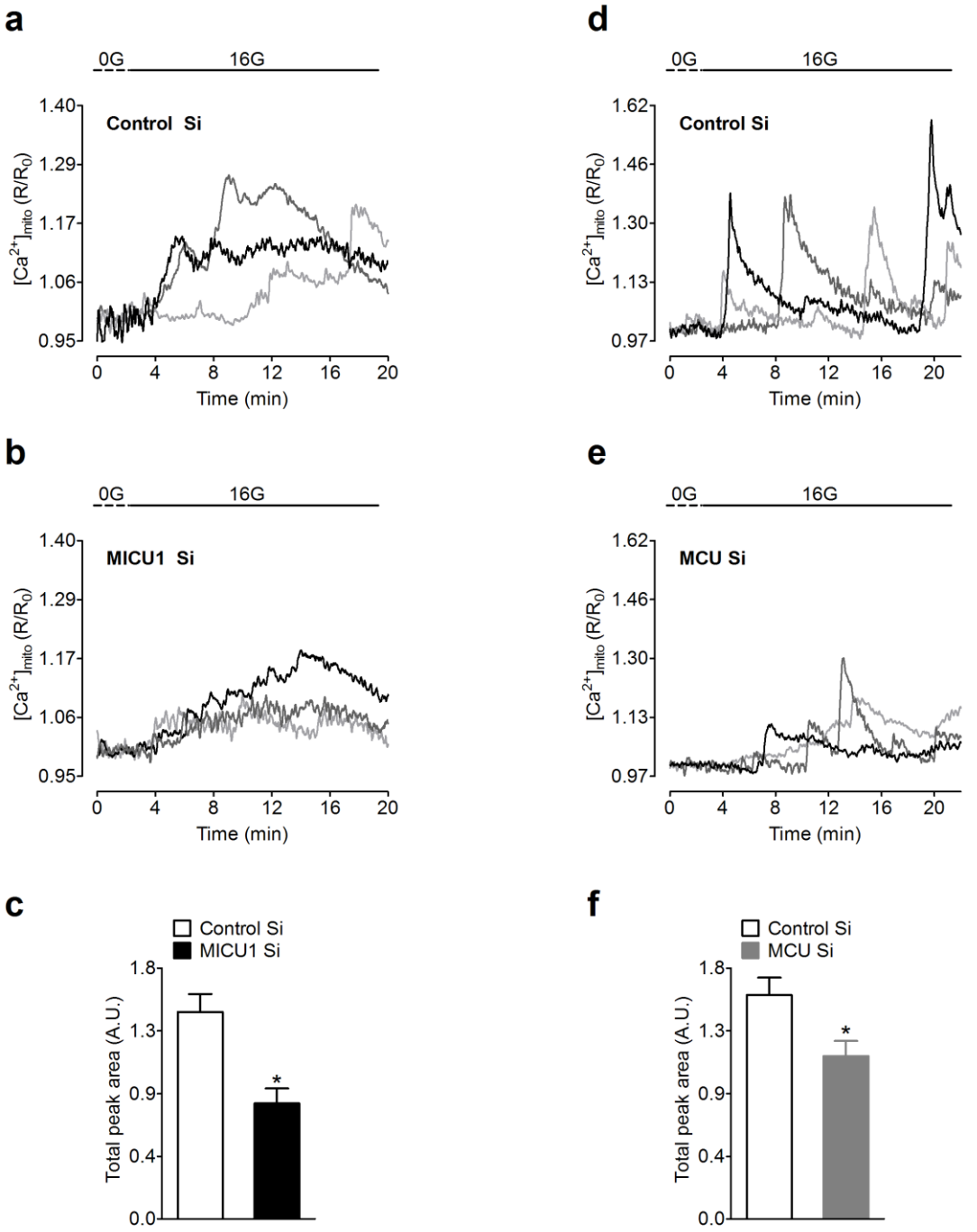

Figure 3.18: *Measurement of glucose – triggered* $[Ca^{2+}]_{mito}$ *rises in MICU1 and MCU silenced cells.* $[Ca^{2+}]_{mito}$ *was measured in cells transiently transfected with 4mD3cpv and respective siRNAs 48 or 72 hours after transfection. Cells were first incubated in 3 mM glucose for 30 minutes followed by 10-15 minutes treatment with a glucose free experimental buffer. On the microscope, cells were perfused with glucose – free buffer (0G) for an additional 3 minutes before switching to 16 mM glucose (16G). a, b, d & e) Three representative curves from MICU1 (b) and MCU (e) knockdown cells along with*

*respective controls (a & d) show [Ca^{2+}]$_{mito}$ responses as corrected ratios. c & f) Total Peak Area (A.U. = arbitrary units) was calculated from all curves and represented as mean ± sem. Silencing of MICU1 (black column; n=12, *P=0.012) and MCU (gray column; n=10, *P=0.011) significantly reduced the total peak area as compared with respective controls.*

3.9 Knockdown of MICU1 and MCU did not alter glucose – induced global cytosolic Ca^{2+} signals

Glucose triggers fast cytosolic Ca^{2+} oscillations and this phenotype is an indispensable feature of pancreatic β-cell physiology. In order to verify whether a MICU1 and MCU – dependent mitochondrial Ca^{2+} uptake contributes to these cytosolic oscillations, global $[Ca^{2+}]_{cyto}$ was measured upon stimulation of the cells with 16 mM glucose following incubation in low glucose as described in section 4.11. Figure 3.19a shows tracing of a cell representing cytosolic Ca^{2+} oscillations in response to 16 mM glucose (16G). In contrast to $[Ca^{2+}]_{mito}$ silencing of MICU1 and MCU did not interfere with the cytosolic Ca^{2+} signals as demonstrated by the Ca^{2+} Peak Area calculated for a continuous 3 minutes time period (Figure 3.19b), frequency of cytosolic Ca^{2+} oscillations (Figure 3.19c) and the percentage of cells responding to 16G (Figure 3.19d).

Figure 3.19: *Glucose – triggered [Ca^{2+}]$_{cyto}$ measurement in MICU1 and MCU knockdown cells. [Ca^{2+}]$_{cyto}$ was measured in cells transiently transfected with D3cpv and respective siRNAs 48 or 72 hours after transfection. Cells were first incubated in 3 mM glucose for 30 minutes followed by 10-15 minutes treatment with a glucose free experimental buffer. On the microscope, cells were perfused with glucose – free buffer (0G) for an additional 3 minutes before switching to 16 mM glucose (16G) followed by a final stimulation 30 mM KCl (30K^+). a). Representative tracing of a cell (% of 30K^+) showing oscillations in response to 16 G. (b)* Ca^{2+} *Peak Area calculated by addition of all values on y axis for every 3 min over the whole measurement period and represented as fold change over basal (0-3 minutes). The corrected ratios were converted into percentage of 30K^+. c) Frequency of peaks/minute/cell under basal (0G) and stimulated (16G) conditions in control, MICU1 and MCU silenced cells. d) Number of cells responding to 16G upon MICU1 and MCU knockdown represented as percentage of control. Data is represented as mean ± sem. (n=3 for all groups).*

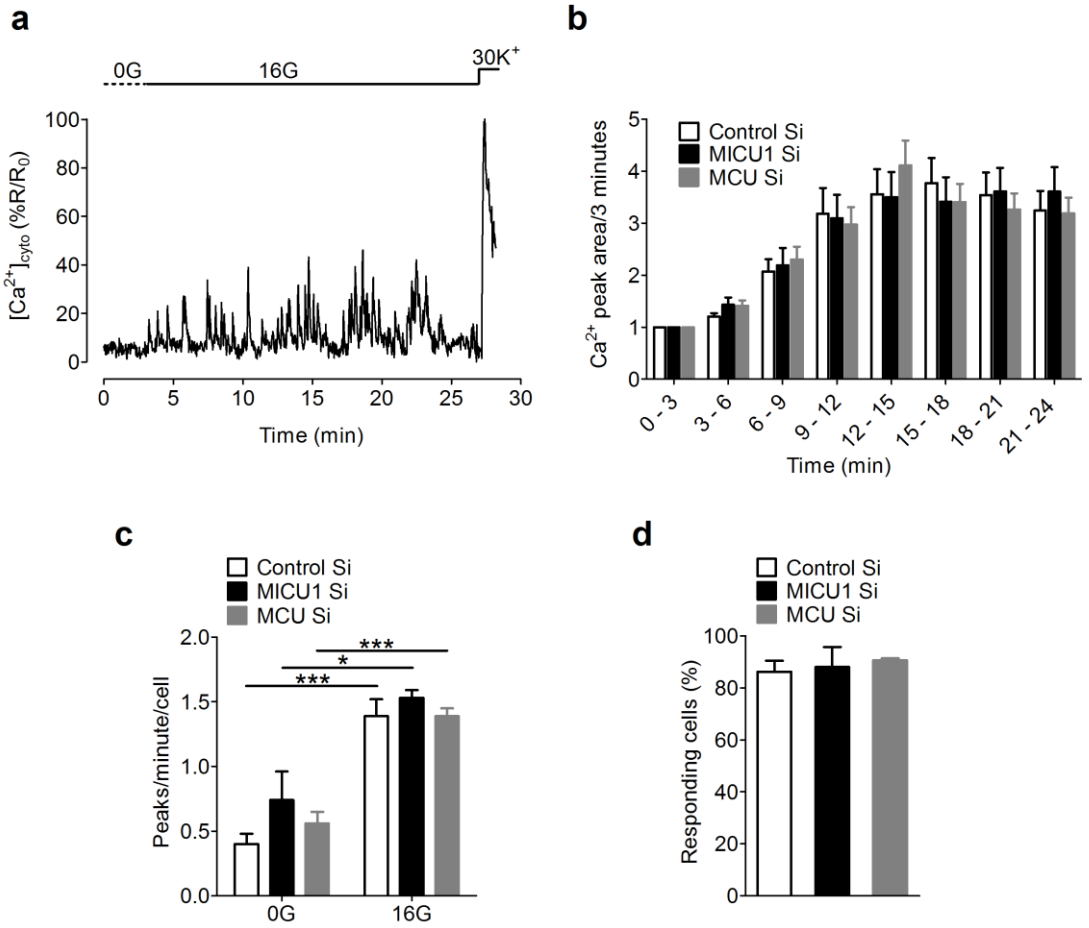

3.10 Glucose – induced cytosolic ATP was reduced in MICU1 and MCU knockdown cells

Mitochondrial Ca^{2+} uptake accelerates the production of ATP by activating some rate limiting dehydrogenases in the matrix. Therefore the influence of MICU1 and MCU – dependent mitochondrial Ca^{2+} uptake on ATP production was investigated. The transfer of cell from 3 mM glucose (3G) to 16 mM glucose (16G) resulted in a slow increase in luminescence signal (indicating cytosolic ATP) which reached a maximum level in 10-15 minutes (Figure 3.20a). The peak cytosolic ATP was elevated by 25 % in 16G as compared to basal glucose (3G). However this decrease was significantly hindered in MICU1 and MCU – silenced cells. The chelation of extracellular Ca^{2+} with 1 mM EGTA had a similar but much stronger effect on the cytosolic ATP levels (Figure 3.20b).

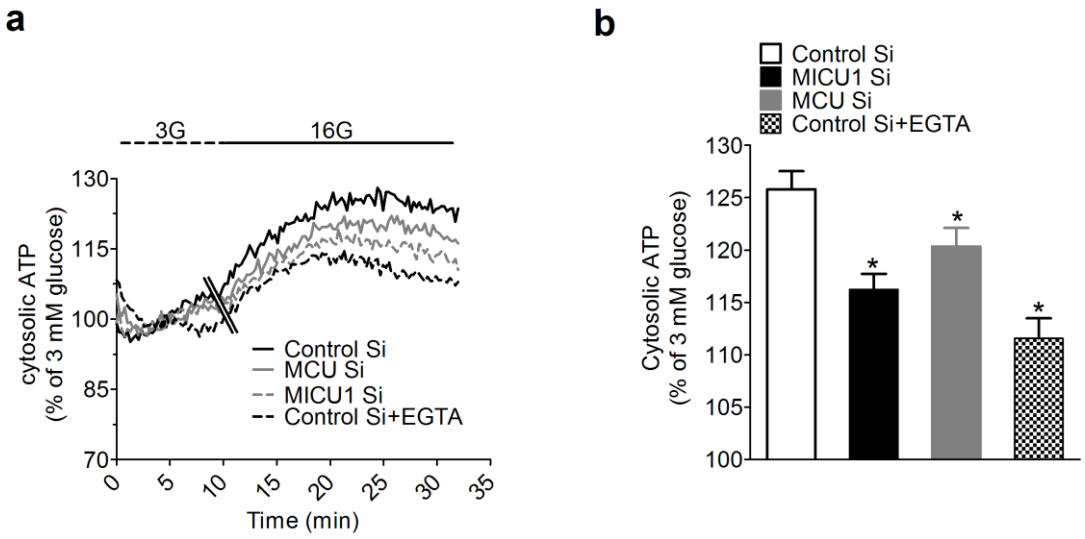

Figure 3.20: *Cytosolic ATP measurement in MICU1 and MCU silenced cells. Cytosolic ATP was measured in INS-1 cells co-transfected with cytosolic luciferase and respective siRNAs 48 hours after transfection. Cells were pre-incubated in 3mM glucose (3G) before switching to 16 mM glucose (16G). a) Average curves expressed as percentage of basal (3G) showing cytosolic ATP in control and knockdown cells. EGTA was used as a positive controls b) Peak cytosolic ATP upon stimulation with 16G expressed as mean ± sem in control, MICU/ MCU – silenced cells (n=32, *P<0.05 vs control)*

3.11 Silencing of MICU1 and MCU hampered glucose – stimulated insulin secretion

As MICU1 and MCU – mediated mitochondrial Ca^{2+} uptake contributes to the ATP production; it is plausible to speculate that it also plays a role in GSIS. In order to demonstrate the involvement of MICU1 and MCU in GSIS, further experiments were carried out to determine insulin release in INS-1 cells upon stimulation with 16 mM glucose with transient knockdown of both proteins. Although there was a ~3 fold increase in insulin secretion in response to 16 mM glucose in control cells, silencing of MICU1 and MCU significantly reduced this effect (Figure 3.21a). In order to rule out the possibility of a defect in insulin biosynthesis pathway as a result of knockdown of MICU1/MCU, total insulin content was also measured in the cell lysate. Data in Figure 3.21b precludes the chances of any such interference with insulin synthesis upon silencing of these proteins.

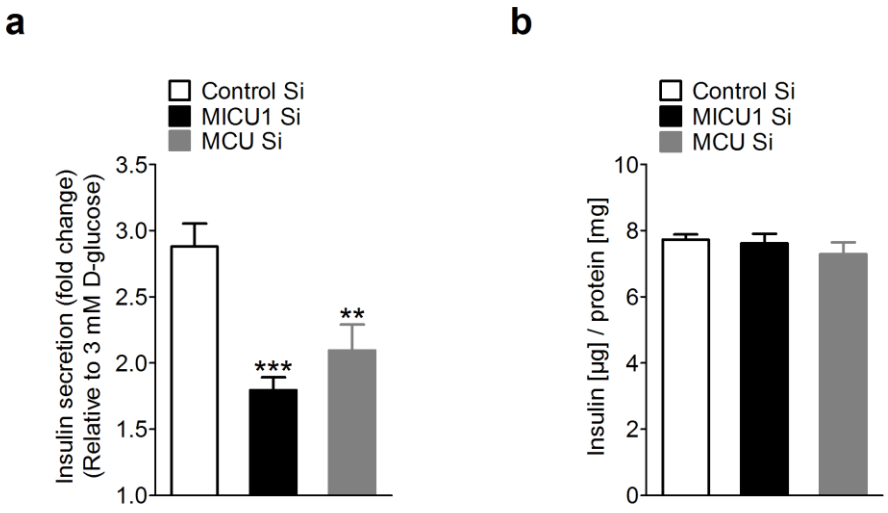

Figure 3.21: *Measurement of GSIS in MICU1 and MCU knockdown cells. GSIS was measured in INS-1 cells 48-72 hours after transfection with the respective siRNA. a) Cells were first incubated in 3 mM glucose for 1 hour followed by a 1 hour treatment with 16 mM glucose. Insulin release was expressed as fold change over basal (3 mM glucose) upon silencing of MICU1 (n=28) and MCU (n=12). b) Total cellular insulin content measured from lysates of cells transfected with MICU1 or MCU (n= 3). (***P= 0.0001, **P=0.01 vs control).*

4. DISCUSSION

Mitochondria are essential players in pancreatic β-cell physiology and their deregulation contributes to the etiopathogenesis of type 2 diabetes mellitus (T2D) (119). The sequestration of Ca^{2+} is a characteristic feature of mitochondria which influences the cellular metabolism, cytosolic Ca^{2+} homeostasis and regulation of cell survival depending on the cell types involved (1). In β-cells the glucose – dependent elevation in matrix Ca^{2+} participates in the activation of mitochondrial metabolism and couples the production of ATP with exocytosis of insulin granule (19). The transport of Ca^{2+} across the IMM is mediated by mitochondrial Ca^{2+} uniporter (54) whose molecular identity has been recently elucidated with the discovery of MCU (51,52) and its regulatory subunit MICU1 (50) In addition, other candidate proteins have also been reported to be involved in mitochondrial Ca^{2+} uptake including RyR1 (55), UCP2/3 (57,58,59) and LETM1 (65,53) While the involvement of RyR1 in mitochondrial Ca^{2+} uptake can be a phenomenon specific for cardiac myocytes, other proteins are either ubiquitous (MICU1 and MCU) or work in more than one cell types (LETM1 and UCP2/3). However the molecular nature mitochondrial Ca^{2+} transport machinery has not yet been elucidated in pancreatic β-cells. Therefore this study was planned to investigate the contribution of MICU1, MCU, LETM1 and UCP2 in mitochondrial Ca^{2+} homeostasis and metabolism – secretion coupling in rat clonal pancreatic β-cells (INS-1). While the role of UCP2 in β-cells is largely debated (125,126,127), no data was available about the function of MICU1, MCU and LETM1 at the beginning of this work.

The initial experiments involved the characterization of cytosolic and mitochondrial Ca^{2+} responses in INS-1 cells. Our data demonstrates that 4mtD3cpv (mito-cameleon), which is a big protein, is correctly targeted to mitochondria of INS-1 cells with very little mistargeting 48 hours after transfection. Mito-cameleon is a FRET – based genetic sensor (128) which has been employed in many different cells types for the measurement mitochondrial Ca^{2+} but its transfection efficiency is not always consistent and many cell types show frequent mistargeting (46). Our data verifies that mito-cameleon is a good sensor for measuring mitochondrial Ca^{2+} in INS-1 in comparison to other cell types (46). INS-1 cells (INS-1 832/13 actually) which have been derived from an extensively studied original rat INS-1 clone have an enhanced responsiveness to glucose compared to their parent clone. They harbor an additional copy of human insulin cDNA inserted into their genome and retain most of the characteristics of parental β-cells (122). Therefore they can

be used as an excellent model for physiological studies. In our hands INS-1 cells responded quite nicely with strong mitochondrial Ca^{2+} responses upon stimulation both with IP_3 – generating agonists (a mixture of carbachol and ATP) or upon depolarization of plasma membrane. A combination of oligomycin and antimycin, which depolarizes mitochondria and inhibits energy – dependent mitochondrial Ca^{2+} uptake (124), was also effective in INS-1 cells confirming the correct targeting of the sensor to mitochondrial matrix.

The recent development of a red – shifted mitochondrial Ca^{2+} sensor (4mtD1GO-Cam) provided us an opportunity to simultaneously measure cytosolic and mitochondrial Ca^{2+} in combination with Fura-2. Due to spectral overlap of CFP/YFP based sensor i.e. mito-cameleon with Fura-2, it is not possible to employ them for simultaneous measurement (129,47). The application 4mD1GO-Cam Ca^{2+} (in combination with Fura-2) highlighted many interesting aspects of the transfer of Ca^{2+} signals from cytosol into mitochondria in INS-1 cells. Our findings reveal that upon VGCCs – mediated Ca^{2+} influx there was a slight delay in the uptake of Ca^{2+} by mitochondria after cytosolic Ca^{2+} elevation confirming the existence of a time interval, which allows Ca^{2+} to cross a threshold before it starts passing through MCU (130). Moreover it also points out towards the formation of Ca^{2+} microdomains on the surface of mitochondrial which can be a time dependent phenomenon. (47). These results further explain that although the slope of rise in Ca^{2+} in both cytosol and mitochondria was similar, the extrusion of Ca^{2+} from mitochondria was much slower than cytosol. The inactivation of mitochondrial Ca^{2+} uptake after first pulse of repetitive stimulation with high K^+ points towards a Ca^{2+} - dependent desensitization of MCU due to slow extrusion of Ca^{2+} from β-cells (131,130). The regulation of mitochondrial Ca^{2+} uptake seems to be an intricate process which has also been reported in other cell types.(132).

In a series of further experiments we investigated the expression of candidate proteins in INS-1 cells in addition to their involvement in mitochondrial Ca^{2+} transport. Along with UCP2 whose expression has already been demonstrated in β-cells (133,134) our data demonstrate the existence of MICU1, MCU and LETM1 in INS-1 cells. The analysis of freshly isolated pancreatic islets also revealed the presence of MICU1 and MCU in primary cells as well. MICU1 and MCU have been shown to express ubiquitously in many mice tissues in addition to some human cells lines but the level of expression varies from tissue to tissue (50,51,52). The detection of all four candidates in INS-1 cells provided us a possibility to systematically compare the contribution of these proteins in mitochondrial

Ca^{2+} uptake in INS-1 cells. Using a combination of previously described FRET – based genetic sensor (mito-cameleon) and siRNA – mediated knockdown we were able to analyze the role of these protein in mitochondrial Ca^{2+} transport. Silencing of MICU1 and MCU could effectively inhibit mitochondrial Ca^{2+} sequestration upon stimulation of cells with IP_3 – generating agonists and direct depolarization. The diminishing effect on mitochondrial Ca^{2+} was dependent on the efficiency of siRNA knockdown. These results coincide with the initial reports which described the participation of MICU1 and MCU in agonist – induced mitochondrial Ca^{2+} uptake in HeLa cell line (50,51,52).

While the contribution of MCU has also been demonstrated in depolarization – induced mitochondrial Ca^{2+} uptake in pancreatic β-cells (135,120,121) along with a similar role in other cells types (136,18), such an involvement of MICU1 in agonist – induced mitochondrial Ca^{2+} import has only been described by two studies (135,50). However this very role of MICU1 has been challenged by recent study (71). Madesh and co-worker found out that instead of inhibiting the mitochondrial Ca^{2+} uptake upon cell stimulation, MICU1 regulates the basal matrix Ca^{2+} by inhibiting the MCU – mediated uptake under resting conditions. In their hands knockdown of MICU1 in HeLa and endothelial cells resulted in an elevated basal mitochondrial Ca^{2+} and this entry was mediated by MCU (71). In another interesting piece of work silencing of MICU1 did not hampered agonist – induced mitochondrial Ca^{2+} uptake in endothelial cells but this study did not enlighten the influence of MICU1 knockdown on basal mitochondrial Ca^{2+}(53). Moreover some unpublished data from our lab portrays a variable contribution of MICU1 in INS-1 cells compared to other cell types like endothelial and HeLa cells. While these observations indicate that silencing of MICU1 increased the basal mitochondrial Ca^{2+} in endothelial and HeLa cells without affecting agonist – induced uptake, these clearly showed a diminished mitochondrial Ca^{2+} sequestration in INS-1 cells as described in this study However, this effect was not accompanied by an elevated basal mitochondrial Ca^{2+} in INS-1 cells. These results point towards a more dynamic role of MICU1 in different cells types and raise many questions about its regulatory role in mitochondrial Ca^{2+} transport. One possible explanation could be the variable expression pattern of MICU1 and/or MCU which might contribute to differential stoichiometric interaction of MICU1 with MCU. This variation in the interaction might be responsible for a different function in various cell types. The existence of more than one isoforms of MICU1 and MCU, which might interact differently, raises another possibility about the divergent regulatory pattern of MICU1. A

third possibility proposes the involvement the post-translational modification of these proteins which might be variable depending on the function and metabolic status of different cell types. As Ca^{2+} is a crucial modulator of mitochondrial respiration, MICU1 might function as an activator of mitochondrial Ca^{2+} uptake to boots mitochondrial metabolism in one cell type (e.g. pancreatic β-cells) while it may not be involved or may have an inhibitory role in other cell types where mitochondrial metabolism is not very crucial for the energy production (e.g. HeLa and endothelial cells). Future studies will hopefully clarify the exact contribution of MICU1 in mitochondrial Ca^{2+} sequestration under stimulated and resting conditions (135).

MICU1 and MCU may also be involved to different pathways of mitochondrial Ca^{2+} transport. In order to rule this possibility, further experiments were carried out to measure mitochondrial Ca^{2+} in cells with simultaneous knockdown of both proteins. The measurement of mitochondrial Ca^{2+} uptake upon stimulation of cells with direct depolarization or IP_3 – generating agonists in double knockdown cells did not have any additional inhibitory effect which further confirm that both of these proteins are part of an identical Ca^{2+} transfer pathway in the inner mitochondrial membrane (50,51,52). Additionally the present data also demonstrates a rescuing effect of MCU overexpression in MCU – silenced cells which also substantiates the concept of MCU as a part of the mitochondrial Ca^{2+} uniporter. However overexpression of MICU1 could not rescue its inhibitory phenotype. Instead it produced aberrant changes in the structure of mitochondrial which might provide a clue about an additional involvement of this protein in mitochondrial ultra-structure.

In contrast to the contribution of MICU1 and MCU in both agonist – and depolarization induced mitochondrial Ca^{2+} uptake, LETM1 and UCP2 appear to be associated with mitochondrial Ca^{2+} transport in a mode/source depending manner. Our data reveals that LETM1 and UCP2 silencing could only hamper mitochondrial Ca^{2+} sequestration upon cell stimulation with direct depolarization and IP_3 – generating agonists respectively. These findings verify some previous reports from our group which described that the contribution of UCP2/3 (58,59) and LETM1 (53) in mitochondrial Ca^{2+} uptake crucially depends on the source and mode of mobilized Ca^{2+} in HeLa and endothelial cells. The involvement of LETM1 in the uptake of Ca^{2+} coming from extracellular milieu correlates with previous reports (65) along with a study from our group (53) which highlight the role of this protein as a high affinity mitochondrial Ca^{2+} carrier.

The reduction in mitochondrial Ca^{2+} uptake can also result due to changes in the global cytosolic Ca^{2+} signals (137). In addition reduced mitochondrial Ca^{2+} buffering can also be expected to increase the cytosolic Ca^{2+}. Intriguingly our data reveals that the global cytosolic Ca^{2+} remained unchanged upon silencing of either of candidates proteins (MICU1, MCU, LETM1 and UCP2) regardless of the nature of the stimulus. This confirms the direct inhibitory effect of these proteins in mitochondrial Ca^{2+} sequestration and correlates with previous studies from our group (59,58,57). These findings highlight an intricate role of mitochondria in the regulation of cellular Ca^{2+} homeostasis with their contribution in refilling of ER, store – operated Ca^{2+} entry and maintenance of normal cytosolic Ca^{2+} (124,100,1).

Glucose is the major nutrient secretagogue which generates mitochondria – dependent cytosolic Ca^{2+} transients due to activation of VGCCs that ultimately trigger GSIS. These Ca^{2+} signals are also relayed into mitochondria where they further accelerate the oxidative metabolism producing certain coupling factors necessary for the amplifying phase of GSIS (19,111). As MICU1 and MCU appear to be involved in both types of Ca^{2+} uptake pathways (Ca^{2+} release from ER and influx from extracellular milieu), therefore we further investigated their participation in glucose – induced cytosolic and mitochondrial Ca^{2+} signals. Our data shows that glucose triggered fast Ca^{2+} oscillations in the cytosol which were also transferred to mitochondria. However there was a large heterogeneity in glucose - induced Ca^{2+} responses between individual INS-1 and it is consistent with a recent study which described a similar finding in the this cell type (138). Notably, the transfer of Ca^{2+} transients from cytosol to mitochondria was significantly hampered in cells with a knockdown of MICU1 and MCU which further confirms the participation of these proteins in mitochondrial Ca^{2+} uptake in pancreatic β-cells in response to a physiological stimulus. Interestingly, the silencing of MICU1 and MCU did not alter the cytosolic Ca^{2+} oscillations in response to glucose which confirms the results of a previous study where matrix Ca^{2+} was buffered by the overexpression of a Ca^{2+} - binding protein in mitochondria (19). This outcome can be explained by the existence of certain subplasmalemmal Ca^{2+} microdomains which cannot be detected by our methods or it could also highlight the contribution of other coupling factors whose production is also modulated by mitochondrial Ca^{2+}. These coupling factors might be a trigger for a sustained insulin secretion without yielding a further increase in the cytosolic Ca^{2+} concentration (19,139). Two recent studies also confirm this concept that inhibition of mitochondrial Ca^{2+} uptake

by silencing of MCU does not impair glucose – triggered cytosolic Ca^{2+} oscillations (121,120).

Glucose – induced uptake of Ca^{2+} by mitochondria activates matrix dehydrogenases which boost the production of ATP. Therefore it is reasonable to expect a contribution of MICU1 and MCU – dependent mitochondrial Ca^{2+} uptake in ATP production. The data presented here reveals a reduction of glucose – induced cytosolic ATP elevation in MICU1 and MCU – silenced cells which confirm the previous reports about participation of matrix Ca^{2+} in the acceleration of glucose – dependent mitochondrial metabolism (85,140,90). In addition to acting as a trigger for GSIS, cytosolic ATP along with other coupling factors has also been proposed to contribute to a sustained amplifying phase of insulin secretion (84).Therefore it is tempting to speculate a role of MICU1 and MCU – dependent mitochondrial Ca^{2+} sequestration in GSIS. Our data demonstrate a significant reduction of insulin secretion in response to glucose upon silencing of MICU1 and MCU. However, knockdown of these proteins did not alter the total cellular insulin content indicating an inhibitory effect only at the level of insulin release rather than its biosynthesis. These finding confirm the previous studies about the role of matrix Ca^{2+} in GSIS (19).and elaborate a function of MICU1 and MCU which places them at a strategically important location where they can provide a positive feedback effect for sustained insulin secretion in pancreatic β-cells.

To conclude, this work provided us an opportunity to compare the individual contribution of MICU1, MCU, LETM1 and UCP2 in mitochondrial Ca^{2+} uptake in pancreatic β-cells. Although the role of LETM1 and UCP2 seem to be dependent on the mode and source of mobilized Ca^{2+} which supports already existing information, MICU1 and MCU are involved in both agonist – and depolarization induced mitochondrial Ca^{2+} sequestration. Thus we propose MICU1 and MCU as the major players in mitochondrial Ca^{2+} transport in β-cells. Moreover their contribution to the regulation of Ca^{2+} - dependent mitochondrial metabolism, ATP production and insulin secretion makes them integral components of β-cell physiology. Future research might expand our understanding of the MICU1 and MCU function in β-cells along with obtaining more information about their role in the pathogenesis of T2D and whether or not these proteins can serve as targets for the development of a therapeutic strategy to improve GSIS.

REFERENCES

1. Rizzuto R, De Stefani D, Raffaello A, Mammucari C. Mitochondria as sensors and regulators of calcium signalling. **Nat Rev Mol Cell Biol.** 2012;13(9):566-78.

2. Galluzzi L, Kepp O, Kroemer G. Mitochondria: master regulators of danger signalling. **Nat Rev Mol Cell Biol.** 2012;13(12):780-8.

3. DiMauro S, Garone C. Historical perspective on mitochondrial medicine. **Developmental disabilities research reviews.** 2010;16(2):106-13.

4. Vafai SB, Mootha VK. Mitochondrial disorders as windows into an ancient organelle. **Nature.** 2012;491(7424):374-83.

5. Ernster L, Schatz G. Mitochondria: a historical review. **J Cell Biol.** 1981;91(3 Pt 2):227s-55s.

6. Nass MM. Mitochondrial DNA: Advances, Problems, and Goals. **Science.** 1969;165(3888):25-35.

7. Mitchell P. Keilin's respiratory chain concept and its chemiosmotic consequences. **Science.** 1979;206(4423):1148-59.

8. Pizzo P, Drago I, Filadi R, Pozzan T. Mitochondrial Ca^{2+} homeostasis: mechanism, role, and tissue specificities. **Pflugers Arch.** 2012;464(1):3-17.

9. Drago I, Pizzo P, Pozzan T. After half a century mitochondrial calcium in- and efflux machineries reveal themselves. **EMBO J.** 2011;30(20):4119-25.

10. O-Uchi J, Pan S, Sheu SS. Perspectives on: SGP symposium on mitochondrial physiology and medicine: molecular identities of mitochondrial Ca^{2+} influx mechanism: updated passwords for accessing mitochondrial Ca^{2+}-linked health and disease. **J Gen Physiol.** 2012;139(6):435-43.

11. Carafoli E. Calcium signaling: a tale for all seasons. **Proc Natl Acad Sci U S A.** 2002;99(3):1115-22.

12. Clapham DE. Calcium signaling. **Cell.** 2007;131(6):1047-58.

13. VASINGTON FD, MURPHY JV. Ca ion uptake by rat kidney mitochondria and its dependence on respiration and phosphorylation. **J Biol Chem.** 1962;237:2670-7.

14. DELUCA HF, ENGSTROM GW. Calcium uptake by rat kidney mitochondria. **Proc Natl Acad Sci U S A.** 1961;47:1744-50.

15. Jouaville LS, Pinton P, Bastianutto C, Rutter GA, Rizzuto R. Regulation of mitochondrial ATP synthesis by calcium: evidence for a long-term metabolic priming. **Proc Natl Acad Sci U S A.** 1999;96(24):13807-12.

16. Babcock DF, Herrington J, Goodwin PC, Park YB, Hille B. Mitochondrial participation in the intracellular Ca^{2+} network. **J Cell Biol.** 1997;136(4):833-44.

17. David G, Barrett JN, Barrett EF. Evidence that mitochondria buffer physiological Ca^{2+} loads in lizard motor nerve terminals. **J Physiol.** 1998;509 (Pt 1):59-65.

18. Drago I, De Stefani D, Rizzuto R, Pozzan T. Mitochondrial Ca^{2+} uptake contributes to buffering cytoplasmic Ca^{2+} peaks in cardiomyocytes. **Proc Natl Acad Sci U S A.** 2012;109(32):12986-91.

19. Wiederkehr A, Szanda G, Akhmedov D, Mataki C, Heizmann CW, Schoonjans K et al. Mitochondrial matrix calcium is an activating signal for hormone secretion. **Cell Metab.** 2011;13(5):601-11.

20. Pizzo P, Drago I, Filadi R, Pozzan T. Mitochondrial Ca^{2+} homeostasis: mechanism, role, and tissue specificities. **Pflugers Arch.** 2012;464(1):3-17.

21. Leo S, Bianchi K, Brini M, Rizzuto R. Mitochondrial calcium signalling in cell death. **FEBS J.** 2005;272(16):4013-22.

22. Hajnóczky G, Csordás G, Das S, Garcia-Perez C, Saotome M, Sinha Roy S et al. Mitochondrial calcium signalling and cell death: approaches for assessing the role of mitochondrial Ca^{2+} uptake in apoptosis. **Cell Calcium.** 2006;40(5-6):553-60.

23. Nicholls DG, Crompton M. Mitochondrial calcium transport. **FEBS Lett.** 1980;111(2):261-8.

24. Patergnani S, Suski JM, Agnoletto C, Bononi A, Bonora M, De Marchi E et al. Calcium signaling around Mitochondria Associated Membranes (MAMs). **Cell communication and signaling : CCS.** 2011;9:19.

25. Berridge MJ, Bootman MD, Roderick HL. Calcium signalling: dynamics, homeostasis and remodelling. **Nat Rev Mol Cell Biol.** 2003;4(7):517-29.

26. English AR, Zurek N, Voeltz GK. Peripheral ER structure and function. **Curr Opin Cell Biol.** 2009;21(4):596-602.

27. Mikoshiba K. IP3 receptor/Ca^{2+} channel: from discovery to new signaling concepts. **J Neurochem.** 2007;102(5):1426-46.

28. Choe CU, Ehrlich BE. The inositol 1,4,5-trisphosphate receptor (IP3R) and its regulators: sometimes good and sometimes bad teamwork. **Sci STKE.** 2006;2006(363):re15.

29. Vanderheyden V, Devogelaere B, Missiaen L, De Smedt H, Bultynck G, Parys JB. Regulation of inositol 1,4,5-trisphosphate-induced Ca^{2+} release by reversible phosphorylation and dephosphorylation. **Biochim Biophys Acta.** 2009;1793(6):959-70.

30. Bezprozvanny I. The inositol 1,4,5-trisphosphate receptors. **Cell Calcium.** 2005;38(3-4):261-72.

31. Van Petegem F. Ryanodine receptors: structure and function. **J Biol Chem.** 2012;287(38):31624-32.

32. Zalk R, Lehnart SE, Marks AR. Modulation of the ryanodine receptor and intracellular calcium. **Annu Rev Biochem.** 2007;76:367-85.

33. Brini M, Carafoli E. Calcium pumps in health and disease. **Physiol Rev.** 2009;89(4):1341-78.

34. Sammels E, Parys JB, Missiaen L, De Smedt H, Bultynck G. Intracellular Ca^{2+} storage in health and disease: a dynamic equilibrium. **Cell Calcium.** 2010;47(4):297-314.

35. Van Coppenolle F, Vanden Abeele F, Slomianny C, Flourakis M, Hesketh J, Dewailly E et al. Ribosome-translocon complex mediates calcium leakage from endoplasmic reticulum stores. **J Cell Sci.** 2004;117(Pt 18):4135-42.

36. Weber KH, Lee EK, Basavanna U, Lindley S, Ziegelstein RC, Germino GG et al. Heterologous expression of polycystin-1 inhibits endoplasmic reticulum calcium leak in stably transfected MDCK cells. **Am J Physiol Renal Physiol.** 2008;294(6):F1279-86.

37. Supnet C, Bezprozvanny I. Presenilins function in ER calcium leak and Alzheimer's disease pathogenesis. **Cell Calcium.** 2011;50(3):303-9.

38. Pinton P, Rizzuto R. Bcl-2 and Ca^{2+} homeostasis in the endoplasmic reticulum. **Cell Death Differ.** 2006;13(8):1409-18.

39. Soboloff J, Rothberg BS, Madesh M, Gill DL. STIM proteins: dynamic calcium signal transducers. **Nat Rev Mol Cell Biol.** 2012;13(9):549-65.

40. Parekh AB. Store-operated CRAC channels: function in health and disease. **Nat Rev Drug Discov.** 2010;9(5):399-410.

41. Song MY, Yuan JXJ. Introduction to TRP channels: structure, function, and regulation. **Adv Exp Med Biol.** 2010;661:99-108.

42. Ramsey IS, Delling M, Clapham DE. An introduction to TRP channels. **Annu Rev Physiol.** 2006;68:619-47.

43. Brini M, Carafoli E. The plasma membrane Ca²+ ATPase and the plasma membrane sodium calcium exchanger cooperate in the regulation of cell calcium. **Cold Spring Harbor perspectives in biology.** 2011;3(2).

44. Lytton J. Na+/Ca^{2+} exchangers: three mammalian gene families control Ca^{2+} transport. **Biochem J.** 2007;406(3):365-82.

45. Sanjurjo CIL, Tovey SC, Prole DL, Taylor CW. Lysosomes shape IP_3-evoked Ca^{2+} signals by selectively sequestering Ca^{2+} released from the endoplasmic reticulum. **J Cell Sci.** 2012

46. Jean-Quartier C, Bondarenko AI, Alam MR, Trenker M, Waldeck-Weiermair M, Malli R et al. Studying mitochondrial Ca^{2+} uptake - A revisit. **Mol Cell Endocrinol.** 2012;353 (1-2): 114-27.

47. Waldeck-Weiermair M, Alam MR, Khan MJ, Deak AT, Vishnu N, Karsten F et al. Spatiotemporal correlations between cytosolic and mitochondrial Ca^{2+} signals using a novel red-shifted mitochondrial targeted cameleon. **PloS one.** 2012;7(9):e45917.

48. Shoshan-Barmatz V, De Pinto V, Zweckstetter M, Raviv Z, Keinan N, Arbel N. VDAC, a multi-functional mitochondrial protein regulating cell life and death. **Mol Aspects Med.** 2010;31(3):227-85.

49. Malli R, Graier WF. Mitochondrial Ca^{2+} channels: Great unknowns with important functions. **FEBS Lett.** 2010;584(10):1942-7.

50. Perocchi F, Gohil VM, Girgis HS, Bao XR, McCombs JE, Palmer AE et al. MICU1 encodes a mitochondrial EF hand protein required for Ca^{2+} uptake. **Nature.** 2010;467(7313):291-6.

51. Baughman JM, Perocchi F, Girgis HS, Plovanich M, Belcher-Timme CA, Sancak Y et al. Integrative genomics identifies MCU as an essential component of the mitochondrial calcium uniporter. **Nature.** 2011;476(7360):341-5.

52. De Stefani D, Raffaello A, Teardo E, Szabò I, Rizzuto R. A forty-kilodalton protein of the inner membrane is the mitochondrial calcium uniporter. **Nature.** 2011;476(7360):336-40.

53. Waldeck-Weiermair M, Jean-Quartier C, Rost R, Khan MJ, Vishnu N, Bondarenko AI et al. Leucine Zipper EF Hand-containing Transmembrane Protein 1 (Letm1) and Uncoupling Proteins 2 and 3 (UCP2/3) Contribute to Two Distinct Mitochondrial Ca^{2+} Uptake Pathways. **J Biol Chem.** 2011;286(32):28444-55.

54. Kirichok Y, Krapivinsky G, Clapham DE. The mitochondrial calcium uniporter is a highly selective ion channel. **Nature.** 2004;427(6972):360-4.

55. Beutner G, Sharma VK, Giovannucci DR, Yule DI, Sheu SS. Identification of a ryanodine receptor in rat heart mitochondria. **J Biol Chem.** 2001;276(24):21482-8.

56. Ryu SY, Beutner G, Kinnally KW, Dirksen RT, Sheu SS. Single channel characterization of the mitochondrial ryanodine receptor in heart mitoplasts. **J Biol Chem.** 2011;286(24):21324-9.

57. Trenker M, Malli R, Fertschai I, Levak-Frank S, Graier WF. Uncoupling proteins 2 and 3 are fundamental for mitochondrial Ca^{2+} uniport. **Nat Cell Biol.** 2007;9(4):445-52.

58. Waldeck-Weiermair M, Duan X, Naghdi S, Khan MJ, Trenker M, Malli R et al. Uncoupling protein 3 adjusts mitochondrial Ca^{2+} uptake to high and low Ca^{2+} signals. **Cell Calcium.** 2010;48(5):288-301.

59. Waldeck-Weiermair M, Malli R, Naghdi S, Trenker M, Kahn MJ, Graier WF. The contribution of UCP2 and UCP3 to mitochondrial Ca^{2+} uptake is differentially determined by the source of supplied Ca^{2+}. **Cell Calcium.** 2010;47(5):433-40.

60. De Marchi U, Castelbou C, Demaurex N. Uncoupling protein 3 (UCP3) modulates the activity of Sarco/endoplasmic reticulum Ca^{2+}-ATPase (SERCA) by decreasing mitochondrial ATP production. **J Biol Chem.** 2011;286(37):32533-41.

61. Zotova L, Aleschko M, Sponder G, Baumgartner R, Reipert S, Prinz M et al. Novel components of an active mitochondrial K(+)/H(+) exchange. **J Biol Chem.** 2010;285(19):14399-414.

62. Dimmer KS, Navoni F, Casarin A, Trevisson E, Endele S, Winterpacht A et al. LETM1, deleted in Wolf-Hirschhorn syndrome is required for normal mitochondrial morphology and cellular viability. **Hum Mol Genet.** 2008;17(2):201-14.

63. Piao L, Li Y, Kim SJ, Byun HS, Huang SM, Hwang SK et al. Association of LETM1 and MRPL36 contributes to the regulation of mitochondrial ATP production and necrotic cell death. **Cancer Res.** 2009;69(8):3397-404.

64. Tamai S, Iida H, Yokota S, Sayano T, Kiguchiya S, Ishihara N et al. Characterization of the mitochondrial protein LETM1, which maintains the mitochondrial tubular shapes and interacts with the AAA-ATPase BCS1L. **J Cell Sci.** 2008;121(Pt 15):2588-600.

65. Jiang D, Zhao L, Clapham DE. Genome-wide RNAi screen identifies Letm1 as a mitochondrial Ca^{2+}/H+ antiporter. **Science.** 2009;326(5949):144-7.

66. Nowikovsky K, Pozzan T, Rizzuto R, Scorrano L, Bernardi P. Perspectives on: SGP symposium on mitochondrial physiology and medicine: the pathophysiology of LETM1. **J Gen Physiol.** 2012;139(6):445-54.

67. Sparagna GC, Gunter KK, Sheu SS, Gunter TE. Mitochondrial calcium uptake from physiological-type pulses of calcium. A description of the rapid uptake mode. **J Biol Chem.** 1995;270(46):27510-5.

68. Bogeski I, Gulaboski R, Kappl R, Mirceski V, Stefova M, Petreska J et al. Calcium binding and transport by coenzyme Q. **J Am Chem Soc.** 2011;133(24):9293-303.

69. Michels G, Khan IF, Endres-Becker J, Rottlaender D, Herzig S, Ruhparwar A et al. Regulation of the human cardiac mitochondrial Ca^{2+} uptake by 2 different voltage-gated Ca^{2+} channels. **Circulation.** 2009;119(18):2435-43.

70. von Stockum S, Basso E, Petronilli V, Sabatelli P, Forte MA, Bernardi P. Properties of Ca^{2+} transport in mitochondria of Drosophila melanogaster. **J Biol Chem.** 2011;286(48):41163-70.

71. Mallilankaraman K, Doonan P, Cárdenas C, Chandramoorthy HC, Müller M, Miller R et al. MICU1 Is an Essential Gatekeeper for MCU-Mediated Mitochondrial Ca^{2+} Uptake that Regulates Cell Survival. **Cell.** 2012;151(3):630-44.

72. Joiner MLA, Koval OM, Li J, He BJ, Allamargot C, Gao Z et al. CaMKII determines mitochondrial stress responses in heart. **Nature.** 2012;

73. Martell JD, Deerinck TJ, Sancak Y, Poulos TL, Mootha VK, Sosinsky GE et al. Engineered ascorbate peroxidase as a genetically encoded reporter for electron microscopy. **Nat Biotechnol.** 2012;30(11):1143-8.

74. Fedorenko A, Lishko PV, Kirichok Y. Mechanism of fatty-acid-dependent UCP1 uncoupling in brown fat mitochondria. **Cell.** 2012;151(2):400-13.

75. Mallilankaraman K, Cárdenas C, Doonan PJ, Chandramoorthy HC, Irrinki KM, Golenár T et al. MCUR1 is an essential component of mitochondrial Ca^{2+} uptake that regulates cellular metabolism. **Nat Cell Biol.** 2012;14(12):1336-43.

76. Wei AC, Liu T, Winslow RL, O'Rourke B. Dynamics of matrix-free Ca^{2+} in cardiac mitochondria: two components of Ca^{2+} uptake and role of phosphate buffering. **J Gen Physiol.** 2012;139(6):465-78.

77. Carafoli E, Tiozzo R, Lugli G, Crovetti F, Kratzing C. The release of calcium from heart mitochondria by sodium. **J Mol Cell Cardiol.** 1974;6(4):361-71.

78. Palty R, Silverman WF, Hershfinkel M, Caporale T, Sensi SL, Parnis J et al. NCLX is an essential component of mitochondrial Na+/Ca^{2+} exchange. **Proc Natl Acad Sci U S A.** 2010;107(1):436-41.

79. Nita II, Hershfinkel M, Fishman D, Ozeri E, Rutter GA, Sensi SL et al. The mitochondrial Na+/Ca^{2+} exchanger upregulates glucose dependent Ca^{2+} signalling linked to insulin secretion. **PloS one.** 2012;7(10):e46649.

80. Kim B, Takeuchi A, Koga O, Hikida M, Matsuoka S. Mitochondria na(+)-ca (2+) exchange in cardiomyocytes and lymphocytes. **Adv Exp Med Biol.** 2013;961:193-201.

81. Gunter TE, Buntinas L, Sparagna G, Eliseev R, Gunter K. Mitochondrial calcium transport: mechanisms and functions. **Cell Calcium.** 2000;28(5-6):285-96.

82. Ichas F, Jouaville LS, Mazat JP. Mitochondria are excitable organelles capable of generating and conveying electrical and calcium signals. **Cell.** 1997;89(7):1145-53.

83. Kroemer G, Galluzzi L, Brenner C. Mitochondrial membrane permeabilization in cell death. **Physiol Rev.** 2007;87(1):99-163.

84. Tarasov AI, Griffiths EJ, Rutter GA. Regulation of ATP production by mitochondrial Ca^{2+}. **Cell Calcium.** 2012.

85. Rutter GA, McCormack JG, Midgley PJ, Denton RM. The role of Ca^{2+} in the hormonal regulation of the activities of pyruvate dehydrogenase and oxoglutarate dehydrogenase complexes. **Ann N Y Acad Sci.** 1989;573:206-17.

86. Sale GJ, Randle PJ. Occupancy of phosphorylation sites in pyruvate dehydrogenase phosphate complex in rat heart in vivo. Relation to proportion of inactive complex and rate of re-activation by phosphatase. **Biochem J.** 1982;206(2):221-9.

87. Behal RH, Buxton DB, Robertson JG, Olson MS. Regulation of the pyruvate dehydrogenase multienzyme complex. **Annu Rev Nutr.** 1993;13:497-520.

88. Habelhah H, Laine A, Erdjument-Bromage H, Tempst P, Gershwin ME, Bowtell DDL et al. Regulation of 2-oxoglutarate (alpha-ketoglutarate) dehydrogenase stability by the RING finger ubiquitin ligase Siah. **J Biol Chem.** 2004;279(51):53782-8.

89. McLain AL, Szweda PA, Szweda LI. α-Ketoglutarate dehydrogenase: a mitochondrial redox sensor. **Free Radic Res.** 2011;45(1):29-36.

90. Denton RM. Regulation of mitochondrial dehydrogenases by calcium ions. **Biochim Biophys Acta.** 2009;1787(11):1309-16.

91. Boyer PD. The ATP synthase--a splendid molecular machine. **Annu Rev Biochem.** 1997;66:717-49.

92. Capaldi RA, Aggeler R. Mechanism of the F(1)F(0)-type ATP synthase, a biological rotary motor. **Trends Biochem Sci.** 2002;27(3):154-60.

93. Boerries M, Most P, Gledhill JR, Walker JE, Katus HA, Koch WJ et al. Ca^{2+} - dependent interaction of S100A1 with F1-ATPase leads to an increased ATP content in cardiomyocytes. **Mol Cell Biol.** 2007;27(12):4365-73.

94. Das AM. Regulation of the mitochondrial ATP-synthase in health and disease. **Mol Genet Metab.** 2003;79(2):71-82.

95. von Ballmoos C, Wiedenmann A, Dimroth P. Essentials for ATP synthesis by F1F0 ATP synthases. **Annu Rev Biochem.** 2009;78:649-72.

96. Wernette ME, Ochs RS, Lardy HA. Ca^{2+} stimulation of rat liver mitochondrial glycerophosphate dehydrogenase. **J Biol Chem.** 1981;256(24):12767-71.

97. Kirichenko AV, Pfitzner U, Ludwig B, Soares CM, Vygodina TV, Konstantinov AA. Cytochrome c oxidase as a calcium binding protein. Studies on the role of a conserved aspartate in helices XI-XII cytoplasmic loop in cation binding. **Biochemistry.** 2005;44(37):12391-401.

98. Palmieri L, Pardo B, Lasorsa FM, del Arco A, Kobayashi K, Iijima M et al. Citrin and aralar1 are Ca^{2+}-stimulated aspartate/glutamate transporters in mitochondria. **EMBO J.** 2001;20(18):5060-9.

99. Osellame LD, Blacker TS, Duchen MR. Cellular and molecular mechanisms of mitochondrial function. **Best Pract Res Clin Endocrinol Metab.** 2012;26(6):711-23.

100. Naghdi S, Waldeck-Weiermair M, Fertschai I, Poteser M, Graier WF, Malli R. Mitochondrial Ca^{2+} uptake and not mitochondrial motility is required for STIM1-Orai1-dependent store-operated Ca^{2+} entry. **J Cell Sci.** 2010;123(Pt 15):2553-64.

101. Glitsch MD, Bakowski D, Parekh AB. Store-operated Ca^{2+} entry depends on mitochondrial Ca^{2+} uptake. **EMBO J.** 2002;21(24):6744-54.

102. Billups B, Forsythe ID. Presynaptic mitochondrial calcium sequestration influences transmission at mammalian central synapses. **J Neurosci.** 2002;22(14):5840-7.

103. Duchen MR. Mitochondria and calcium: from cell signalling to cell death. **J Physiol.** 2000;529 Pt 1:57-68.

104. Cancela JM, Van Coppenolle F, Galione A, Tepikin AV, Petersen OH. Transformation of local Ca^{2+} spikes to global Ca^{2+} transients: the combinatorial roles of multiple Ca^{2+} releasing messengers. **EMBO J.** 2002;21(5):909-19.

105. Sheng ZH, Cai Q. Mitochondrial transport in neurons: impact on synaptic homeostasis and neurodegeneration. **Nat Rev Neurosci.** 2012;13(2):77-93.

106. Celsi F, Pizzo P, Brini M, Leo S, Fotino C, Pinton P et al. Mitochondria, calcium and cell death: a deadly triad in neurodegeneration. **Biochim Biophys Acta.** 2009;1787(5):335-44.

107. Cárdenas C, Miller RA, Smith I, Bui T, Molgó J, Müller M et al. Essential regulation of cell bioenergetics by constitutive InsP3 receptor Ca^{2+} transfer to mitochondria. **Cell.** 2010;142(2):270-83.

108. Green DR, Wang R. Calcium and energy: making the cake and eating it too? **Cell.** 2010;142(2):200-2.

109. Wiederkehr A, Wollheim CB. Mitochondrial signals drive insulin secretion in the pancreatic β-cell. **Mol Cell Endocrinol.** 2011;

10. Joseph JW, Jensen MV, Ilkayeva O, Palmieri F, Alárcon C, Rhodes CJ et al. The mitochondrial citrate/isocitrate carrier plays a regulatory role in glucose-stimulated insulin secretion. **J Biol Chem.** 2006;281(47):35624-32.

111. Kibbey RG, Pongratz RL, Romanelli AJ, Wollheim CB, Cline GW, Shulman GI. Mitochondrial GTP regulates glucose-stimulated insulin secretion. **Cell Metab.** 2007;5(4):253-64.

112. Rorsman P, Braun M. Regulation of Insulin Secretion in Human Pancreatic Islets. **Annu Rev Physiol.** 2012.

113. MacDonald MJ, Longacre MJ, Stoker SW, Kendrick M, Thonpho A, Brown LJ et al. Differences between human and rodent pancreatic islets: low pyruvate carboxylase, atp citrate lyase, and pyruvate carboxylation and high glucose-stimulated acetoacetate in human pancreatic islets. **J Biol Chem.** 2011;286(21):18383-96.

114. Cabrera O, Berman DM, Kenyon NS, Ricordi C, Berggren PO, Caicedo A. The unique cytoarchitecture of human pancreatic islets has implications for islet cell function. **Proc Natl Acad Sci U S A.** 2006;103(7):2334-9.

115. Bouwens L, Rooman I. Regulation of pancreatic beta-cell mass. **Physiol Rev.** 2005;85(4):1255-70.

116. Parnaud G, Bosco D, Berney T, Pattou F, Kerr-Conte J, Donath MY et al. Proliferation of sorted human and rat beta cells. **Diabetologia.** 2008;51(1):91-100.

117. Rutti S, Sauter NS, Bouzakri K, Prazak R, Halban PA, Donath MY. In vitro proliferation of adult human beta-cells. **PloS one.** 2012;7(4):e35801.

118. Rolin B, Larsen MO, Gotfredsen CF, Deacon CF, Carr RD, Wilken M et al. The long-acting GLP-1 derivative NN2211 ameliorates glycemia and increases beta-cell mass in diabetic mice. **Am J Physiol Endocrinol Metab.** 2002;283(4):E745-52.

119. Supale S, Li N, Brun T, Maechler P. Mitochondrial dysfunction in pancreatic β cells. **Trends Endocrinol Metab.** 2012.

120. Tarasov AI, Semplici F, Ravier MA, Bellomo EA, Pullen TJ, Gilon P et al. The mitochondrial Ca^{2+} uniporter MCU is essential for glucose-induced ATP increases in pancreatic β-cells. **PloS one.** 2012;7(7):e39722.

121. Tarasov AI, Semplici F, Li D, Rizzuto R, Ravier MA, Gilon P et al. Frequency-dependent mitochondrial Ca^{2+} accumulation regulates ATP synthesis in pancreatic β cells. **Pflugers Arch.** 2012.

122. Hohmeier HE, Mulder H, Chen G, Henkel-Rieger R, Prentki M, Newgard CB. Isolation of INS-1-derived cell lines with robust ATP-sensitive K+ channel-dependent and -independent glucose-stimulated insulin secretion. **Diabetes.** 2000;49(3):424-30.

123. Li DS, Yuan YH, Tu HJ, Liang QL, Dai LJ. A protocol for islet isolation from mouse pancreas. **Nat Protoc.** 2009;4(11):1649-52.

124. Malli R, Frieden M, Osibow K, Zoratti C, Mayer M, Demaurex N et al. Sustained Ca^{2+} transfer across mitochondria is Essential for mitochondrial Ca^{2+} buffering, sore-operated Ca^{2+} entry, and Ca^{2+} store refilling. **J Biol Chem.** 2003;278(45):44769-79.

125. Robson-Doucette CA, Sultan S, Allister EM, Wikstrom JD, Koshkin V, Bhattacharjee A et al. Beta-cell uncoupling protein 2 regulates reactive oxygen species production, which influences both insulin and glucagon secretion. **Diabetes.** 2011;60(11):2710-9.

126. Affourtit C, Jastroch M, Brand MD. Uncoupling protein-2 attenuates glucose-stimulated insulin secretion in INS-1E insulinoma cells by lowering mitochondrial reactive oxygen species. **Free Radic Biol Med.** 2011;50(5):609-16.

127. Brownlee M. A radical explanation for glucose-induced beta cell dysfunction. **J Clin Invest.** 2003;112(12):1788-90.

128. Palmer AE, Giacomello M, Kortemme T, Hires SA, Lev-Ram V, Baker D et al. Ca^{2+} indicators based on computationally redesigned calmodulin-peptide pairs. **Chem Biol.** 2006;13(5):521-30.

129. Carlson HJ, Campbell RE. Genetically encoded FRET-based biosensors for multiparameter fluorescence imaging. **Curr Opin Biotechnol.** 2009;20(1):19-27.

130. Collins TJ, Lipp P, Berridge MJ, Bootman MD. Mitochondrial Ca^{2+} uptake depends on the spatial and temporal profile of cytosolic Ca^{2+} signals. **J Biol Chem.** 2001;276(28):26411-20.

131. Kennedy ED, Rizzuto R, Theler JM, Pralong WF, Bastianutto C, Pozzan T et al. Glucose-stimulated insulin secretion correlates with changes in mitochondrial and cytosolic Ca^{2+} in aequorin-expressing INS-1 cells. **J Clin Invest.** 1996;98(11):2524-38.

132. Moreau B, Parekh AB. Ca^{2+} -dependent inactivation of the mitochondrial Ca^{2+} uniporter involves proton flux through the ATP synthase. **Curr Biol.** 2008;18(11):855-9.

133. Li Y, Maedler K, Shu L, Haataja L. UCP-2 and UCP-3 proteins are differentially regulated in pancreatic beta-cells. **PloS one.** 2008;3(1):e1397.

134. Medvedev AV, Robidoux J, Bai X, Cao W, Floering LM, Daniel KW et al. Regulation of the uncoupling protein-2 gene in INS-1 beta-cells by oleic acid. **J Biol Chem.** 2002;277(45):42639-44.

135. Alam MR, Groschner LN, Parichatikanond W, Kuo L, Bondarenko AI, Rost R et al. Mitochondrial Ca^{2+} uptake 1 (MICU1) and mitochondrial Ca^{2+} uniporter (MCU) contribute to metabolism-secretion coupling in clonal pancreatic β-cells. **J Biol Chem.** 2012;287(41):34445-54.

136. Marchi S, Lupini L, Patergnani S, Rimessi A, Missiroli S, Bonora M et al. Downregulation of the Mitochondrial Calcium Uniporter by Cancer-Related miR-25. **Curr Biol.** 2013;23(1):58-63.

137. Palty R, Raveh A, Kaminsky I, Meller R, Reuveny E. SARAF inactivates the store operated calcium entry machinery to prevent excess calcium refilling. **Cell.** 2012;149(2):425-38.

138. Goehring I, Gerencser AA, Schmidt S, Brand MD, Mulder H, Nicholls DG. Plasma membrane potential oscillations in insulin secreting ins-1 832/13 cells do not require glycolysis and are not initiated by fluctuations in mitochondrial bioenergetics. **J Biol Chem.** 2012;287(19):15706-17.

139. Ravier MA, Cheng-Xue R, Palmer AE, Henquin JC, Gilon P. Subplasmalemmal Ca^{2+} measurements in mouse pancreatic beta cells support the existence of an amplifying effect of glucose on insulin secretion. **Diabetologia.** 2010;53(9):1947-57.

140. Robb-Gaspers LD, Burnett P, Rutter GA, Denton RM, Rizzuto R, Thomas AP. Integrating cytosolic calcium signals into mitochondrial metabolic responses. **EMBO J.** 1998;17(17):4987-5000.

PUBLICATIONS

This dissertation is based no following papers which have been published in peer reviewed journals.

1- Alam MR, Groschner LN, Parichatikanond W, Kuo L, Bondarenko AI, Rost R et al. Mitochondrial Ca^{2+} uptake 1 (MICU1) and mitochondrial Ca^{2+} uniporter (MCU) contribute to metabolism-secretion coupling in clonal pancreatic β-cells. **J Biol Chem.** 2012;287(41):34445-54

2- Waldeck-Weiermair M, **Alam MR**, Khan MJ, Deak AT, Vishnu N, Karsten F et al. Spatiotemporal correlations between cytosolic and mitochondrial Ca^{2+} signals using a novel red-shifted mitochondrial targeted cameleon. **PloS one.** 2012;7(9):e45917

I have also contributed to following studies during the period of my PhD.

1- Jean-Quartier C, Bondarenko AI, **Alam MR**, Trenker M, Waldeck-Weiermair M, Malli R et al. Studying mitochondrial Ca^{2+} uptake - A revisit. **Mol Cell Endocrinol.** 2012;353 (1-2): 114-27

2- Khan MJ, **Rizwan Alam M**, Waldeck-Weiermair M, Karsten F, Groschner L, Riederer M et al. Inhibition of Autophagy Rescues Palmitic Acid-induced Necroptosis of Endothelial Cells. **J Biol Chem.** 2012;287(25):21110-20

3- Deak AT, Groschner LN, **Alam MR**, Seles E, Bondarenko AI, Graier WF et al. The endocannabinoid N-arachidonoyl glycine (NAGly) inhibits store-operated Ca^{2+} entry by abrogating STIM1/Orai1 interaction. **J Cell Sci.** 2012